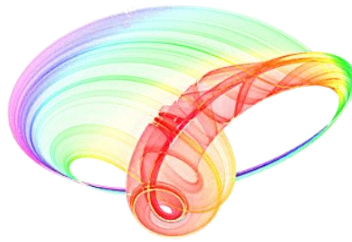


Book of abstracts



IX International School and Conference on Photonics

PHOTONICA2023

with joint events:

Understanding interaction light - biological surfaces: possibility for new electronic materials and devices

&

Biological and bioinspired structures for multispectral surveillance

&

Quantum sensing integration within microfluidic Lab-on-a Chips for biomedical applications

&

Advanced Biophysical Methods for Soil Targeted Fungi-Based Biocontrol Agents

August 28 - September 01, 2023, Belgrade, Serbia

Editors

Jelena Potočnik, Maja Popović, Dušan Božanić

Vinča Institute of Nuclear Sciences – National Institute of the Republic of Serbia, University of Belgrade

Belgrade, 2023

ABSTRACTS OF TUTORIAL, KEYNOTE, INVITED LECTURES,
PROGRESS REPORTS AND CONTRIBUTED PAPERS

of

IX International School and Conference on Photonics

PHOTONICA2023

August 28 - September 01, 2023, Belgrade, Serbia

Editors

Jelena Potočnik, Maja Popović, Dušan Božanić

Publisher

Vinča Institute of Nuclear Sciences – National Institute of the Republic of
Serbia, University of Belgrade
Mike Petrovića Alasa 12-14
11351 Vinča, Belgrade, Serbia

Printed by

Serbian Academy of Sciences and Arts

Number of copies

200

ISBN 978-86-7306-165-8

ISBN 978-86-7306-168-9 (Online)



This work is licensed under a Creative Commons Attribution-NonCommercial-NoDerivatives 4.0 International License, <http://creativecommons.org/licenses/by-nc-nd/4.0/>

PHOTONICA2023 – IX International School and Conference on Photonics (www.photonica.ac.rs) is organized by Vinča Institute of Nuclear Sciences - National Institute of the Republic of Serbia, University of Belgrade (www.vin.bg.ac.rs), Serbian Academy of Sciences and Arts (www.sanu.ac.rs), and Optical Society of Serbia (www.ods.org.rs).



Other institutions that helped the organization of this event are: Institute of Physics Belgrade, University of Belgrade (www.ipb.ac.rs), Faculty of Physics, University of Belgrade (www.ff.bg.ac.rs), School of Electrical Engineering, University of Belgrade (www.etf.bg.ac.rs), Institute of Chemistry, Technology and Metallurgy, University of Belgrade (www.ihtm.bg.ac.rs), Faculty of Technical Sciences, University of Novi Sad (www.ftn.uns.ac.rs), Faculty of Sciences and Mathematics, University of Niš (www.pmf.ni.ac.rs), Faculty of Biology, University of Belgrade (www.bio.bg.ac.rs) and Faculty of Sciences and Mathematics, University of Kragujevac (www.pmf.kg.ac.rs).

PHOTONICA2023 is organized under auspices and with support of the Ministry of Science, Technological Development and Innovation, Republic of Serbia (www.nitra.gov.rs). PHOTONICA2023 is supported and recognized by Optica (Formerly OSA) - The Optical Society (www.optica.org).



Committees

Scientific Committee

- Aleksandar Krmpot, Serbia
- Aleksandra Maluckov, Serbia
- Bojan Resan, Switzerland
- Boris Malomed, Israel
- Branislav Jelenković, Serbia
- Carsten Ronning, Germany
- Concita Sibilica, Italy
- Darko Zibar, Denmark
- Dmitry Budker, Germany
- Dragan Inđin, United Kingdom
- Edik Rafailov, United Kingdom
- Francesco Cataliotti, Italy
- Giannis Zacharakis, Greece
- Goran Isić, Serbia
- Goran Mašanović, United Kingdom
- Ivana Vasić, Serbia
- Jasna Crnjanski, Serbia
- Jelena Radovanović, Serbia
- Jelena Stašić, Serbia
- Jerker Widengren, Sweden
- Jovan Bajić, Serbia
- Ljupčo Hadžievski, Serbia
- Luca Antonelli, United Kingdom
- Marco Canepari, France
- Marko Krstić, Serbia
- Marko Spasenović, Serbia
- Milan Kovačević, Serbia
- Milena Milošević, Serbia
- Milivoj Belić, Qatar
- Mirjana Novaković, Serbia
- Nikola Stojanović, Germany
- Nikola Vuković, Serbia
- Nikos Pleros, Greece
- Pavle Anđus, Serbia
- Petra Beličev, Serbia
- Sergei Turitsyn, United Kingdom
- Vladan Pavlović, Serbia
- Vladan Vuletić, United States of America
- Vladana Vukojević, Sweden
- Zoran Grujić, Serbia

Organizing Committee

- Dušan Božanić, Vinča Institute of Nuclear Sciences, Belgrade (Chair)
- Jelena Pajović, Faculty of Physics, University of Belgrade (Deputy Chair)
- Radovan Dojčilović, Vinča Institute of Nuclear Sciences, Belgrade (Deputy Chair)
- Maja Popović, Vinča Institute of Nuclear Sciences, Belgrade (Deputy Chair)
- Jelena Potočnik, Vinča Institute of Nuclear Sciences, Belgrade
- Goran Gligorić, Vinča Institute of Nuclear Sciences, Belgrade
- Danijela Danilović, Vinča Institute of Nuclear Sciences, Belgrade
- Kolja Bugarski, Vinča Institute of Nuclear Sciences, Belgrade
- Milica Nedić, Vinča Institute of Nuclear Sciences, Belgrade
- Miljana Piljević, Institute of Physics Belgrade
- Đorđe Trpkov, Vinča Institute of Nuclear Sciences, Belgrade
- Dragana Tošić, Vinča Institute of Nuclear Sciences, Belgrade
- Anamarija Abu el Rub, Vinča Institute of Nuclear Sciences, Belgrade
- Vanja Ralić, Vinča Institute of Nuclear Sciences, Belgrade

Technical Organizer

 **Lufthansa City Center**
Panacomp Wonderland
Travel

<http://www.panacomp.net/>

Tel: +381 21 466 075

Tel: +381 21 466 076

Tel: +381 21 466 077

Dear Colleagues, friends of photonics,

We are honored by your participation at our PHOTONICA 2023 and your contribution to the tradition of this event. It is our pleasure to host you in Belgrade and in Serbia. Welcome to the world of photonics.

The International School and Conference on Photonics, PHOTONICA, is a biennial event held in Belgrade since 2007. The first meeting in the series was called ISCOM (International School and Conference on Optics and Optical Materials), but it was later renamed to PHOTONICA to reflect more clearly the aims of the event as a forum for education of young scientists, exchanging new knowledge and ideas, and fostering collaboration between scientists working within emerging areas of photonic science and technology. A particular educational feature of the program is to enable students and young researchers to benefit from the event, by providing introductory lectures preceding most recent results in many topics covered by the regular talks. In other words, tutorial and keynote speakers will give lectures specifically designed for students and scientists starting in this field. Apart from the oral presentations PHOTONICA hosts vibrant poster sessions. A significant number of best posters will be selected and the authors will have opportunity to present their work through short oral presentations – contributed talks.

The wish of the organizers is to provide a platform for discussing new developments and concepts within various disciplines of photonics, by bringing together researchers from academia, government and industrial laboratories for scientific interaction, the showcasing of new results in the relevant fields and debate on future trends.

PHOTONICA 2023 will host three joint events: PhoBioS COST Action “Understanding interaction light - biological surfaces: possibility for new electronic materials and devices”, NATO Science for Peace and Security Program (grant G5618) workshop “Biological and bioinspired structures for multispectral surveillance”, workshop on “Quantum sensing integration within microfluidic Lab-on-a Chips for biomedical applications” and BioPhysFUN workshop “Advanced Biophysical Methods for Soil Targeted Fungi-Based Biocontrol Agents”. Following the official program, the participants will also have plenty of opportunities to mix and network outside of the lecture theatre with planned free time and social events.

This book contains 130 abstracts of all presentations at the IX International School and Conference on Photonics, PHOTONICA2023. Authors from all around the world, from all the continents, will present their work at this event. There will be 4 tutorial and 7 keynote lectures to the benefits of students and early stage researches. The most recent results in various research fields of photonics will be presented through 16 invited lectures and 8 progress reports of early-stage researchers. Within the poster sessions and a number of contributed talks, authors will present 95 presentations on their new results in a cozy atmosphere of the building of Serbian Academy of Science and Arts.

Belgrade, August 2023

Editors

Conference Topics

1. Quantum optics and ultracold systems
2. Nonlinear optics
3. Optical materials
4. Biophotonics
5. Devices and components
6. Optical communications
7. Laser spectroscopy and metrology
8. Ultrafast optical phenomena
9. Laser - material interaction
10. Optical metamaterials and plasmonics
11. Machine learning in photonics
12. Other topics in photonics

Joint Events

PhoBioS COST Action - Understanding interaction light - biological surfaces: possibility for new electronic materials and devices

NATO Science for Peace and Security Program - Biological and bioinspired structures for multispectral surveillance

Workshop - Quantum sensing integration within microfluidic Lab-on-a Chips for biomedical applications

BioPhysFUN workshop - Advanced Biophysical Methods for Soil Targeted Fungi-Based Biocontrol Agents

Table of Contents

Tutorial Lectures

T.1	Measurements beyond the Heisenberg uncertainty bound <i>E.S. Polzik</i>	2
T.2	The intelligent microscope at the nanoscale: multimodal microscopy from fluorescence to label-free <i>A. Diaspro</i>	3
T.3	Nanoplasmonics: Fundamentals & Applications <i>S.I. Bozhevolnyi</i>	4
T.4	VUV Circularly-Polarized Light as a symmetry-breaking driving force: implications for the origin of life's homochirality <i>L. Nahon</i>	5

Keynote Lectures

K.1	Recent trends in superfluid atomic gases: ferromagnetic, liquid and supersolid states <i>A. Recati</i>	7
K.2	Nonlinear optics in atomically thin materials <i>G. Soavi</i>	8
K.3	Three-dimensional imaging flow cytometry <i>A. Bassi</i>	9
K.4	From French fries to Foie Gras, turning around a synchrotron <i>F. Jamme, J. Pajovic, F. Wien and M. Réfrégiers</i>	10
K.5	Einstein-Podolsky-Rosen experiment with two Bose-Einstein condensates <i>P. Colciaghi, Y. Li, P. Treutlein and T. Zibold</i>	11
K.6	Development of table-top ultrafast soft-X spectroscopy for material science <i>C. Vozzi</i>	12
K.7	Ultrafast chirality: the road to efficient chiral measurements <i>O. Smirnova</i>	13

Invited Lectures

I.1	Optical control of topological and correlated electronic states <i>M. Hafezi</i>	15
I.2	Scanning quantum microscopy <i>F. Setzpfandt</i>	16
I.3	A single ion meets a single Rydberg atom <i>R. Löw</i>	17
I.4	Photonic Landau levels <i>M. Rechtsman</i>	18
I.5	Shape-changing microstructures for multifunctional microfluidics <i>S. Nocentini, S. Donato, D. Martella, C. Credi, C. Parmeggiani and D.S. Wiersma</i>	19
I.6	Deeper and faster: new tools for nonlinear bioimaging <i>L. Bonacina</i>	20

I.7	Polymeric SERS-fluidic platforms for the non-destructive optical analysis of liquid samples <i>C. Credi</i>	21
I.8	Rapid and sensitive cancer detection with fluorescence lifetime imaging microscopy <i>W. Su, M. Ji, J. Ma, R. Guo and L. Mi</i>	22
I.9	Photonic integrated circuits based on linearly coupled waveguide arrays <i>J. Petrovic</i>	23
I.10	Excursion of a biophysicist to the quantum world <i>A. Dér</i>	24
I.11	Light-enhanced transdermal drug delivery <i>R. Boukherroub</i>	25
I.12	Luminescent thermometry using lanthanide and transition metal-activated phosphors <i>Ž. Antić</i>	26
I.13	Black box certification of resources for photonic quantum technologies <i>S. Neves, L. dos Santos Martins, V. Yacoub, P. Lefevbre, I. Šupić, D. Markham and E. Diamanti</i>	27
I.14	Femtosecond laser direct writing of fiber optic microstructure devices <i>X. Shu</i>	28
I.15	Microscopic theory of transport and optics in superlattices and applications to metabolomics and novel device functionalities <i>M.F. Pereira, A. Apostolakis, H. Zafar, V. Vaks and V. Anfertev</i>	29
I.16	Blue and red diode pumped low-cost ultrafast lasers for biomedical applications <i>B. Resan</i>	30

Progress Reports

P.1	Broadband photonic quantum memory in atomic ensembles <i>K. Shinbrough, B.D. Hunt, S. Park, K. Oolman, T. Loveridge, J.G. Eden and V.O. Lorenz</i>	32
P.2	Measuring the dipolar interaction shift of the BEC critical temperature <i>M. Krstajic</i>	33
P.3	Crystal structure, optical properties and photo/electrocatalytic activity of nanostructured $Zn_{1-x}Fe_yO_{(1-x+1.5y)}$ <i>V. Rajic, S. Markovic, M. Popovic, M. Novakovic, Lj. Veselinovic, I. Stojkovic Simatovic, S.D. Skapin, S. Stojadinovic and V. Rac</i>	34
P.4	Synchrotron radiation photoemission spectroscopy study of the valence band electronic structure of Ag-Ag ₂ S Janus nanoparticles for the development of nanomotors propelled by NIR light <i>D. Danilović, D.K. Božanić, J. Pajović, G.A. Garcia, L. Nahon, T. Marić and V. Djoković</i>	35
P.5	Photosensitizer potential of doped and undoped nanostructured TiO ₂ <i>M. Matijević, L. Korićanac, Đ. Nakarada, J. Žakula, M. Stepić, M. Radoičić, M. Mojović, M. Petković and M.D. Nešić</i>	36
P.6	Application of laser-induced breakdown spectroscopy for the determination of trace metals in oils <i>M. Vinić</i>	37

P.7	Influence of thin oxide layer to photoacoustic signal of nano-mechanical structures <i>K.Lj. Đorđević, S.P. Galović, M.A. Dragaš, D.K. Markushev and D.D. Markushev</i>	38
P.8	Modeling microwave ablation for tumor treatment using open-source software components <i>N. Boskovic, M. Radmilovic-Radjenovic and B. Radjenovic</i>	39
Contributed Papers		
1. Quantum optics and ultracold systems		
QO.1	Exploiting the quantumness of coherent states: toward macroscopic quantum light <i>C. Hermann Avigliano</i>	42
QO.2	Anomalous diffusion and mixed dynamics in a classical Bose-Hubbard chain <i>D. Markovic and M. Cubrovic</i>	43
QO.3	Correlated photon pairs by Four Wave Mixing in alkali vapor for imaging application <i>M.M. Ćurčić, D. Arsenović and B. Jelenković</i>	44
QO.4	Transport of cold bosonic atoms in optical lattices <i>I. Vasić and J. Vučićević</i>	45
QO.5	Experimental and theoretical study of the phase response of M_x magnetometer to modulating transversal magnetic field <i>M.M. Ćurčić, A. Milenković, A. Bunjac, T. Scholtes and Z. Grujić</i>	46
QO.6	Spontaneous emission of three-level ladder-type atom coupled to one-dimensional rectangular waveguide <i>Lj. Stevanović and M. Perić</i>	47
QO.7	Quantized vortices in dipolar BECs when crossing the superfluid-supersolid phase transition <i>M. Sindik, A. Recati, S.M. Rocuzzo, L. Santos and S. Stringari</i>	48
2. Nonlinear optics		
NO.1	Absorption coefficients and refractive index changes in a strongly prolate and strongly oblate ellipsoidal quantum dot <i>V. Pavlovic and Lj. Stevanovic</i>	50
NO.2	Impact of nonlinearity on the zero-mode lasing in optical lattices <i>M. Nedić, G. Gligorić, J. Petrovic and A. Maluckov</i>	51
NO.3	The modulation instability triggered band relaxation in photonic Chern insulator <i>A. Mančić, M. Nedić, D. Leykam and A. Maluckov</i>	52
NO.4	Coupled vortex generator in active multi-core fibers <i>P.P. Beliĉev, G. Gligorić and A. Maluckov</i>	53
NO.5	Electric-field induced SHG (EFISHG) in graphene? <i>J. Woeste, N. Stojanovic and M. Gensch</i>	54
NO.6	Rogue wave clusters of the nonlinear Schrödinger equation composed of Akhmediev breathers and Kuznetsov-Ma solitons <i>S.N. Nikolić, S. Alwashahi, N.B. Aleksić and M.R. Belić</i>	55

NO.7	Counterpropagating rogue waves <i>M.S. Petrovic, N.B. Aleksic, A.I. Strinic and M.R. Belic</i>	56
NO.8	Solutions to nematic liquid crystals systems with cubic-quintic and septic nonlinearities using the Jacobi elliptic function expansion method <i>N. Petrović</i>	57
3. Optical materials		
OM.1	Centrosymmetric, non-symmorphic, non-magnetic, spin-orbit coupled layers without Dirac cones: a tight-binding example <i>V. Damljanović</i>	59
OM.2	Helical and square-spiral copper nanostructures: The effect of thickness and deposition conditions on the structural and optical properties <i>J. Potočnik, N. Božinović, M. Popović, M. Nenadović and M. Novaković</i>	60
OM.3	Luminescent lanthanide molecular materials for photonics applications <i>D. Mara</i>	61
OM.4	Interference effect in surface modified ZnS nanoparticles/Poly (methylmethacrylate) nanocomposites <i>N. Romčević, B. Hadžić, M. Curčić, V. Radojević, N. Paunović and M. Romčević</i>	62
OM.5	Metal ion-implanted TiN thin films: Induced effects on structural and optical properties <i>M. Popović, M. Novaković, D. Pjević, D. Vaňa, D. Jugović and P. Noga</i>	63
OM.6	Real-time fabrication of microstructures on the modified chitosan <i>B. Murić, S. Savić-Šević, A. Kovačević, D. Pantelić and B. Jelenković</i>	64
OM.7	Optimization of UV LED design using evolutionary algorithms <i>L. Leguay, H. Mączko, A. Schliwa and S. Birner</i>	65
OM.8	Yellow fluorescent, water soluble N-doped graphene quantum dots: synthesis, photoluminescence and functionalization with L-Phenylalanine <i>Dj. Trpkov, D. Sredojević, D. Tošić, J. Pajović, D.K. Božanić and V. Djoković</i>	66
OM.9	Large thermally irreversible photoinduced shift of selective light reflection in hydrazone-containing cholesteric polymer systems <i>M. Cigl, A. Boychuk, V. Shibaev, V. Hamplová, V. Novotná and A. Bobrovsky</i>	67
OM.10	Strain-induced modulation of electronic and optical properties in hBN/group III monochalcogenide heterostructures <i>A. Solajić and J. Pesić</i>	68
OM.11	Anthocyanin-functionalized biopolymer films as pH-sensitive indicators <i>D. Tosić, R. Dojčilo, D. Božanić, Dj. Trpkov and V. Djoković</i>	69
4. Biophotonics		
B.1	Design of femtosecond microstructured Poly Lactic Acid temporal cellular scaffolds coated with hydroxyapatite by PLD method for bone tissue regeneration <i>L. Angelova, A. Daskalova, R. Mincheva, E. Filipov, A. Dikovska, M.H. Fernandes and I. Buchvarov</i>	71
B.2	Non-linear excitation fluorescence imaging through two-photon laser polymerized microlenses	

	<i>G. Chirico, M. Marini, R. Martínez Vázquez, R. Osellame, A. Nardini, C. Conci, E. Jacchetti,,M.T. Raimondi</i>	72
B.3	SERS-based immunosensor for sensitive detection of cancer protein biomarkers in serum <i>M. Kahraman, A.M. Saridağ and I.D. Karagoz</i>	73
B.4	Fabrication of flexible diatomite-based SERS active platforms <i>A.M. Saridağ and M. Kahraman</i>	74
B.5	Development of two-dimensional superresolution fluorescence microscope with structured illumination <i>A. Denčevski, A.J. Krmpot and M.D. Rabasović</i>	75
B.6	Smart optical assay based on novel bioorthogonal SERS nanoprobe for the β -amyloid peptide quantification <i>C. Dallari, C. Credi and F.S. Pavone</i>	76
B.7	Bioactive compounds of <i>Carlina acanthifolia</i> roots obtained by fractional extraction and their 3D fluorescence spectra <i>N. Petkova, I. Ivanov, E. Saraliev, D. Georgieva, K. Nikolova, T. Eftimov, G. Gentsheva and L. Vladimirova–Mihaleva</i>	77
B.8	Carbon quantum dots/silver based metal organic framework composites in light enhanced wound healing <i>I. Popović, A. Valenta Šobot, J. Filipović Tričković, L. Korićanac, J. Žakula, V. Ralić,,M.D. Nešić</i>	78
B.9	Anti-cancer and imaging potential of fluorescent black carrot Carbon Dot nanoparticles <i>M.D. Nešić, J. Filipović Tričković, A. Valenta Šobot, J. Žakula, L. Korićanac, I. Popović,,M. Petković</i>	79
B.10	In search of conditions for Gd-TiO ₂ activation by light irradiation in photodynamic treatment of pancreatic cancer cells <i>A. Abu el Rub, M.D. Nešić, J. Žakula, V. Ralić, M. Petković, I. Popović, M. Matijević, M. Radočić and M. Stepić</i>	80
B.11	Quantum sensing and imaging with entangled photons <i>B. Jelenković</i>	81
B.12	Optical skin biopsy through multispectral approach and prototype device <i>Ts. Genova, V. Mircheva, Al. Zhelyazkova, A. Markovski and P. Troyanova</i>	82
B.13	Novel approach for colon cancer detection through fluorescence spectroscopy <i>Ts. Genova, Al. Zhelyazkova, B. Vladimirov and N. Pankov</i>	83
B.14	<i>In vivo</i> multiphoton imaging of a filamentous fungus <i>Phycomyces blakesleeanus</i> : the effect of small ambient temperature increase on mitochondrial morphology and lipid droplets density <i>T. Pajic, S. Kozakijevic, A.J. Krmpot, M. Zivic, N.V. Todorovic and M.D. Rabasovic</i>	84
B.15	Synthesis of europium-doped fluorapatite as a promising luminescent biomaterial <i>V. Stanic, M. Omerasevic, D. Mutavdzic, A. Mrakovic, Dj. Veljovic, M. Marinovic Cincovic and D. Jovanovic</i>	85
B.16	FEM analysis of natural photonic structures of insects in the IR band <i>B. Salatic, D. Pavlovic and D. Pantelic</i>	86
B.17	Dynamics of optomechanical array revealed by holography <i>H. Skenderović, A.M. Dezfouli, D. Abramović, M. Rakić, and N. Demoli</i>	87

B.18	Functionalization of biological/bioinspired structures for multispectral surveillance <i>D. Pavlović, B. Salatić, H. Skenderović, M. Rakić and D. Pantelić</i>	88
B.19	A compact, holographic imaging sensor for biophotonic structures <i>D. Pantelic, D. Pavlovic, D. Grujic, B. Salatic, P. Atanasijevic and P. Mihailovic</i>	89
B.20	Cutting edge technique for determination of spatial resolution limits of nonlinear laser scanning microscopy <i>M. Bukumira, J. Jelić, A. Denčevski, M.D. Rabasović, N. Vujičić, A. Senkić, A. Supina and A. Krmpot</i>	90
B.21	Optical fiber curing of a dental composite: a holographic, thermographic, and Raman study <i>E. Novta, T. Lainović, D. Grujić, S. Savić-Šević, E. Toth, Ž. Cvejić, L. Blažić and D. Pantelić</i>	91
B.22	Exploring the nano-scale world using a custom-made Fluorescence Correlation Spectroscopy (FCS) instrument <i>J.Z. Jelić, M.D. Rabasović, S. Nikolić, V. Vukojević and A.J. Krmpot</i>	92
B.23	Calcium imaging of cerebellar granular neurons in culture acutely treated with cerebrospinal fluid of patients with neurodegenerative diseases <i>A. Laudanović, A. Antić, A. Palibrk, P. Andjus, Z. Stević, D. Lutz and M. Milošević</i>	93
B.24	Mid-Infrared quantum scanning microscopy with visible light <i>J.R. León-Torres, J. Fuenzalida, M. Gilaberte, S. Töpfer, V. Gili and M. Gräfe</i>	94
B.25	Fluorescent products upon heme degradation as potential biomarkers: Understanding their formation via Hemoglobin oxidation <i>M.D. Radmilović, I.T. Drvenica, M.D. Rabasović, V.Lj. Ilić and A.J. Krmpot</i>	95
5. Devices and components		
DC.1	High-power diffraction-limited laser systems with variable output characteristics oscillating in visible spectral range on atomic copper self-terminating transitions for advanced material microprocessing <i>I. Kostadinov, K. Temelkov, S. Slaveeva and G. Yankov</i>	97
DC.2	Interband cascade lasers: advantages of bulk AlGaAsSb claddings <i>B. Petrović, A. Bader, F. Hartmann, R. Weih, F. Jabeen and S. Höfling</i>	98
DC.3	Dependence of transport parameters on interface composition diffusion and doping segregation in longitudinal optical phonon, bound to continuum and hybrid THz quantum cascade laser designs <i>N. Stanojević, A. Demić, N. Vuković, D. Indjin and J. Radovanović</i>	99
DC.4	Investigation of intersubband transitions in wide bandgap oxide quantum well structures for optoelectronic device applications <i>A. Atić, N. Vuković and J. Radovanović</i>	100
DC.5	Multipoint splitters based on waveguide arrays <i>K. Bugarski, P. Vildoso, M. Stojanovic, A. Maluckov, G.Z. Mashanovich, R.A. Vicencio and J. Petrovic</i>	101
DC.6	Optical interconnects and filters based on waveguide arrays <i>J. Krsic, M. Stojanovic, K. Bugarski, N. Stojanovic, A. Maluckov, P. Veerman and J. Petrovic</i>	102

DC.7	Photo-electronic security device based on photonics integrated circuits <i>C. Cid-Lara and R.A. Vicencio</i>	103
DC.8	The influence of injection barriers on performance of organic solar cells studied by drift-diffusion model with transport layers <i>T. Pavlicevic, J. Gojanovic and S. Zivanovic</i>	104
DC.9	Characterization and performance evaluation of a dual loop Sagnac interferometer as sensing system for intrusion location detection <i>M. Vasiljević Toskić, J.S. Bajić, L. Manojlović and B. Batinić</i>	105
6. Optical communications		
OC.1	Free-space OAM wave transmission: a short dipole modeling study <i>A.Ž. Ilić, J.Z. Trajković, S.V. Savić and M.M. Ilić</i>	107
OC.2	OAM mode quality comparisons for discrete EM radiating sources <i>J.Z. Trajković, A.Ž. Ilić, S.V. Savić, N. Maletić, E. Grass and M.M. Ilić</i>	108
7. Laser spectroscopy and metrology		
LS.1	An upgrade of the primary length standard of Republic of Serbia <i>Z.D. Grujić, M.G. Nikolić, S. Zelenika and M.D. Rabasović</i>	110
LS.2	Combined spectroscopic approach for the characterization of pigments used in prehistoric pottery from the region of Western Bulgaria <i>V. Tankova, V. Atanassova, V. Mihailov and A. Pirovska</i>	111
LS.3	Fluorescence spectroscopy and sucrose presence in onion genotypes after long-term storage <i>L. Vladimirova-Mihaleva, M. Mihalev, V. Slavova, G. Pevicharova, S. Genova and V. Boteva</i>	112
LS.4	Measurement of the heading error of a free alignment precession magnetometer <i>Z.D. Grujić, M. Ćurčić, A. Milenkovic, J. Hinkel and T. Scholtes</i>	113
8. Ultrafast optical phenomena		
UO.1	Femtosecond laser spectroscopy for exploration of space <i>Y. Ha, O. Gueckstock, G. Kourfakas, J. Petrovic, M. Rabasovic, A. Krmpot, T. Seifert,,M. Gensch</i>	115
9. Laser - material interaction		
LM.1	Preparing the bioactive surface of Ti/Zr/Ti system by femtosecond laser pre-patterning of substrate <i>N. Božinović, V. Rajić, K. Savva, J. Potočnik, E. Stratakis and S. Petrović</i>	117
LM.2	Selective ablation and laser induced periodical surface structures (LIPSS) produced on (Ni/Ti) nano layer thin film with ultrafast laser pulses <i>S. Petrović, B. Gaković, C. Siogka, D. Milovanović and G. Tsibidis</i>	118
LM.3	Experimental demonstration of vectorial spin-orbital Hall effect of light <i>A. Porfirev, S. Khonina, A. Ustinov, N. Ivliev and I. Golub</i>	119
LM.4	Structured laser beams: generation and applications <i>D. Porfirev, A. Porfirev, S. Khonina and S. Karpeev</i>	120
LM.5	Carbon dots nanoparticles as an effective gate for PDT	

	<i>M. Algarra, M.D. Nešić, J. Soto, M. Stepić, A. Urrutia, J.J. Imas, T. Dučić and M. Petković</i>	121
LM.6	All PM, 14 W, 2.8 GHz intra-burst repetition rate Yb-doped fiber laser <i>E. Hasar and P. Elahi</i>	122
LM.7	The analysis of the influence of optical absorbance on photothermally induced surface temperature variations in a thin sample of high optical transparency <i>M. Nesic, M. Popovic, S. Galovic, V. Miletic and Lj. Kostic</i>	123
LM.8	Interaction of ns laser with 316L-NiB stainless steel obtained by powder metallurgy – morphological effects and LIBS analysis <i>J. Stasic, M. Trtica, M. Kuzmanovic, J. Savovic, J. Ruzic, M. Simic, X. Chen and D. Bozic</i>	124
LM.9	ns-Laser – titanium interaction: hydrogen ambience <i>M. Trtica and J. Stasic</i>	125
10. Optical metamaterials and plasmonics		
OMP.1	All-dielectric optical metasurfaces for sensing of substances with identical real parts of refractive index <i>M. Obradov, Z. Jakšić, I. Mladenović, M. Rašljić Rafajilović and D. Vasiljević Radović</i>	127
OMP.2	Electron energy loss spectroscopy of multilayered structures: Theoretical aspects and the role of graphene-insulator distance <i>I. Radović, A. Kalinić, L. Karbunar and Z.L. Mišković</i>	128
OMP.3	Plasmon-phonon hybridization in drift-current biased supported graphene <i>I. Radović, A. Kalinić, L. Karbunar and Z.L. Mišković</i>	129
OMP.4	Terahertz transmission through metal-insulator-metal cavity arrays infiltrated by liquid crystals <i>G. Isić, D.C. Zografopoulos and B. Vasić</i>	130
OMP.5	Ellipsometric Study of Interactions of Erufosine with Solid-supported by Metasurfaces Lipid Films <i>D. Georgieva, M. Tanovska, V. Vassilev, R. Tzoneva, M. Berger, M. Rahmani, D. Neshev and L. Vladimirova-Mihaleva</i>	131
OMP.6	Rosette based metamaterial for circularly polarized terahertz waves manipulation <i>D.B. Stojanovic, U. Ralevic, Y. Demirhan, G. Aygun and L. Ozyuzer</i>	132
11. Machine learning in photonics		
MLP.1	Remote temperature sensing using upconverting phosphor and artificial neural networks <i>M.S. Rabasovic, M.G. Nikolic and D. Sevic</i>	134
MLP.2	Reverse sigmoid-like nonlinearity in Fabry-Perot injection-locked lasers <i>P. Atanasijević, M. Banović, J. Crnjanski, M. Krstić, P. Mihailović, S. Petričević and D. Gvozdić</i>	135
MLP.3	Low-cost raspberry Pi based imaging system for analysis of Fiber Specklegram Sensors <i>L. Brestovacki, M. Golubovic, J. Bajic, A. Joža and V. Rajs</i>	136

12. Other topics in photonics

OP.1	Revealing non-equilibrium dynamics by holography: The case of Briggs-Rauscher reaction <i>M. Pagnacco, M. Simovic Pavlovic, A. Radulovic, B. Bokic, D. Vasiljevic and B. Kolaric</i>	138
OP.2	Using Laser-Induced Fluorescence technique for interdisciplinary natural sciences school experiment <i>L. Zaharieva, M. Stoyanova, V. Dimova, V. Deneva, Ts. Genova, A. Markovski, L. Antonov and C. Andreeva</i>	139
OP.3	One dimensional SP lattices based on photonic molecules <i>D. Román-Cortés, G. Cáceres-Aravena, B. Real and R.A. Vicencio</i>	140
OP.4	Wave-packets induced by the radiation of an atom coupled to the continuum in photonic lattices <i>B. Real, D. Guzmán-Silva and R.A. Vicencio</i>	141
OP.5	Multi-orbital lattices based on photonic molecules <i>R.A. Vicencio</i>	142
OP.6	Pushing the boundaries of metasurface engineering: Hierarchical supercells and experimental validation <i>T. Contino and M. Tamagnone</i>	143
OP.7	Unraveling the phononic mysteries: BIC revealed in hBN resonators through phonon polaritons <i>H. Gupta, J. Edgar, F. De Angelis, A. Toma and M. Tamagnone</i>	144
OP.8	Refractive index change caused by biomolecular adsorption and structural transformations of adsorbed molecules in ultrasensitive plasmonic biosensors <i>I. Jokić, O. Jakšić, M. Frantlović, Z. Jakšić and K. Radulović</i>	145
OP.9	Characterization and testing of fiber optic curvature sensor as an optical mode converter for deformation measurement <i>S. Babić, J.S. Bajić, M. Vasiljević Toskić, A. Joža and V. Rajs</i>	146
OP.10	Application of polymer optical fiber sensor for urine parameter measurements: a preliminary study <i>P. Sokołowski, K. Cierpiak, P. Wityk, A. Drabik-Kruczkowska and M. Szczerska</i>	147
Index		148

Tutorial Lectures

Measurements beyond the Heisenberg uncertainty bound

E.S. Polzik

Niels Bohr Institute, University of Copenhagen

e-mail: polzik@nbi.ku.dk

This tutorial will revisit quantum limits for measurement and sensing. It is well known that a measurement of a position of an object imposes a random quantum back action perturbation on its momentum. This randomness translates with time into position uncertainty, thus leading to the uncertainty of the measurement of motion. The Heisenberg microscope is a textbook example illustrating this fundamental effect. As a consequence, the precision of sensing of position, velocity and force becomes limited in quantum mechanics. Remarkably, those limits can be surpassed by performing measurements in a special reference frame with an effective negative mass [1]. A spin polarized atomic ensemble can play the role of such reference oscillator. Evasion of quantum back action of the measurement and generation of an entangled state of a sensor and of the reference frame has been demonstrated in [2,3]. Sensing of fields and motion beyond standard quantum limits has become possible using this principle. Examples of applications include sensing of tiny magnetic fields [4] and detection of gravitational waves [5].

REFERENCES

- [1] E.S. Polzik, K.Hammerer, *Ann. Phys.* 527, A15 (2015).
- [2] C.B. Møller *et al.*, *Nature* 547, 191 (2017).
- [3] R.A. Thomas *et al.*, *Nat. Phys.* 17, 228 (2021).
- [4] W. Wasilewski *et al.*, *PRL* 104, 133601 (2010).
- [5] F.Ya. Khalili, E.S. Polzik, *PRL* 121, 031101 (2018).

The intelligent microscope at the nanoscale: multimodal microscopy from fluorescence to label-free

A. Diaspro^{1,2,3}

¹*DIFILAB, Dipartimento di Fisica, Università di Genova, Italia*

²*Nanoscopy, Istituto Italiano di Tecnologia, CHT, Erzell, Genova, Italia*

³*Istituto di Biofisica, CNR, Genova, Italia*

e-mail: diaspro@fisica.unige.it

Advanced optical microscopes, from super resolved methods to quantum optical microscopy, are analytical instruments able to produce images that are rich sources of quantitative information towards an unprecedented insight into the molecular mechanisms that govern and determine the fate of living cells. Their developments are positioned at the interface between biology and physics, and today in. More specifically, multimodal optical microscopy is a growing attitude boosted by artificial intelligence that makes intelligent the microscope. In the era of super-resolved fluorescence microscopy, fluorescence plays a significant role, including its photochemical parameters, from brightness to lifetime, and non-linear approaches, like those associated with multi-photon excitation able to exploit intrinsic fluorescence and SHG/THG. In this framework, polarization methods like Mueller matrix microscopy expand those contrast mechanisms available for imaging towards label-free. The intelligent microscope is AI-guided through a computational core based on independent component analysis (ICA) un-supervised machine learning towards supervised deep learning with the ambitious target to create a robust virtual environment "to see what we could not perceive before". An interesting case study is related to understanding the visualization of chromatin organization [1-3].

REFERENCES

- [1] A. Diaspro, *Confocal and Two-Photon Microscopy: Foundations, Applications and Advances*, Wiley (2021).
- [2] A. Diaspro, P. Bianchini, *Riv. Nuovo Cim.* 43, 385 (2020).
- [3] A. Diaspro, *Expedition into the Nanoworld*, Springer (2022).

Nanoplasmonics: Fundamentals & Applications

S.I. Bozhevolnyi

Centre for Nano Optics, University of Southern Denmark, Odense, Denmark

e-mail: seib@mci.sdu.dk

Surface plasmon polaritons, often shortened to surface plasmons (SPs), represent hybrid excitations involving free electron oscillations in metals and electromagnetic fields in dielectrics that propagate along and strongly bound to metal-dielectric interfaces. These surface electromagnetic waves enable deeply subwavelength confinement of guided modes along with strong enhancement of optical fields, two major features of SP modes that have been and continue being advantageously exploited in plasmon-empowered nanophotonics [1]. It would be impossible to overview, even very briefly, all fascinating topics found within plasmonics that include metasurfaces, graphene and other 2D materials, strong-coupling phenomena, topological plasmonics, quantum plasmonics, hot-electron phenomena, and many other interesting topics (Fig. 1).

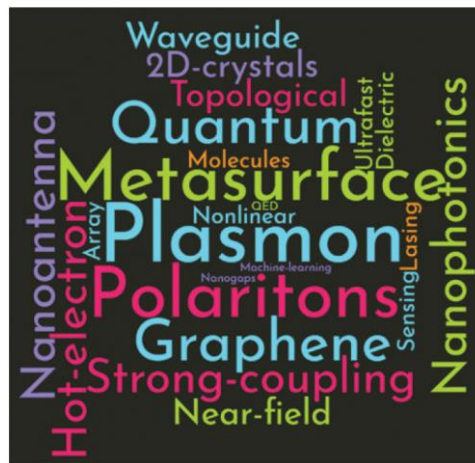


Figure 1. The breadth of research topics within plasmonics illustrated by a word cloud compiled from the book of abstract from the 9th International Conference on Surface Plasmon Photonics (SPP9) held in 2019 [2].

In this tutorial, the first part is devoted to introducing various SP modes supported by different configurations and their main physical characteristics that in turn determine the scope of their applications [1]. In the second part, special attention is given to the progress in ultra-compact photonic circuitry, including modulators and detectors, and plasmonic metasurfaces dynamically controlling propagation of light. In particular, the most efficient and ultrafast electro-optical modulators utilizing the commercially viable material, LiNbO_3 , in which the radiation transport is controlled using the same metal circuitry for both guiding SP modes and delivering electrical signals, are presented [3]. Plasmonic metasurfaces, which can be considered as the two-dimensional analogue of metal-based metamaterials, used for room-temperature generation of single-photon streams carrying orbital angular momenta [4] and dynamic control of optical birefringence [5] are also discussed. A personal view on the nearest perspectives for plasmon-empowered nanophotonics concludes this talk.

REFERENCES

- [1] D.K. Gramotnev, S.I. Bozhevolnyi, *Nat. Photon.* 4, 83 (2010).
- [2] N.A. Mortensen *et al.*, *Nanophotonics* 9, 245 (2020).
- [3] M. Thomaschewski *et al.*, *Nat. Commun.* 11, 748 (2020).
- [4] C. Wu *et al.*, *Sci. Adv.* 8, eabk3075 (2022).
- [5] C. Meng *et al.*, *Nat. Commun.* 13, 2071 (2022).

VUV Circularly-Polarized Light as a symmetry-breaking driving force: implications for the origin of life's homochirality

L. Nahon

Synchrotron SOLEIL, Saint Aubin, France

e-mail: laurent.nahon@synchrotron-soleil.fr

Circularly Polarized Light (CPL) is a chiral object, and as such its interaction with chiral matter may induced enantio-specific photo-processes which could be involved in an astrophysical scenario linked to the origin of life's homochirality, the fact that in the biosphere only L-amino acids and D-sugars are found. Assuming an extra-terrestrial formation of building blocks of life such as amino acids (aa), a possible abiotic explanation for the selection of L-amino acid could then be the exposure to CPL in space.

We have been using synchrotron radiation to simulate the VUV spectrum of light encountered in the Inter-Stellar Medium, and especially the DESIRS beamline [1] at SOLEIL providing an intense and tunable VUV CPL radiation allowing the study of photon-induced processes leading to noticeable enantiomeric excesses (e.e.) on aa.

After a broad introduction on chirality, homochirality and CPL, and on the instrumentation available on the DESIRS beamline, we will present several asymmetric photon-induced processes such as:

- (i) The photon wavelength-controlled enantio-selective photolysis of racemic solid-films on alanine leading to e.e. of up to 4 % [2].
- (ii) The asymmetric photochirogenesis on CPL-irradiated interstellar achiral ice analogs (H₂O, NH₃, CH₃OH) leading to the asymmetric production of several aa with e.e. up to 2.5 % for alanine [3].
- (iii) The one-photon photoelectron Circular Dichroism (PECD) on gas phase aa. PECD is new type of Circular Dichroism in the angular distribution of photoelectrons produced by CPL-ionization of pure enantiomers. This chiroptical effect is observed as a very intense (up to 35 %) forward/backward asymmetry (for a review see Ref. [4]). PECD happens to be a subtle probe of molecular structures such as conformers [5], chemical substitution and isomers [6]. After a large introduction to PECD and some of its properties, we will show how the asymmetric photoemission process may lead to e.e of up to 4 % in the case of alanine [7] and 12 % for proline [8,9] at the astrophysical-relevant Lyman- α wavelength.

REFERENCES

- [1] L. Nahon *et al.*, *J. Synchrotron Rad.* 19, 508 (2012).
- [2] C. Meinert *et al.*, *Angew. Chem. Int. Edit.* 53, 210 (2014).
- [3] P. Modica *et al.*, *Astrophys. J.* 788, 79 (2014).
- [4] L. Nahon *et al.*, *J. Electron Spectros. Relat. Phenomena* 204, 322 (2015).
- [5] J. Dupont *et al.*, *J. Phys. Chem. Lett.* 13, 2313 (2022).
- [6] L. Nahon *et al.*, *Phys. Chem. Chem. Phys.* 18, 12696 (2016).
- [7] M. Tia *et al.*, *J. Phys. Chem. Lett.* 4, 2698 (2013).
- [8] R. Hadidi *et al.*, *Adv. Phys. X* 3, 1477530 (2018).
- [9] R. Hadidi *et al.*, *Commun. Chem.* 4, 72 (2021).

Keynote Lectures

Recent trends in superfluid atomic gases: ferromagnetic, liquid and supersolid states

A. Recati

Pitaevskii Center on Bose-Einstein Condensation, INO-CNR and Trento University

e-mail: alessio.recati@unitn.it

After almost 30 years from the realisation of atomic Bose-Einstein condensation (BEC), the field of ultra-cold gases is still expanding and providing new insights on quantum states of matter. The reason is rooted in the strong synergy between theoreticians and experimentalists in the field and the development of new experimental tools to trap and manipulate different atomic species. This talk will focus on some new states recently realised using Bose atomic gases.

The first part of the talk will be devoted to introducing **coherently coupled BECs** and their peculiar ground and excited states due to the explicit breaking of one $U(1)$ symmetry, and, for large inter-species interaction, of a \mathbb{Z}_2 symmetry leading to ferromagnetic behaviour. I will show how the spin dynamics is well described by a dissipationless Landau-Lifshitz equation, and report on the first experimental evidence of false vacuum decay and bubble creation for the ferromagnetic first order phase transition.

The second part will focus on the so-called Lee-Huang-Yang (LHY) liquid or droplet phase, where beyond mean-field effects are fundamental for the system's description, leading in particular to new density functional theories. Such LHY states have been realised in both **Bose-Bose mixtures and dipolar Bose gases**. The latter platform has notably allowed experimentalists to realise the long sought **supersolid (SS)** phase, which is attracting much attention also outside the cold atomic field. The properties of the excitation spectrum and the vortices due to the spontaneous breaking of both $U(1)$ and translational invariance are presented. A brief comparison between the SS phase realized in dipolar gases, in optical cavities and in spin-orbit coupled gases will conclude the talk.

Nonlinear optics in atomically thin materials

G. Soavi

Institute of Solid State Physics, Friedrich Schiller University Jena, Germany
e-mail: giancarlo.soavi@uni-jena.de

Two-dimensional materials, such as graphene and transition metal dichalcogenides (TMDs), have attracted enormous interest in recent years as a viable platform for nonlinear optics [1]. On one hand, their atomically thin nature allows for frequency conversion without phase matching constraints, leading to ultra broadband parametric amplification and down-conversion of photons. On the other hand, 2D materials are easy to integrate on photonic platforms, and thus they are ideal candidates for in-fiber and on-chip nonlinear operations with platforms that would otherwise display negligible nonlinear effects. In this talk I will discuss some of our recent results and activities in this growing field of research, with a focus on the following aspects: (1) electrical and all-optical modulation of nonlinearities in graphene [2] and TMDs [3]; (2) nonlinear photonic integrated devices based on graphene for gas sensing [4] and logic operations [5] and (3) ultrafast nonlinear valleytronics in TMDs [6].

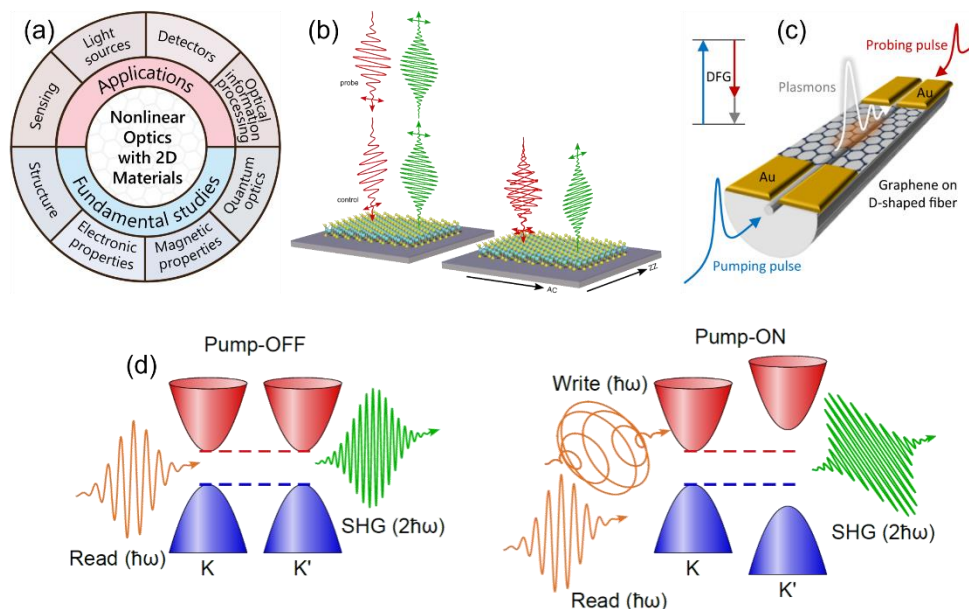


Figure 1. (a) Overview of applications and fundamental studies enabled by nonlinear optics in 2D materials, from Ref. [1]; (b) schematic of all-optical modulation of SHG in TMDs, from Ref. [3]; (c) graphene on a D-shaped fiber for logic operations enabled by difference frequency generation, from Ref. [5]; (d) operating principle of valley SHG for all-optical generation and detection of a valley imbalance in TMDs, from Ref. [6].

REFERENCES

- [1] O. Dogadov *et al.*, *Laser Photonics Rev.* 16, 2100726 (2022).
- [2] G. Soavi *et al.*, *Nat. Nanotechnol.* 13, 583 (2018).
- [3] S. Klimmer *et al.*, *Nat. Photon.* 15, 837 (2021).
- [4] N. An *et al.*, *Nano Lett.* 20, 6473 (2020).
- [5] Y. Li *et al.*, *Nat. Commun.* 13, 3138 (2022).
- [6] P. Herrmann *et al.*, *Small*, <https://doi.org/10.1002/sml.202301126>.

Three-dimensional imaging flow cytometry

A. Bassi

Politecnico di Milano, Milano, Italy

e-mail: andrea1.bassi@polimi.it

Imaging flow cytometry (IFC) is a powerful technique that combines the advantages of flow cytometry and optical microscopy. By capturing microscopy images of cells as they move along a liquid stream, IFC provides high-throughput collection of morphological and spatial information from thousands of cells. Recently optofluidic manufacturing technologies have shown their potential in the field of imaging flow cytometry enabling high throughput, and three-dimensional imaging.

The keynote speech will discuss the design and applications of miniaturized optofluidic devices for 3D imaging flow cytometry [1]. First, an optofluidic chip that incorporates light-sheet illumination and automatic sample delivery will be illustrated. This device upgrades a standard inverted microscope to automatic, three-dimensional, Light Sheet Fluorescence Microscope. Then a miniaturized device, based on integrated waveguides will be shown, as a new source for structured illumination microscopy. Finally, the combination of these two technologies will be described to demonstrate automatic imaging of cells at enhanced resolution.

Example applications will be discussed, together with the technological solutions for automatic sample alignment, including automatic imaging of tumour spheroids, *Drosophila* embryos, and high-resolution imaging of single cells [2].

REFERENCES

- [1] P. Paiè *et al.*, *Cyto. A* 93, 987 (2018).
- [2] F. Sala *et al.*, *Biomed. Opt. Express* 11, 4397 (2020).

From French fries to Foie Gras, turning around a synchrotron

F. Jamme¹, J. Pajovic², F. Wien¹ and M. Réfrégiers³

¹DISCO Beamline, Synchrotron SOLEIL, Gif-sur-Yvette, France

²University of Belgrade, Faculty of Physics, Studentski trg 12, Belgrade, Serbia

³CBM CNRS UPR430, rue Charles Sadron, Orléans, France

e-mail: matthieu.refregiers@cnrs.fr

Probably the best way to enter a synchrotron and to understand the usefulness of parasitic effects in accelerator physics is through its applications.

We will take a tour of the quasi-relativistic nature of accelerated particles - the ultimate for an electron in a synchrotron - and some original applications we've come across at the SOLEIL synchrotron in life sciences and cultural heritage.

Of particular interest, deep ultraviolet (DUV: from 180 to 380 nm), have enough energy to interact with a very broad range of biomolecules [1], pigments [2], semiconductors, etc., and at the same time, not so energetic that they can continue to travel through air and water. It is therefore a perfect energy range for studying those molecules in their natural environment. Controlling the delivered power, it is even possible to work with living microorganisms [3].

Most applications will be based on natural luminescence observed in a diversity of samples, but time resolved circular dichroism using the natural polarization of the upper and lower parts of the synchrotron beam extracted from a bending magnet will also be illustrated [4].

We will discuss the diversity of applications in structural biology, food science, cultural heritage, pharmacological research and medical diagnostics developed in DUV at SOLEIL, a large-scale facility open to a broad range of research communities.

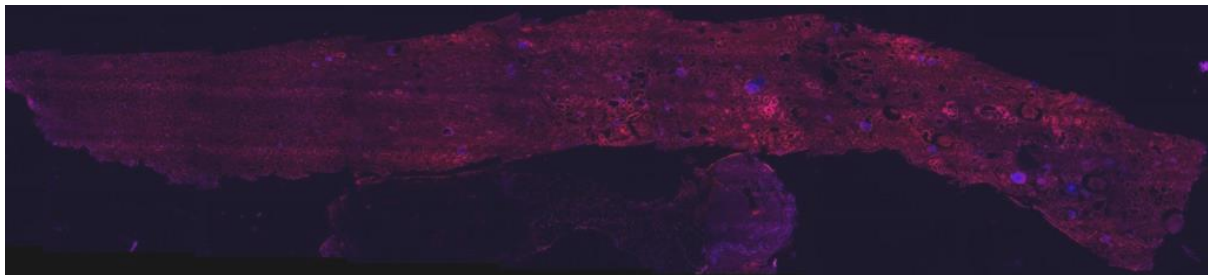


Figure 1. Direct observation of calcium oxalates precipitation (blue) in a kidney biopsy (tissue autofluorescence shown in red).

REFERENCES

- [1] <https://doi.org/10.1111/boc.201200075>.
- [2] <https://doi.org/10.1017/S1431927622000873>.
- [3] <https://doi.org/10.1038/s42003-020-0929-x>.
- [4] <https://doi.org/10.1063/1.5120346>.

Einstein-Podolsky-Rosen experiment with two Bose-Einstein condensates

P. Colciaghi, Y. Li, P. Treutlein and T. Zibold

University of Basel, Department of Physics, Klingelbergstrasse 82, 4056 Basel, Switzerland

e-mail: philipp.treutlein@unibas.ch

In 1935, Einstein, Podolsky, and Rosen (EPR) conceived a gedanken experiment which became a cornerstone of quantum technology and still challenges our understanding of reality and locality today. While the experiment has been realized with small quantum systems, a demonstration of the EPR paradox with massive many-particle systems remains an important challenge, as such systems are particularly closely tied to the concept of local realism in our everyday experience and may serve as probes for new physics at the quantum-to-classical transition.

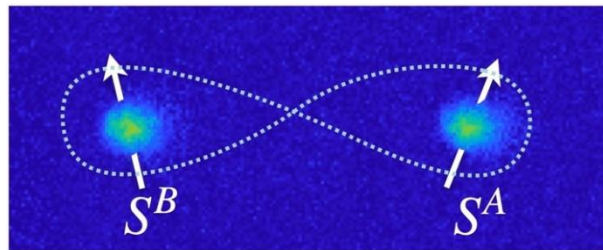


Figure 1. Absorption image of two Bose-Einstein condensates whose collective spins S^A and S^B are entangled.

In this work we report an EPR experiment with two spatially separated Bose-Einstein condensates, each containing about 700 rubidium atoms [1]. Entanglement between the condensates results in strong correlations of their collective spins, allowing us to demonstrate the EPR paradox between them. Our results represent the first observation of the EPR paradox with spatially separated, massive many-particle systems. They show that the conflict between quantum mechanics and local realism does not disappear as the system size increases to more than a thousand massive particles. Furthermore, EPR entanglement in conjunction with individual manipulation of the two condensates on the quantum level, as we demonstrate here, constitutes an important resource for quantum metrology and information processing with many-particle systems.

REFERENCES

[1] P. Colciaghi *et al.*, Phys. Rev. X 13, 021031 (2023).

Development of table-top ultrafast soft-X spectroscopy for material science

C. Vozzi

Istituto di Fotonica e Nanotecnologie, Consiglio Nazionale delle Ricerche, Milano, Italy
e-mail: caterina.vozzi@ifn.cnr.it

Ultrafast XUV and X-ray spectroscopy play a pivotal role in material science and biochemistry by enabling real-time observation of dynamic processes at the atomic and molecular levels, leading to profound insights into structure-function relationships and facilitating the design of innovative materials.

High-order harmonics (HHG) are generated from the interaction of intense femtosecond laser pulses with noble gases. Recently, HHG led to the realization of table-top sources of coherent XUV and Soft-X Ray radiation. With these sources, ultrafast spectroscopy can be performed with extreme temporal resolutions, down to the attosecond regime (1 as = 10^{-18} s), and with the site and chemical selectivity. These peculiar features grant access to purely electronic dynamics in molecules and solids, initiated by ultrafast laser pulses, and to fundamental processes of light-matter interaction.

One of the most promising all-optical techniques to perform these experiments is transient absorption in the XUV. However, the full exploitation of ultrafast spectroscopy in this spectral range is somehow hindered, even today, by the technological complexity of the required setups and the low generation efficiency of the HHG sources, particularly when moving toward higher photon energies.

Here, we report the efficient XUV generation inside a microfluidic device fabricated by femtosecond laser irradiation followed by chemical etching [1]. This microfluidic approach allows controlling and manipulating the harmonic generation conditions in gas on the micro-meter scale with unprecedented flexibility, enabling a high photon-flux and phasematching on broadband harmonics up to 200 eV [2]. We also report on the design and commissioning of a new beamline for transient absorption/reflectivity measurements in molecules and solids recently developed at CNR-IFN and equipped with a flexible XUV spectrometer for high-resolution and high dynamic range measurement, with a polarimeter for the characterization of the HHG polarization.

REFERENCES

- [1] A.G. Ciriolo *et al.*, *J. Phys. Photonics* 2, 024005 (2020).
- [2] A.G. Ciriolo *et al.*, *APL Photonics* 7, 110801 (2022).

Ultrafast chirality: the road to efficient chiral measurements

O. Smirnova^{1,2,3}

¹Max Born Institute, Max Born Str 2A, 12 489 Berlin Germany

²Technische Universität Berlin, Straße des 17. Juni 135

³Technion-Israel Institute of Technology, Haifa, Israel

e-mail: olga.smirnova@mbi-berlin.de

I will describe several new, extremely efficient approaches (Fig. 1) to chiral discrimination and enantio-sensitive molecular manipulation, which take advantage of ultrafast electronic response [1]. One of them is combines the new concept of synthetic chiral light [2], with vortex beams to create chiral topological light [3] and imprint topological properties on high harmonic emission, generated by such light in chiral molecules. The other is based on the new concept of geometric magnetism in photoionization of chiral molecules and leads to a new class of enantiosensitive observables in photoionization [4]. Crucially, the emergence of these new observables is associated with ultrafast excitation of chiral electronic or vibronic currents prior to ionization and can be viewed as their unique signature.

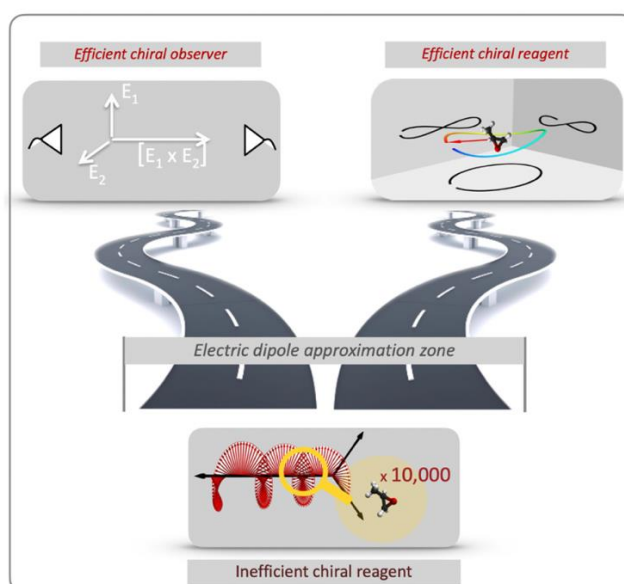


Figure 1. Two roads to efficient enantio-discrimination: chiral reagent (approaches that substitute the inefficient (non-local) light helix in space by an efficient (local) light helix in time) and chiral observer (approaches that do not rely on the chiral properties of light).

REFERENCES

- [1] D. Ayuso *et al.*, *Phys. Chem. Chem. Phys.* 24, 26962 (2022).
- [2] D. Ayuso *et al.*, *Nat. Photonics* 13, 866 (2019).
- [3] N. Mayer *et al.*, <https://doi.org/10.48550/arXiv.2303.10932>.
- [4] A.F. Ordonez *et al.*, <https://doi.org/10.21203/rs.3.rs-2679380/v1>.

Invited Lectures

Optical control of topological and correlated electronic states

M. Hafezi

Minta Martin Professor of Physics and ECE
Joint Quantum Institute, University of Maryland
e-mail: hafezi@umd.edu

Given tremendous progress in controlling individual photons and other excitations such as spin, excitonic, phononic in solid-state systems, it is intriguing to explore whether these quantum optical control techniques could pave a radically new way to prepare, detect and manipulate non-local and correlated electronic states [1]. After discussing several broad theoretical schemes, as the first experimental example, we report on optical and electrical tunable Bose-Fermi mixtures in hetero-bilayer systems and the observation of an excitonic Mott insulator [2]. As the second experimental example, we report on the optical manipulation of quantum Hall states in graphene using twisted light [3]. Specifically, we show that, by going beyond the dipole-approximation in light-matter interaction, one can optically manipulate the electronic wave function, which is manifested in photocurrent measurements.

REFERENCES

- [1] J. Bloch *et al.*, Nature 606, 41 (2022).
- [2] B. Gao *et al.*, arXiv:2304.09731 [cond-mat.mes-hall] (2023).
- [3] D. Session *et al.* (in preparation)

Scanning quantum microscopy

F. Setzpfandt^{1,2}

¹Institute of Applied Physics, Abbe Center of Photonics, Friedrich Schiller University Jena, Jena, Germany

²Fraunhofer Institute of Applied Optics and Precision Engineering IOF, Jena, Germany

e-mail: f.setzpfandt@uni-jena.de

Quantum correlations of photon pairs in time and space have been widely employed for quantum-enhanced measurements and specially in the field of quantum imaging [1]. Imaging approaches based on such correlations fundamentally enable to image below the shot-noise limit, thus allowing to extract more information from a sample than classically possible with the same number of photons. Wide-field imaging schemes using correlations, however, are often limited by the properties of the needed sources for correlated photon pairs. In particular, for reaching a high spatial resolution, very short photon-pair sources would be necessary [2], which in turn limits the generation rate and thus increases the measurement time.

One approach that overcomes these limitations is based on scanning imaging. In my talk, I will discuss our implementation of a scanning microscope exploiting the correlations of photon pairs to enable infrared imaging [3]. This approach greatly reduces the demands on the photon-pair source while still allowing to access the advantages enabled by using correlations. I will show that the spatial resolution of our system is now only limited by the used optics. Furthermore, I will discuss first experiments towards hyperspectral imaging of biological specimen.

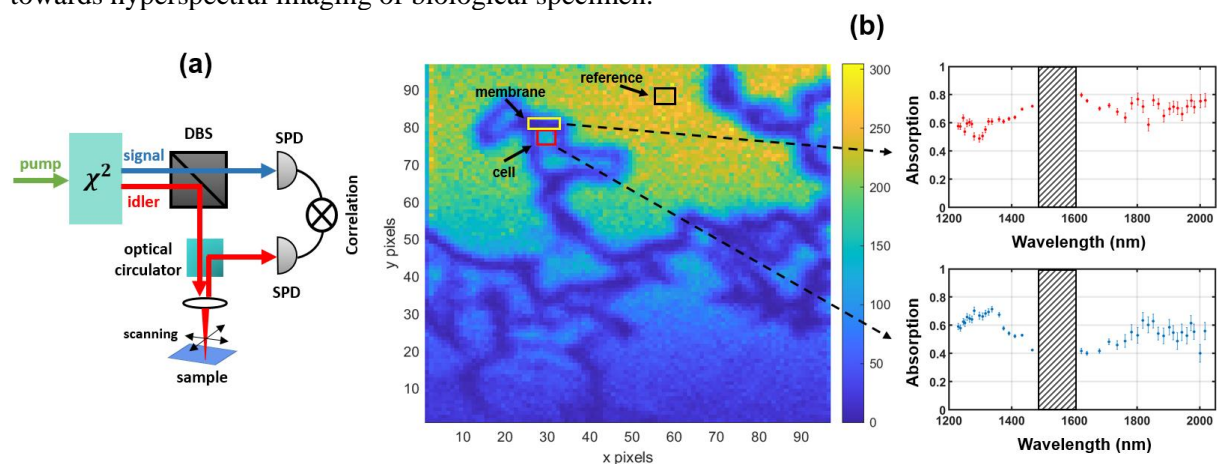


Figure 1. (a) Scheme of the implementation of the scanning quantum microscope and (b) measurement results for HEK 293 T cells, where the image is taken at 1465 nm wavelength, while the two insets show spectra obtained with the microscope at the membrane and core regions of one cell in the sample.

REFERENCES

- [1] I. Ruo-Berchera, I.P. Degiovanni, *Metrologia* 56, 024001 (2019).
- [2] A. Vega *et al.*, *Phys. Rev. Research* 4, 033252 (2022).
- [3] V.F. Gili *et al.*, *Appl. Phys. Lett.* 121, 104002 (2022).

A single ion meets a single Rydberg atom

R. Löw

University of Stuttgart, Stuttgart, Germany

e-mail: r.loew@physik.uni-stuttgart.de

Highly excited Rydberg atoms can form quite unusual bonds, which lead to long-range Rydberg molecules with exotic properties. Here we study a molecular ion that is formed due to the interaction between an ionic charge and a flipping-induced dipole of a highly excited Rydberg atom [1]. This molecule feature an unusual large bond length, therefore dynamical processes are slowed down drastically. This leads to a vibrational dynamics in the microsecond regime [2] that can be observed in real space by using a high-resolution ion microscope [3]. By applying a weak external electric field of a few mV/cm, it is possible to control the orientation of the ionic ultralong-range Rydberg molecules directly during the creation process. When the field is quenched off in a subsequent step, the vibrational dynamics can be initialized and observed under the ion microscope in real space. In the end we will look at the unbound collision dynamics of a Rydberg atom and an Ion.

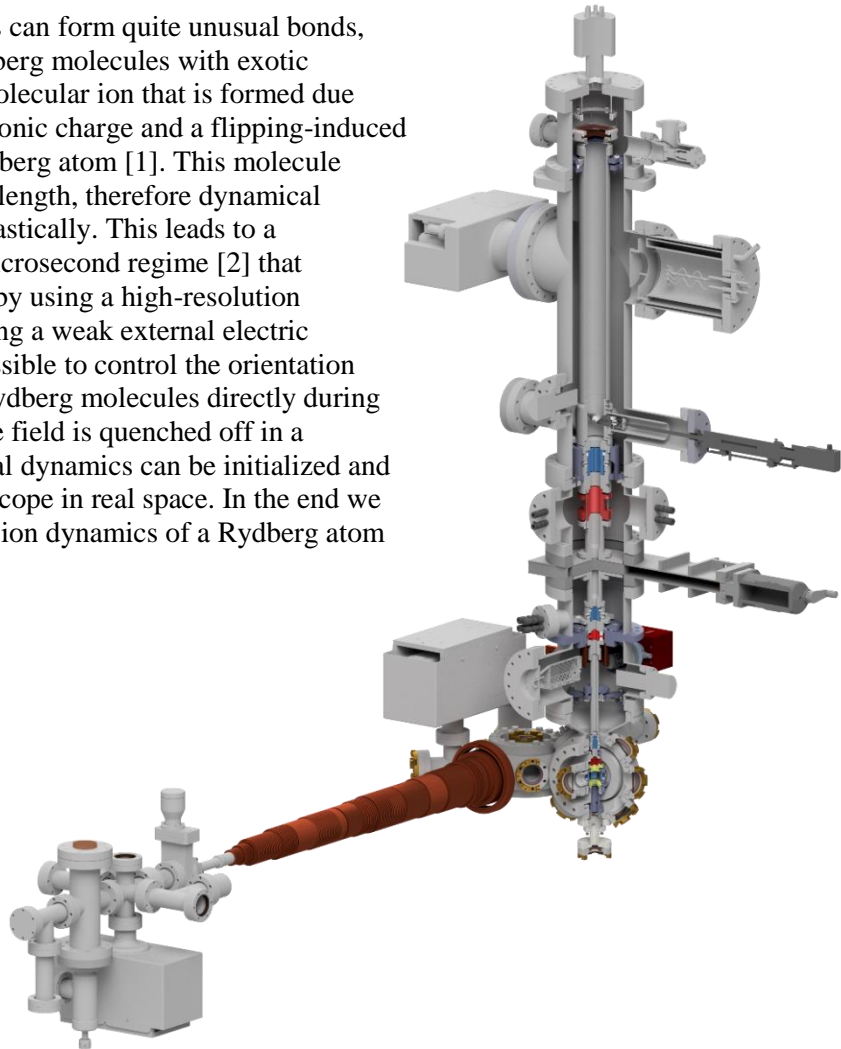


Figure 1. Schematics of a new type of ion microscope for probing ultracold gases beyond the typical optical resolution. The setup consists of a traditional cooling chamber (Zeeman-slower, MOT, evaporation) and a science chamber connected to a spatially resolving detector including three magnifying ion lenses.

REFERENCES

- [1] N. Zuber *et al.*, Nature 605, 453 (2022).
- [2] Y.-Q. Zou *et al.*, PRL 130, 023002 (2023).
- [3] C. Veit *et al.*, PRX 11, 011036 (2021).

Photonic Landau levels

M. Rechtsman

Department of Physics, The Pennsylvania State University, University Park, PA, USA

e-mail: mcr22@psu.edu

Breaking Lorentz reciprocity (or time-reversal symmetry) strongly is hard for photons because they don't carry charge and therefore don't respond directly to an external magnetic field. Here, I'll present our experimental results on how straining a photonic crystal with a Dirac point generates an artificial magnetic field, and we directly observe Landau levels as a result. Adding another kind of strain, corresponding to a pseudoelectric field, can remove the dispersion of the Landau levels, making them flat bands.

Shape-changing microstructures for multifunctional microfluidics

S. Nocentini^{1,2}, S. Donato², D. Martella^{1,2}, C. Credi^{2,3}, C. Parmeggiani^{2,4} and D.S. Wiersma^{1,2,5}

¹Istituto Nazionale di Ricerca Metrologica INRiM, Turin, Italy

²European Laboratory for Non-linear Spectroscopy, Sesto Fiorentino, Italy

³National Institute of Optics, National Research Council, Sesto Fiorentino, Italy

⁴Department of Chemistry Ugo Schiff, University of Florence, Sesto Fiorentino, Italy

⁵Department of Physics and Astronomy, University of Florence, Sesto Fiorentino, Italy.

e-mail: nocentini@lens.unifi.it

The miniaturization of functional components and actuators within active microfluidic circuits constitutes a fascinating technological challenge. The role of pumps, valves and mechanical filter is of paramount importance to dynamically operate with microfluidic devices, and their implementation can be tackled by the 3D micro patterning of smart materials with a shape changing behavior. To avoid the complex integration of batteries or electronic circuits, the activation of such active micro-components can be obtained by optically driven micro machines and actuators that exploit optical stimuli as fuel, converting light energy into mechanical work. Among photo-responsive materials, shape-changing polymers such as liquid crystalline networks (LCN) offer reversible deformations in the millisecond time range [1,2]. In this contribution, we will present the patterning of LCN with a laser-based printing technique based on two-photon polymerization that allows to micropattern functional polymers in 3D shapes even in microfluidic channels (Figure 1). By tailoring the material choice and the printing parameters, structures made by the same material capable of different deformations can be printed on the same chip in a single fabrication process. The design of the structure reversible deformation enlarges the reshaping and functional properties of integrated soft microstructures also determining the dynamics of the structure deformation both in dry and liquid environments.

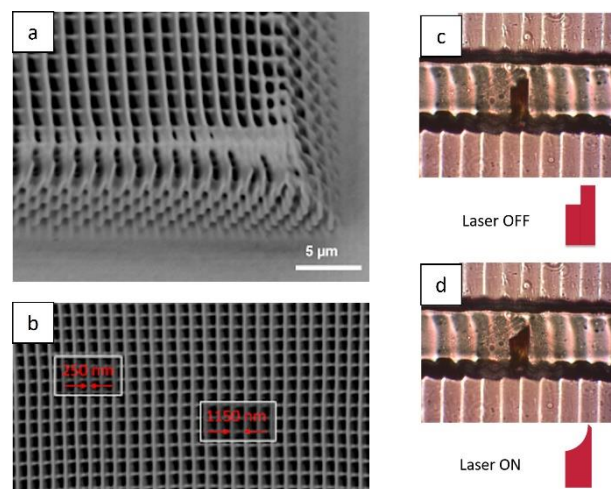


Figure 1. Soft elastic microstructures printed by two photon direct laser writing: on the left, a LCN woodpile (a-b); on the right, a LCN valve in a micro-fluidic channel (c) under light illumination (d).

REFERENCES

- [1] I. De Bellis *et al.*, *Adv. Funct. Mater.* 2213162 (2023).
 [2] S. Nocentini *et al.*, *Adv. Opt. Mater.* 6, 1800167 (2018).

Deeper and faster: new tools for nonlinear bioimaging

L. Bonacina

Department of Applied Physics, University of Geneva, Switzerland

e-mail: luigi.bonacina@unige.ch

While the majority of studies on the nonlinear properties of micro- and nano-structures focus on the production of distinct signals, like second and third harmonic, we recently showed that the new generation of rugged commercial dual output sources designed for microscopy (OPO, OPA) can easily expand the accessible parameter space and enable the simultaneous excitation and detection of multiple nonlinear emissions from individual objects, including several harmonics and parametric signals derived from different frequency mixing processes [1]. This rich response, which in our case features 10 distinct emissions and spans from the deep ultraviolet to the short-wave infrared, is demonstrated using various metal-oxide materials (harmonic nanoparticles, HNPs) while being characterized and numerically simulated both in the temporal and spectral domains [2]. HNPs offer excitation flexibility and quasi-instantaneous optical response and their use as imaging probes can be leveraged to increase speed in scanning microscopy, achieving dwell times as short as 1 nanosecond, faster than typical fluorophore lifetimes.

Our strategy combining nonlinear optical excitation and HNPs labelling is illustrated in the context of the preclinical assessment of cell therapies. Specifically, we apply it to a recently proposed protocol based on the use of mesenchymal stem cells to regenerate dystrophic muscles affected by Duchenne myopathy. Our imaging experiments reveal HNP detection in tissues at depths greater than 1 mm [3], as well as high-sensitivity detection of labelled stem cells in whole blood and characterization of their morphology and aggregation-state at framerates exceeding 15'000 images per second [4]. At these imaging rates, blood volumes consistent with preclinical animal research could be monitored in a matter of minutes without the need of sample prefiltration.

REFERENCES

- [1] L. Bonacina *et al.*, *J. Appl. Phys.* 127, 230901 (2020).
- [2] G. Campargue *et al.*, *Nano Lett.* 20, 8725 (2020).
- [3] L. Dubreil *et al.*, *ACS Nano* 11, 6672 (2017).
- [4] S. Karpf *et al.*, submitted

Polymeric SERS-fluidic platforms for the non-destructive optical analysis of liquid samples

C. Credi^{1,2}

¹European Laboratory for Non-Linear Spectroscopy (LENS), Via Nello Carrara 1, 50019 Sesto Fiorentino, Italy

²National Institute of Optics, National Research Council (INO-CNR), Via Nello Carrara 1, 50019 Sesto Fiorentino, Italy

e-mail: catarina.credi@ino.cnr.it

The recent technological advances in micro- and nano-fabrication processes paved the way to the possibility to downsize optical detection techniques within microfluidic devices thus opening interesting perspectives towards the development of low-cost and portable (bio)sensors. These could be widely exploited for the optical analysis of liquid samples with potential applications in the clinic-diagnostic field, to precociously reveal pathological biomarkers in the biofluids as well as in the environmental and agrifood sectors to reveal contaminants [1]. Among all techniques, surface enhanced Raman spectroscopy (SERS) exploiting metal plasmonic gold nanoparticles (NPs) constitutes the one of the most promising analytical methods as alternative to current traditional bioassays [2]. Indeed, NPs with unique physical and chemical properties are exploited as high performing optical transducers that selectively capture and amplify (up to 10^6) the Raman signal scattered from analytes located near NPs with respect to the overall background matrices [3]. Despite all these advantages, SERS measurements guaranteeing picomolar sensitivity still rely on the exploitation of bulky confocal Raman set-up that cannot be used outside laboratories and leading to uncontrolled evaporation phenomena when tight focusing the excitation laser thus possibly inducing conformational changes of analyzed molecules [4]. To address these issues and to develop accurate portable systems, recent approaches are focused on synergically merge photonics and fluidics into miniaturized lab-on-a-chip (LoC) devices for light and fluids manipulation at the micrometric scale. Indeed, LoC technology enables easier handling of very small liquid volumes avoiding cross-contamination, efficient NPs-sample mixing [5] and, more interestingly, LoCs channels can be exploited to host optical fibers and waveguides for straight light delivering and collection at the fluids level [6]. Here, novel SERS-fluidic devices for the straightforward analysis of liquids have been developed by implementing time- and cost-saving manufacturing processes of polymers. The exploitation of low-cost traditional manufacturing processes and laser-based 3D printing guarantees high design versatility and smart interfacing with compact fiber-based Raman set-ups. To this end, the devices are constituted by network of channels for fluid handling and for optical fiber housing with embedded microfeatures used to control their relative positioning and to guarantee the highest signal delivering and collection. Within the detection chambers, SERS functionality is achieved by the selective interaction of the target analytes with gold NPs of varied size and shape attached to the bottom of the channel or pre-mixed with the samples. The resulting SERS-fluidic devices represent highly versatile sensing platforms providing high repeatability, high sensitivity and speed of analysis, possibly revolutionizing liquid analysis by making it costless, on-chip, handy, and easy to use.

REFERENCES

- [1] R. Gao *et al.*, ACS Sens. 4, 938 (2019).
- [2] L. Cheng *et al.*, ACS Appl. Mater. Interfaces 10, 34869 (2018).
- [3] B. Sharma *et al.*, Mater. Today 15, 16 (2012).
- [4] L. Yap *et al.*, Nanoscale 9, 7822 (2017).
- [5] D. Psaltis *et al.*, Nature 442, 381 (2006).
- [6] H. Liu *et al.*, Opt. Commun. 352, 148 (2015).

Rapid and sensitive cancer detection with fluorescence lifetime imaging microscopy

W. Su, M. Ji, J. Ma, R. Guo and L. Mi

Department of Optical Science and Engineering, Fudan University, Shanghai, China

e-mail: lanmi@fudan.edu.cn

Fluorescence Lifetime Imaging Microscopy (FLIM) has great potential for cancer detection. In this talk, I will introduce the FLIM method and related techniques for noninvasive cancer screening and diagnosis. First, a pH-sensitive AgInS₂(AIS)/ZnS quantum dots (QDs) with long fluorescence lifetimes are introduced as an intracellular pH sensor. The FLIM technique is used in combination with AIS/ZnS QDs to distinguish cancer cells from normal cells, with promising results for noninvasive cervical cancer screening [1]. I will also talk about an endogenous coenzyme (reduced nicotinamide adenine dinucleotide (phosphate), NAD(P)H) as an indicator of cellular energy metabolism. FLIM is used to detect NAD(P)H in unstained exfoliated cervical cells to evaluate cellular metabolic status. FLIM images are analyzed by unsupervised machine learning to build a prediction model for cervical cancer risk. The FLIM method combined with unsupervised machine learning (FLIM-ML) demonstrates significantly higher sensitivity and specificity than cytology approaches, making it a promising tool for cervical cancer screening and follow-up care [2].

This talk highlights the potential of FLIM and related techniques for noninvasive cancer screening and diagnosis, providing a convenient and accurate tool for early cancer detection and follow-up cancer care.

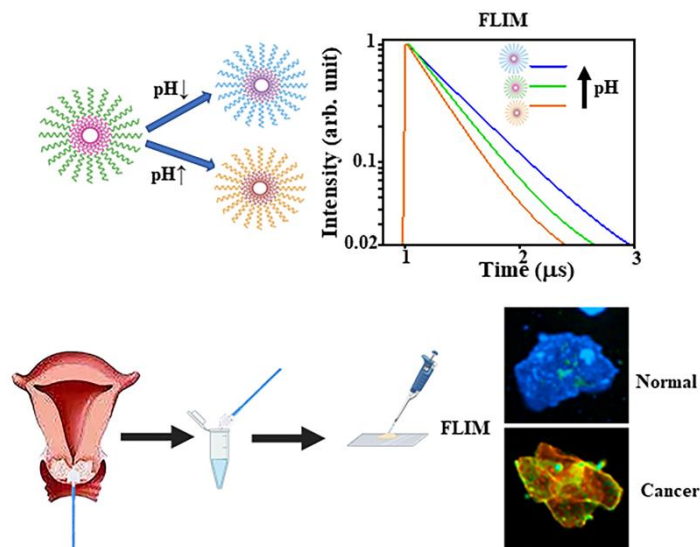


Figure 1. An intracellular pH sensor AIS/ZnS QDs combined with FLIM are used for noninvasive cervical cancer screening, and the method may be applied to other pH-related diseases in the future.

REFERENCES

- [1] W. Su *et al.*, *Nano Res.* 15, 5193 (2022).
 [2] M. Ji *et al.*, *Int. J. Mol. Sci.* 23, 11476 (2022).

Photonic integrated circuits based on linearly coupled waveguide arrays

J. Petrovic

Vinca Institute of Nuclear Sciences - National Institute of the Republic of Serbia, University of Belgrade, Serbia
e-mail: jovanap@vin.bg.ac.rs

Photonic integrated circuits (PICs) are a promising route towards the next generation of classical and quantum information technologies. The main challenges before their widespread implementation are achievements of the competitive footprint, speed and number of simultaneous operations. This translates into requirements for miniaturization, broad bandwidth and extensive spatial and wavelength multiplexing. Current PIC designs commonly rely on directional couplers for operations and waveguides for information transfer. However, their miniaturization potential is limited by the trade-off between losses and bend radii in the former case and the crosstalk between densely packed waveguides in the latter case. On the other hand, operationally successful nanophotonic inverse designs are achieved only with substantial time and energy resources per device [1,2].

Here, we present and discuss an innovative solution for design of PICs which utilizes the linear crosstalk between waveguides [3]. We demonstrate construction of interconnects, couplers, interferometers, filters and dichroic splitters [4-6]. As the only fundamental assumption is the linear coupling between waveguides, these designs are applicable to all photonic fabrication platforms. We show components in glass, silicon nitride and silicon-on-insulator, and offer strategies for optimization of their footprint and bandwidth. The concept has been experimentally validated by fabrication of equal power splitters in glass. The optimization capability was proven by the achieved negligible insertion loss, large bandwidth and footprint scalability [7].

The proposed PICs are highly cost effective. Our simple semi-analytical design algorithm ensures efficient design, 20-100 times faster than the competing nanodesigns [1,2], and production realizable by any waveguide fabrication technique.

Finally, we show that the quantum walk through the proposed linearly coupled waveguide arrays offers numerous possibilities for exploitation of qudits and construction of quantum logic gates.

REFERENCES

- [1] H. Xie *et al.*, IEEE Photon. J. 10, 1 (2018).
- [2] A.Y. Piggott *et al.*, Sci. Rep. 7, 1786 (2017).
- [3] J. Petrovic, J. Veerman, Ann. Phys. 392, 128 (2018).
- [4] J. Petrovic *et al.*, J. Opt. Las. Technol. 163, 109381 (2023).
- [5] J. Petrovic, Opt. Lett. 40, 139 (2015).
- [6] J. Petrovic *et al.*, Opt. Quantum Electron. 54, 687 (2022).
- [8] P. Vildoso *et al.*, Opt. Express 31, 12704 (2023).

Excursion of a biophysicist to the quantum world

A. Dér

Institute of Biophysics, Biological Research Centre, H-6726 Szeged, Temesvári krt. 62, Hungary
 e-mail: der.andras@brc.hu

Novel imaging techniques utilizing nondegenerate, correlated photon pairs sparked intense interest during the last couple of years among scientists of the quantum optics community and beyond. It is a key property of such “ghost imaging” or “quantum interference” methods that they use those photons of the correlated pairs for imaging that never interacted with the sample, allowing detection in a spectral range different from that of the illumination of the object. Extensive applications of these techniques in spectroscopy and microscopy are envisioned, however, their limited spatial resolution to date has not yet supported real-life microscopic investigations of tiny biological objects. In the lecture, a modification of the method based on quantum interference [1] will be outlined (“SIMUP”), by using a seeding laser and confocal scanning, that allows the improvement of the resolution of imaging with undetected photons by more than an order of magnitude [2]. Examples of its application in the microscopy of biological samples will also be presented.

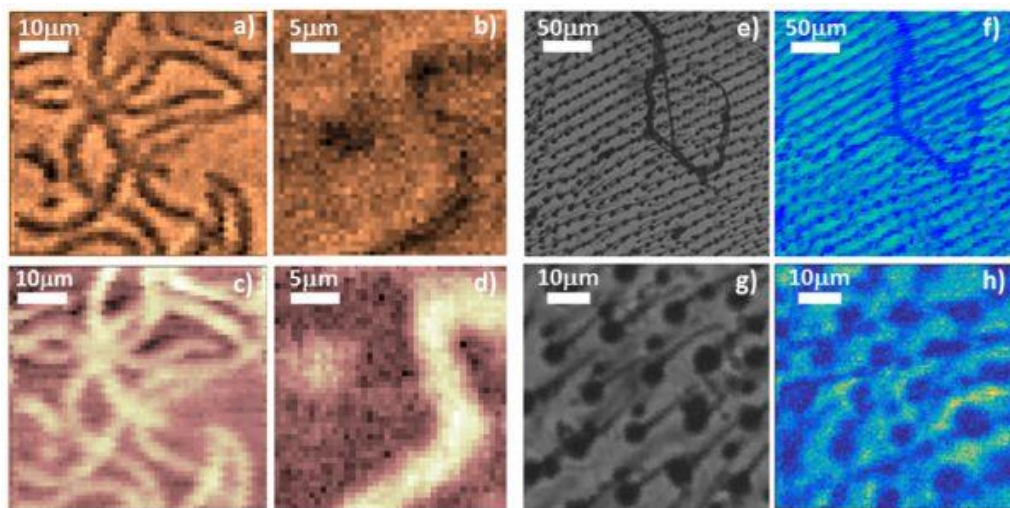


Figure 1. Amplitude (a and b) and phase (c and d) images of *Spirulina* filaments at different scan areas and step sizes (50 μm by 50 μm and 1 μm in a) and c), while 25 μm by 25 μm and 0.5 μm in b) and d), respectively). Normal microscopic (e and g) and SIMUP amplitude images (f and h) of a wasp wing at different scan areas and step sizes for the latter (250 μm by 250 μm and 5 μm , and 50 μm by 50 μm and 0.5 μm , respectively).

REFERENCES

- [1] G.B. Lemos *et al.*, *Nature* 512, 409 (2014).
 [2] A. Búzás *et al.*, *IEEE Access* 8, 107539 (2020).

Light-enhanced transdermal drug delivery

R. Boukherroub

Université de Lille, CNRS, Centrale Lille, Univ. Polytechnique Hauts-de-France, IEMN, UMR CNRS 8520, F-59000 Lille, France

e-mail: rabah.boukherroub@univ-lille.fr

Advances in materials science and bio-nanotechnology have allowed the refinements of current drug delivery systems, expected to facilitate the development of personalized medicine. While dermatological topical pharmaceutical formulations, such as foams, creams, lotions, gels, etc., have been developed and used for decades, these systems target mainly skin-based diseases. To treat systemic medical conditions as well as localized problems such as joint or muscle diseases, transdermal delivery systems (TDDSs), which use the skin as the main route of drug delivery, are very appealing [1,2].

Over the years, these systems have shown to offer important advantages over oral as well as intravenous drug delivery routes. Besides being non-invasive and painless, TDDSs are able to deliver drugs with a short-half-life time more easily and are well-adapted to eliminate frequent administrations to maintain constant drug delivery [3,4].

However, the transdermal market still remains limited to a narrow range of drugs. While small and lipophilic drugs have been successfully delivered using TDDSs, this approach fails to deliver therapeutic macromolecules due to size-limited transport across the *stratum corneum*, the outermost layer of the *epidermis*. The low permeability of the *stratum corneum* to water soluble drugs as well as macromolecules poses important challenges to transdermal administration [5,6].

To widen the scope of drugs for transdermal delivery, new procedures to enhance skin permeation to hydrophilic drugs and macromolecules are under development. Next to iontophoresis and microneedle-based concepts, thermal-based approaches have shown great promise to enhance transdermal drug delivery of different therapeutics [6].

In this presentation, I will discuss our original contribution on the on-demand delivery of drugs *via* light activation for the treatment of chronic diseases, such as diabetics, hypertension, but also for wound treatment.

REFERENCES

- [1] A. Voronova *et al.*, ACS Appl. Bio Mater. 5, 771 (2022).
- [2] B. Demir *et al.*, Nanoscale Horiz. 7, 174 (2022).
- [3] S. Szunerits *et al.*, Chem. Soc. Rev. 50, 2102 (2021).
- [4] Q. Pagneux *et al.*, Nanoscale Horiz. 5, 663 (2020).
- [5] S. Szunerits, R. Boukherroub, Front. Bioeng. Biotechnol. 6, 151 (2018).
- [6] F. Teodorescu *et al.*, J. Control. Release 246, 164 (2017).

Luminescent thermometry using lanthanide and transition metal-activated phosphors

Ž. Antić

Center of Excellence for Photoconversion, Vinča Institute of Nuclear Sciences – National Institute of the Republic of Serbia, University of Belgrade
e-mail: zeljkaa@gmail.com

Temperature is both a thermodynamic property and a fundamental unit of measurement. It plays an important role in our daily lives, from determining the clothing we wear to the efficiency of gas turbines and is by far the most measured physical quantity. As our civilization advances, scientific and technological development, environmental and health problems, and market demands generate a continual need for the development of novel measurement concepts and instruments, especially for temperature. Today's standard thermometers are not able to provide a spatial resolution of measurements better than 1 μm , nor inter or intra-cellular, tissue, or temperatures in harsh environments, on fast-moving objects, and in tough-to-access places.

To address the needs, temperature measurements that harness changes in the optical properties of materials are considered promising, among which temperature measurements using luminescent materials have gained significant attention in recent years. This interest is motivated by the near-infinite range of potential sensor materials, the temperature sensitivity of luminescence, and the ease with which luminescence can be detected in comparison to other optical signals. Luminescence thermometry utilizes temperature changes of luminescence properties of specific material to achieve thermal sensing by temporal (rise and decay time) or spectral (intensity, band shape, spectral peak position, bandwidth, and polarization) alterations of the emission. The method offers semi-invasive, fast, precise, and reliable two-dimensional thermal imaging of macroscopic and microscopic systems at temperatures ranging from cryogenic to approximately 1700°C. To date, different types of materials have been used for luminescence thermometry probes: lanthanide and transition metal ion-activated phosphors, semiconductor quantum dots, organic dyes, metal-organic complexes and frameworks, polymers, carbon-based materials, luminescent proteins, etc. Depending on the application, each class of materials presents unique advantages over others. Herein, the focus will be on luminescent thermometry using lanthanide and transition metal-activated phosphors.

Black box certification of resources for photonic quantum technologies

S. Neves, L. dos Santos Martins, V. Yacoub, P. Lefevbre, I. Šupić, D. Markham and E. Diamanti
Sorbonne Université, CNRS, LIP6, 4 Place Jussieu, Paris F-75005, France
e-mail: ivan.supic@lip6.fr

Quantum transmission links are central elements in essentially all implementations of quantum information protocols. Emerging progress in quantum technologies involving such links needs to be accompanied by appropriate certification tools. In adversarial scenarios, a certification method can be vulnerable to attacks if too much trust is placed on the underlying system. Here, we propose a protocol in a device independent framework, which allows for the certification of practical quantum transmission links in scenarios where minimal assumptions are made about the functioning of the certification setup. In particular, we take unavoidable transmission losses into account by modeling the link as a completely-positive trace-decreasing map. We also, crucially, remove the assumption of independent and identically distributed samples, which is known to be incompatible with adversarial settings. Finally, in view of the use of the certified transmitted states for follow-up applications, our protocol moves beyond certification of the channel to allow us to estimate the quality of the transmitted state itself. To illustrate the practical relevance and the feasibility of our protocol with currently available technology we provide an experimental implementation based on a state-of-the-art polarization entangled photon pair source in a Sagnac configuration and analyze its robustness for realistic losses and errors.

Femtosecond laser direct writing of fiber optic microstructure devices

X. Shu

*Wuhan National Laboratory for Optoelectronics, Huazhong University of Science and Technology, Wuhan,
430074, China*

e-mail: xshu@hust.edu.cn

Femtosecond laser direct writing technology has been demonstrated as a very powerful tool to fabricate micro-structures in a wide range of transparent materials. Compared with conventional UV-laser writing technology, femtosecond laser direct writing technology offers some unique advantages such as highly localized modification of the materials and no photosensitivity requirement, which make it very attractive and promising for micro-structure fabrication. The spatial confinement, combined with laser-beam scanning or sample translation, make it possible to write geometrically complex structures in three dimensions. We have recently used femtosecond laser direct writing technology to develop a variety of fiber optic microstructures such as gratings, interferometers and micro-resonators and demonstrated their applications in fiber lasers and sensors. In this talk, we will review our research work on this topic.

Microscopic theory of transport and optics in superlattices and applications to metabolomics and novel device functionalities

M.F. Pereira^{1,2}, A. Apostolakis², H. Zafar¹, V. Vaks³ and V. Anfertev³
¹Department of Physics, Khalifa University of Science and Technology, UAE
²Institute of Physics, Czech Academy of Sciences, Czech Republic
³Institute for Physics of Microstructures, Nizhny Novgorod, 603950, Russia
 e-mail: mauro.pereira@ku.ac.ae

A nonequilibrium many-body approach is used to predict and control giant THz nonlinearities in superlattices at both steady state and time domains in excellent agreement with experiments [1-3]. The resulting superlattice multipliers are applied to the experimental detection of nitrides in the urine of cancer patients treated by chemotherapy, heralding the potential for a new non-invasive metabolomics approach for diagnostics technique that can potentially detect side effects of chemotherapy using THz spectroscopy, much before conventional diagnostics could indicate damage to the kidneys [4]. In the second part of the talk, superlattice waveguides are used to demonstrate theoretically and experimentally functionalities such as rotators and splitters in a silicon on insulator platform [5-8]. Progress in both projects will be presented at the conference, illustrated in Figure 1.

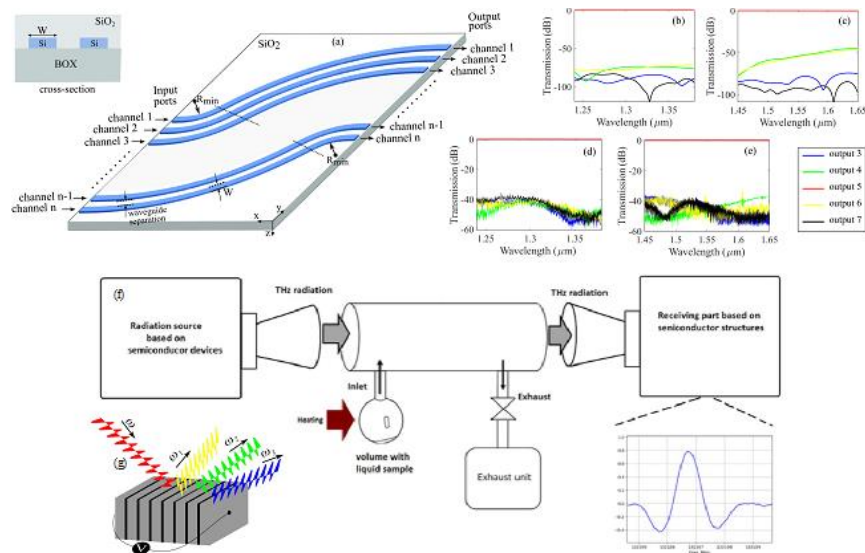


Figure 1. (a) 3D view and cross-section of the n-channel waveguide superlattice. (b, c) simulated transmission spectra for a 9-channel waveguide superlattice with input light at channel 5. (d, e) normalized measured transmissions. The adiabatic bent waveguides are designed with angle $\theta=75^\circ$ and minimum radius of $R_{\min} = 1.5\mu\text{m}$. The crosstalk spectral transmissions are measured through two neighboring ports at either side of the input port 5. (g) Diagram of nitrite detection scheme.

REFERENCES

- [1] M.F. Pereira, *Materials* 11, 2 (2018).
- [2] M.F. Pereira *et al.*, *J. Nanophoton.* 11, 046022 (2017).
- [3] M.F. Pereira *et al.*, *Sci. Rep.* 10, 15950 (2020).
- [4] V. Vaks *et al.*, *Sci. Rep.* 12, 18117 (2022).
- [5] H. Zafar *et al.*, *IEEE J. Sel. Top. Quantum Electron.* 29, 4400109 (2023).
- [6] H. Zafar *et al.*, *Opt. Express* 30, 10087 (2022).
- [7] H. Zafar *et al.*, *AIP Advances* 10, 125214 (2020).
- [8] H. Zafar *et al.*, *J. Nanophoton.* 11, 046022 (2017).

Blue and red diode pumped low-cost ultrafast lasers for biomedical applications

B. Resan

*School of Engineering, University of Applied Sciences and Arts Northwestern Switzerland
Windisch, Switzerland*

e-mail: bojan.resan@fhnw.ch

Last years, we witnessed a huge progress in high power laser diodes and modules in visible wavelength range. The GaN material improvements for blue laser diodes were driven by the high demand for Blue-Ray technology and display industry. kW – class blue diode modules with fiber delivery, are demonstrated for materials processing. Red fiber delivered diode modules generating 100s of W are also reported. Those advances in high power blue and red diodes are enabling direct diode pumping of the mature laser materials with superb output performance, including titanium doped sapphire and alexandrite. Absorption peak of titanium doped sapphire is in green and therefore the common pump laser is a complex frequency doubled solid-state laser. The high cost, large footprint, and low reliability of such pump lasers prevented industrial applications of titanium doped sapphire laser. On the other hand, alexandrite lasers are used in medical applications, but are currently pumped with red flash lamps. We will present our results of the blue laser diode pumped SESAM modelocked femtosecond laser generating 400 mW average power and 70 fs pulse duration [1]. We used such laser for non-linear microscopy and obtained two-photon fluorescence and second-harmonic generation images. We generated up to 70 nm bandwidth from such blue diode pumped titanium-sapphire oscillator, which is a very promising light source for high resolution optical coherence tomography. With a blue diode fiberized module, we obtained >30% small-signal gain in a single pass through the amplifier crystal [2]. We designed a room temperature blue diode pumped titanium-sapphire regenerative amplifier system. On the other hand, we achieved 1 W in CW mode from the red diode pumped alexandrite laser. This is very promising for modelocking, which was not obtained so far with red diode pumping.

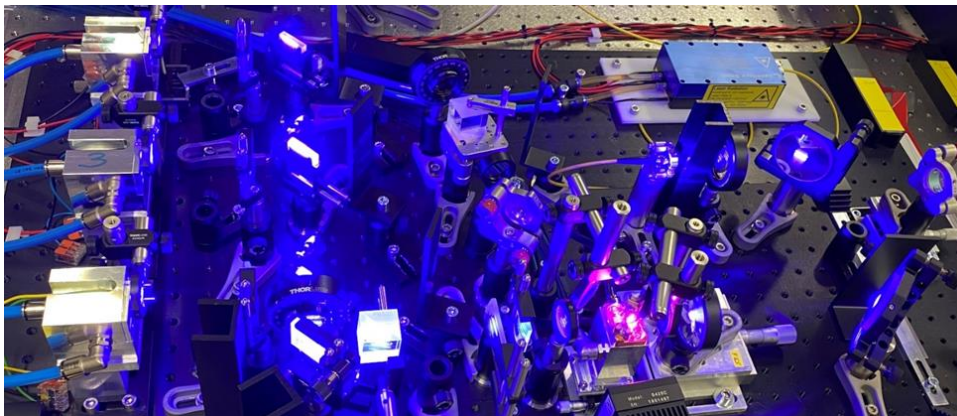


Figure 1. Blue diode pumped Ti:sapphire amplifier.

REFERENCES

- [1] A. Rohrbacher *et al.*, Opt. Express 25, 10677 (2017).
- [2] D. Hug *et al.*, Progress in Blue Diode-Pumped Titanium:Sapphire Regenerative Amplifier at Room Temperature, CLEO EU (2023).

Progress Reports

Broadband photonic quantum memory in atomic ensembles

K. Shinbrough^{1,2}, B.D. Hunt^{1,2}, S. Park³, K. Oolman^{1,2}, T. Loveridge^{1,2}, J.G. Eden³ and V.O. Lorenz^{1,2}

¹Department of Physics, University of Illinois Urbana-Champaign, 1110 W Green St, Urbana, IL 61801, USA

²Illinois Quantum Information Science and Technology (IQIST) Center, University of Illinois Urbana-Champaign, 1101 W Springfield Ave, Urbana, IL 61801, USA

³Department of Electrical and Computer Engineering, University of Illinois Urbana-Champaign, 306 N Wright St, Urbana, IL 61801, USA

e-mail: kais@illinois.edu

Photonic quantum memory constitutes the ability to store and retrieve single-photon-level quantum states of light in a quantum-information-preserving manner. This primitive operation is a critical enabling resource for a wide range of photonic quantum technologies. Of particular importance to the creation of useful, real-world quantum memories is the speed at which the memory can store and retrieve quantum information; quantum memories that operate at high speed need to be compatible with photons that are short in duration and therefore broad in spectral bandwidth. Here we review the state of the art in photonic quantum memory in the broadband regime, we discuss the landscape and limitations of quantum memory protocols based on atomic ensembles, and we present our experimental demonstration of a low-noise, ultra-broadband quantum memory in barium vapor with storage efficiency exceeding 95 %.

Figure 1 shows the performance of all broadband atomic-ensemble quantum memories presently in the literature with respect to two metrics: storage efficiency and bandwidth. We observe that, prior to this work, a tradeoff exists between these two performance criteria, and we trace the cause of this tradeoff to the mismatch between the typically narrowband atomic linewidths in these systems and the broad photon bandwidths they are meant to store [1]. Here we present a resource-efficient method for solving this problem: homogeneous collisional broadening. The introduction of high-density argon perturbers in dilute barium vapor broadens the optical transition linewidths in barium, reducing linewidth-bandwidth mismatch, and allowing for high-efficiency memory operation in the ultra-broadband regime.

In addition to these recent experimental results, we present theoretical results showing that three physically distinct quantum memory protocols - electromagnetically induced transparency (EIT), Autler-Townes splitting (ATS), and absorb-then-transfer (ATT) are smoothly connected via continuous transformation of the control field and memory parameters [2]. Further, we examine the criterion of memory sensitivity (how sensitive a quantum memory is to experimental noise) and show that all resonant memory protocols are ‘stable’, meaning that fluctuations in memory efficiency are always fractionally smaller than the fluctuations in external parameters causing them [3].

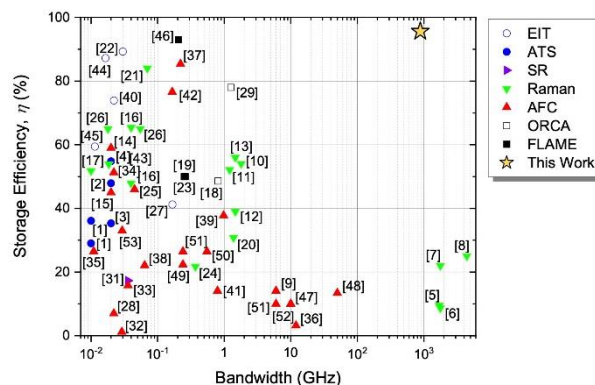


Figure 1. State-of-the-art memory efficiency and bandwidth for atomic ensembles. Adapted from Ref. [1].

REFERENCES

- [1] K. Shinbrough *et al.*, Adv. At. Mol. Opt. Phys. 72 (2023), In Press.
- [2] K. Shinbrough *et al.*, Phys. Rev. A 103, 062418 (2021).
- [3] K. Shinbrough, V.O. Lorenz, Phys. Rev. A 107, 033703 (2023).

Measuring the dipolar interaction shift of the BEC critical temperature

M. Krstajic

Department of Physics, University of Oxford

email: milan.krstajic@physics.ox.ac.uk

The presence of interactions in many-body bosonic systems shifts the critical temperature for Bose-Einstein condensation compared to the ideal gas result. The case of contact interactions has been thoroughly studied, both theoretically and experimentally. This work presents our experimental effort to measure the ‘mean-field’ critical temperature shift due to magnetic dipole-dipole interactions in a harmonically trapped, ultracold erbium gas. Analysing the transition temperature dependence on the orientation of the dipoles in a highly prolate trap, we can isolate the contribution of the anisotropic dipolar interactions and demonstrate the agreement with predictions [1]. Additionally, we investigate the contribution of dipolar interactions to the non-saturation of the thermal gas past the transition [2], and outline a Thomas-Fermi approximation based model to explain the observation. These findings may enhance imaging calibration accuracy in cold atom experiments and could enable studies of beyond-mean field effects in the BEC transition in dipolar gases.

REFERENCES

- [1] K. Glaum *et al.*, Phys. Rev. Lett. 98, 080407 (2007).
- [2] N. Tammuz *et al.*, Phys. Rev. Lett. 106, 230401 (2011).

Crystal structure, optical properties and photo/electrocatalytic activity of nanostructured $\text{Zn}_{1-x}\text{Fe}_y\text{O}_{(1-x+1.5y)}$

V. Rajic¹, S. Markovic², M. Popovic¹, M. Novakovic¹, Lj. Veselinovic¹, I. Stojkovic Simatovic³, S.D. Skapin⁴, S. Stojadinovic⁵ and V. Rac⁶

¹Department of atomic physics, Vinca Institute of Nuclear Sciences - National Institute of the Republic of Serbia, University of Belgrade, Serbia

²Institute of Technical Sciences of SAsA, Belgrade, Serbia

³Faculty of Physical Chemistry, University of Belgrade, Belgrade, Serbia

⁴Jožef Stefan Institute, Ljubljana, Slovenia

⁵Faculty of Physics, University of Belgrade, Belgrade, Serbia

⁶Faculty of Agriculture, University of Belgrade, Zemun, Serbia

e-mail: vladimir.rajic@vin.bg.ac.rs

Zinc oxide-based materials have a great potential to be applied in photo and electro catalysts, optoelectronic (indoor illumination, LED), etc. Attractiveness of ZnO is attributed to wide bandgap energy at room temperature (3.37 eV), high electron mobility and transfer efficiency ($115\text{-}155\text{ cm}^2\cdot\text{V}^{-1}\cdot\text{s}^{-1}$), large exciton binding energy (60 meV), intrinsic stability, nontoxicity, environmental compatibility and also, simple and not expensive synthesis procedure. A lot of different approaches can be used to modify the bandgap (i.e. optical absorption) of ZnO materials: metal and nonmetal ion doping, hydrogenation, the incorporation of crystalline defects in the form of V and I, modification of particles morphology and surface topology, etc.

In this study, eco-friendly and rapid microwave processing of a precipitate was used to produce Fe-doped ZnO nanoparticles with 5, 10, 15 and 20 at.% of Fe ($\text{Zn}_{1-x}\text{Fe}_y\text{O}_{(1-x+1.5y)}$). The influence of different amount of Fe substituted Zn in ZnO on the crystal structure, morphological, textural, and optical properties as well as on functionality of ZnO particles was investigated. The crystal structure and phase purity of the $\text{Zn}_{1-x}\text{Fe}_y\text{O}_{(1-x+1.5y)}$ particles were determined by X-ray diffraction (XRD), Fourier transform infrared spectroscopy (FTIR), Raman spectroscopy and X-ray photoelectron spectroscopy (XPS). Effects of the Fe^{3+} amount on particles morphology and texture properties were observed with field emission scanning electron microscopy (FE–SEM), transmission electron microscopy (TEM) and nitrogen adsorption–desorption isotherm, respectively. Optical properties were studied using UV-Vis diffuse reflectance and photoluminescence spectroscopy. Functionality of ZnO particles was studied due to their photocatalytic and electrochemical activities. Photocatalytic activity was examined via decolorization of methylene blue under direct sunlight irradiation. Electrochemical behavior of the ZnO samples as anode material was evaluated by linear sweep voltammetry in 0.5 M Na_2SO_4 electrolyte.

Synchrotron radiation photoemission spectroscopy study of the valence band electronic structure of Ag-Ag₂S Janus nanoparticles for the development of nanomotors propelled by NIR light

D. Danilović^{1,2}, D.K. Božanić^{1,2}, J. Pajović³, G.A. Garcia⁴, L. Nahon⁴, T. Marić⁵ and V. Djoković^{1,2}

¹Vinca Institute of Nuclear Sciences, University of Belgrade, P.O. Box 522, 11001 Belgrade, Serbia

²Center of Excellence for Photoconversion, Vinča Institute of Nuclear Sciences - National Institute of the Republic of Serbia, University of Belgrade, Serbia,

³Faculty of Physics, University of Belgrade, Studentski trg 12, 11001 Belgrade, Serbia

⁴Synchrotron SOLEIL, l'Orme des Merisiers, St. Aubin, BP48, 91192 Gif sur Yvette Cedex, France

⁵Department of Health Technology, Technical University of Denmark, Kgs Lyngby, 2800 Denmark
e-mail: danijelad@vin.bg.ac.rs

Silver-silver sulfide (Ag-Ag₂S) hybrid nanosystem which consists of plasmonic metal Ag and narrow band gap semiconductor Ag₂S is typically studied as a photocatalyst under visible and NIR light [1,2]. Janus morphology of this system is especially interesting due to the possibility of initiating two different chemical reactions that are spatially separated on two halves of the system. Here, we present the fabrication of Ag-Ag₂S Janus nanoparticles and the examination of their valence electronic structure. For the investigation of the electronic structure of isolated nanoparticles, we performed synchrotron radiation vacuum ultraviolet photoelectron spectroscopy using the velocity map imaging (VMI) technique. By using two different photon energies, $h\nu = 9.5$ eV and $h\nu = 11$ eV, we obtained angle-resolved photoelectron images. Photoemission spectra and the dependence of the asymmetry parameter α on the binding energy are derived from VMI images using modified p-Basex inversion method [3]. In addition, we coupled Ag-Ag₂S nanoparticles to the TiO₂ and studied the actuation of obtained hybrid nanosystem in a liquid medium under visible and NIR light.

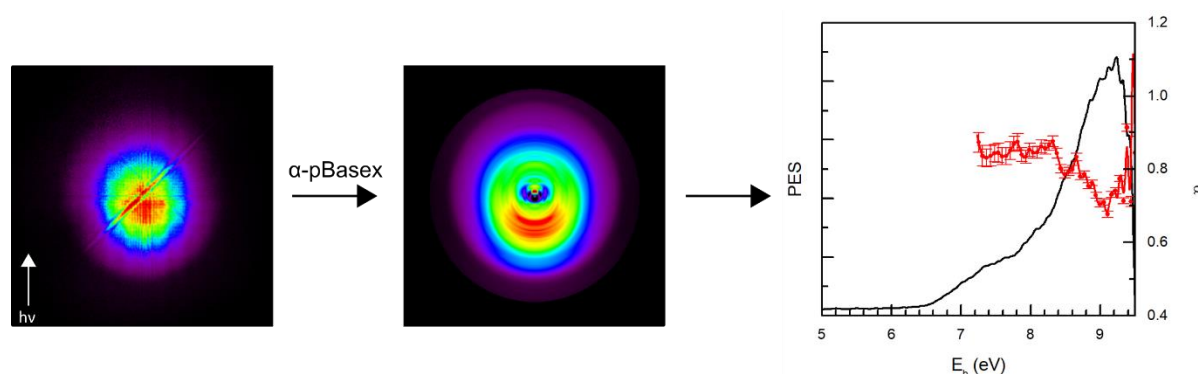


Figure 1. Raw and p-Basex reconstructed photoelectron image of Ag-Ag₂S nanoparticles, and photoemission spectrum and α parameter dependence on the binding energy ($h\nu = 9.5$ eV).

REFERENCES

- [1] X. Zhang *et al.*, Nano Lett. 21, 2625 (2021).
- [2] F. Jiang *et al.*, Cryst. Eng. Comm. 13, 7189 (2011).
- [3] D.K. Božanić *et al.*, Phys. Chem. C 124, 24500 (2020).

Photosensitizer potential of doped and undoped nanostructured TiO₂

M. Matijević¹, L. Korićanac², Đ. Nakarada³, J. Žakula², M. Stepić¹, M. Radoičić², M. Mojović³, M. Petković¹ and M.D. Nešić¹

¹COHERENCE, Department of Atomic Physics, VINČA Institute of Nuclear Sciences - National Institute of the Republic of Serbia, University of Belgrade, Belgrade, Serbia

²VINČA Institute of Nuclear Sciences - National Institute of the Republic of Serbia, University of Belgrade, Belgrade, Serbia

³Faculty of Physical Chemistry, University of Belgrade, Serbia

e-mail: milica.m@vin.bg.ac.rs

Treating cancer remains a major challenge, despite the development of many therapies and advances in general knowledge about the disease. The treatments commonly used are invasive and non-selective, leading to severe side effects and unsatisfactory long-term outcomes. Nevertheless, external stimuli activating therapeutic agents in the affected area can be more beneficial than these aggressive therapies. Photodynamic therapy (PDT) is a minimally invasive, selective treatment that uses photosensitizer (PS) to damage cancer cells. The PS is activated by light, triggering a series of processes that produce reactive oxygen species (ROS), ultimately leading to cancer cell death. Numerous types of nanomaterial possess the capability to act as PS, one of which is TiO₂ [1]. Although nanostructured TiO₂ is biocompatible in the absence of light, its valence band electrons can be stimulated only by ultraviolet (UV) light irradiation. Since the penetration of UV light into tissue is limited, for application in PDT, nanostructured TiO₂ can be doped with heteroatoms like N or C to allow visible light responsiveness [2,3].

This work evaluated the PS properties of unmodified nanostructured TiO₂ (spherical nanoparticles TiO₂ NPs and prolate nanospheroids, TiO₂ PNSs) and doped TiO₂ (N- and C-TiO₂ NPs). After the synthesis, the size of TiO₂ was confirmed to be in the nanoscale range (5-104 nm) by transmission electron microscopy [3,4]. The doped TiO₂ was found to absorb visible light, as demonstrated by UV-Vis spectroscopy and bandgap calculations. Additionally, hydroxyl radicals were detected in water suspensions of TiO₂ PNSs by electron paramagnetic resonance (EPR) spectroscopy, both with and without UV light illumination [4]. However, this radical was observed only with blue light stimulation of the water suspensions of N- and C-TiO₂ NPs [3].

Cell experiments further revealed the internalization process of nanostructured TiO₂ within cells, their cytotoxicity profiles, and the different death modalities triggered by their uptake. After confocal microscopy indicated the successful internalization of the investigated TiO₂, viability tests on different cell lines confirmed their good biocompatibility without light [3,4]. The PDT's efficacy using nanostructured TiO₂ and appropriate light stimuli was evaluated on various cancer cell lines. The most significant viability reduction (60 %) was observed in the HeLa cell line with the combined treatment of C-TiO₂ NPs-blue light. In addition to EPR results, blue light-induced C-TiO₂ NPs-catalyzed generation of ROS was confirmed intracellularly, implying that oxidative stress was the leading cause of HeLa cell death. Fluorescent labeling allowed distinguishing morphological changes inside the cells after the C-TiO₂ NPs, blue light, and the combined C-TiO₂ NPs-blue light treatment. Blue light exposure led to the appearance of large necrotic cells with deformed nuclei, cytoplasm swelling, and membrane blebbing. In contrast, the combined therapy with C-TiO₂ NPs-blue light resulted in controlled cell death, such as autophagy. Since programmed cell death is the desired cancer cell death mechanism, the combined treatment presented here can provide a better outcome of local anticancer therapy.

REFERENCES

- [1] Z. Haijun *et al.*, J. Biomed. Nanotechnol. 10, 1450 (2014).
- [2] Z. Li *et al.*, Nano. Res. Lett. 6, 356 (2011).
- [3] M. Matijević *et al.*, Photochem. & Photobio. Sci. 20, 1087 (2021).
- [4] M. Matijević *et al.*, J. Nanopart. Res. 22, 175 (2020).

Application of laser-induced breakdown spectroscopy for the determination of trace metals in oils

M. Vinić

Institute of Physics, University of Belgrade, 11080 Belgrade, Serbia

e-mail: mvinic@ipb.ac.rs

The subject of this research is a method for preparation and analysis of oils by Laser-Induced Breakdown Spectroscopy (LIBS), aimed to minimize the necessary sample volume and the matrix effect while maximizing the detection sensitivity and measurement's repeatability. The preparation procedure consists in stabilizing the oil sample and silica wafer substrate at a fixed temperature (40°C) and in delivering an oil droplet on the wafer rotated by a spin coater. In this way, an uniform oil film is obtained, which thickness is controlled through the rotational speed.

During the sample preparation, above a certain rotational speed the thickness of the oil film is the same for the two oils although their kinematic viscosities are very different, meaning that the volume sampled by LIBS is the same. The measured oil transmissivity at the laser wavelength of 1064 nm significantly decreases with concentration of impurities, but this effect could be neglected when dealing with very thin oil films. The plasma formation threshold measured on the bulk oil samples decreases with the impurity content. In case of pure oil, also for the maximum laser energy here used (165 mJ), the plasma is mainly initiated on the wafer, while the presence of impurities increases screening of the substrate by the plasma formed directly on the oil. The matrix effect disappears on a very thin film, here of 0.74 μm , where the C I line intensity in plasma does not vary with the total concentration of impurities; simultaneously, the plasma emission becomes stable from one laser pulse to another, contrary to the case of a thick liquid layer. In the optimized experimental conditions, the plasma emission from oil was very intense although the sample volume probed by each laser pulse was of 0.3 nL only. The obtained results show that the LIBS, with the proposed procedure of forming a thin layer of oil, can be very successfully applied for the quantitative analysis. Very low detection limits (in the range of 0.1 to 5 ppm) were obtained with good linearity of calibration curves in the range of 0 to 60 ppm for all tested elements [1].

Spatially and temporally integrated spectral measurements were performed under experimental conditions optimized for elemental analysis of trace metals in oil. Time-resolved values of the spectral line intensities, electron number density, and plasma temperature were obtained by subtracting averaged spectra recorded at different time delays. The electron number density was estimated using the Stark broadened profile of the H_{α} line. Ionization temperatures were derived from Mg ionic to atomic line intensity ratios. Spectra of C_2 and CN molecules were used to evaluate the rotational and vibrational temperature of heavy particles. It is shown that the plasma parameters depend on the total metal concentration in the oil: although the effect is small, it must be taken into account in the quantitative determination of trace metals in the oil using the LIBS technique [2].

REFERENCES

- [1] M. Vinić *et al.*, Spectrochim. Acta Part B: At. Spectrosc. 164, 105765 (2020).
- [2] M. Vinić *et al.*, J. Serb. Chem. Soc. 87, 1 (2022).

Influence of thin oxide layer to photoacoustic signal of nano-mechanical structures

K.Lj. Đorđević¹, S.P. Galović¹, M.A. Dragaš^{2,3}, D.K. Markushev⁴ and D.D. Markushev⁴

¹*Vinča Institute of Nuclear Sciences - National Institute of the Republic of Serbia, University of Belgrade, Belgrade, Serbia*

²*Faculty of Philosophy, University of East Sarajevo, Pale, Bosnia and Herzegovina*

³*Faculty of Physics, University of Belgrade, Serbia*

⁴*Institute of Physics Belgrade - National Institute of the Republic of Serbia, University of Belgrade, Belgrade (Zemun), Serbia*

e-mail: katarina.djordjevic@vin.bg.ac.rs

Nano mechanical structures (NEMS) are being developed for application in pressure and temperature sensors. They consist of a very thin oxide layer on a silicon wafer. This layer is placed to improve their sensitivity to pressure changes. In this paper, it was investigated how much this layer affects the physical properties of such structures. In the research, the photoacoustic gas microphone experimental measurement method was applied and neural networks were developed for solving the inverse photoacoustic problem. The obtained results show that controlling the thickness of the oxide layer can be done by engineering the thermal elastic and optical properties of the NEMS.

REFERENCES

- [1] K.Lj. Djordjević *et al.*, *Materials* 16, 2865 (2023).
- [2] K.Lj. Djordjević *et al.*, *Opt. Quantum Electron.* 52, 247 (2020).
- [3] D.M. Todorović *et al.*, *J. Appl. Phys.* 114, 213510 (2013).

Modeling microwave ablation for tumor treatment using open-source software components

N. Boskovic, M. Radmilovic-Radjenovic and B. Radjenovic
Institute of Physics, Belgrade, Serbia
e-mail: nikolab@ipb.ac.rs

Microwave ablation (MWA) is a minimally invasive medical procedure with a short recovery time for treating various types of cancers. During MWA, a small needle-like probe is inserted inside the tumor. Inside the probe there is a microwave radiator (antenna) that delivers microwave energy, causing tissue heating, and effectively produces necrosis of the tumor tissue. The primary goal of modeling and studying of MWA is to determine ablation zone caused by the particular combination of radiator, input power, time and position of the probe. MWA should cause total necrosis of tumor tissue and minimal damage to surrounding healthy tissue. Simulation of MWA requires calculation of electromagnetic wave propagation, heat transfer, and tissue damage. Physical processes can be described using partial differential equations (PDEs). Multiple effects such as blood flow and change of water content inside the tissue with temperature have a major influence on the MWA.

In our study we have created the complete geometry of MWA including a multi-slot coaxial antenna [1], a real liver tumor taken from the database [2], and the surrounding liver tissue using Gmsh [3]. Geometry is meshed and PDEs are solved using Finite Elements Method (FEM) via GetDP package [4]. The MWA occurs at 2.45 GHz, with an input power of 13 W, during 600 s. The electric field is calculated in frequency domain, while temperature distribution and necrosis are calculated in the time domain using the custom fast fully explicit stable Euler scheme. We have calculated all quantities required in the MWA, including temperature and distribution of tissue necrosis over time, Fig. 1, with results comparable to Comsol [5].

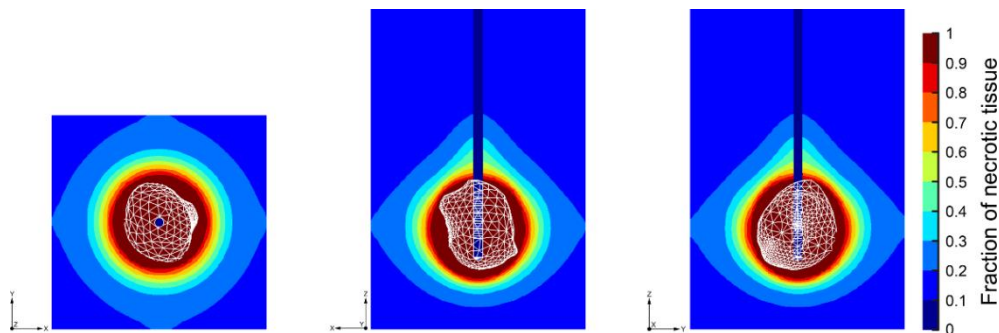


Figure 1. Fraction of necrotic tissue at different cross-sections at 600 s. The shape of the tumor is marked in white and is located in the zone of total tissue damage.

REFERENCES

- [1] M. Radmilović-Radjenović *et al.*, *Bioengineering* 9, 656 (2022).
- [2] M. Radmilović-Radjenović *et al.*, *Biomedicines* 10, 7 (2022).
- [3] Gmsh. Available online: <https://gmsh.info>.
- [4] GetDP. Available online: <https://getdp.info>.
- [5] Comsol Multiphysics. Available online: www.comsol.com.

Contributed Papers

1. Quantum optics and ultracold systems

Exploiting the quantumness of coherent states: toward macroscopic quantum light

C. Hermann Avigliano^{1,2}

¹*Departamento de Física, FCFM, Universidad de Chile, Santiago, Chile.*

²*ANID - Millenium Science Initiative Program - Millenium Institute for Research in Optics (MIRO)*

e-mail: carla.hermann@uchile.cl

Can we harvest useful quantum properties from coherent states? Can we engineer quantum states with them, creating useful nonclassical states from mostly classical light? Our last works attempt to answer both questions with a solid yes. We show how nonlinear light-matter interactions reveal the unambiguous quantum nature of coherent states, creating macroscopic and highly nonclassical light while preserving their coherent photon statistics [1]. Figure 1 shows examples of the generation of such states, where the uncertain region of an initial coherent state in the phase space representation (Wigner Function) nonlinearly evolves into negative values, an unmistakable quantum fingerprint. The emergent non-minimal uncertainty states have a significant metrological advantage, a fundamental resource for quantum metrology. Remarkably, we also show how to deterministically generate Fock states with large photon numbers and high fidelities within the well-known Jaynes–Cummings model, which is a particular case of such nonlinear interactions [2].

Our results highlight how useful quantum features can be extracted from the seemingly most classical states of light, a relevant phenomenon for quantum optics applications.

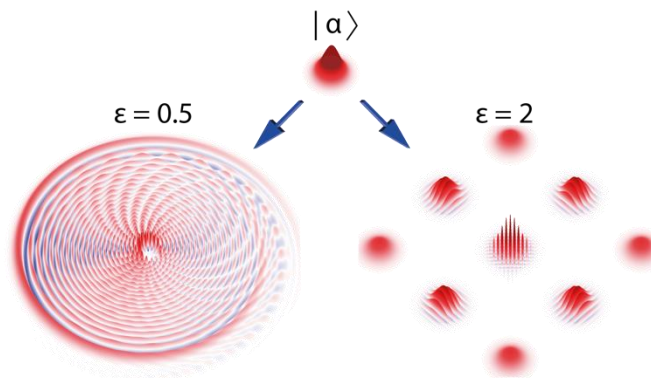


Figure 1. Nonlinear evolution of a coherent state into highly non-Gaussian states.

REFERENCES

- [1] M. Uria *et al.*, Phys. Rev. Research 5, 013165 (2023).
 [2] M. Uria *et al.*, Phys. Rev. Lett. 125, 093603 (2020).

Anomalous diffusion and mixed dynamics in a classical Bose-Hubbard chain

D. Markovic^{1,2} and M. Cubrovic²

¹*Department of Physics, University of Belgrade, Studentski Trg 12-16, Belgrade, Serbia*

²*Center for the Study of Complex Systems, Institute of Physics Belgrade, Pregrevica 118, 11080 Belgrade, Serbia*

e-mail: vokramnagard@gmail.com

We study chaos and anomalous transport in a Bose-Hubbard chain in the semiclassical regime (the limit when the number of particles goes to infinity), which allows us to solve long chains with up to hundred sites. We find that the system has mixed phase space with both regular and chaotic dynamics. The consequence is strongly anomalous diffusion with a discrete set of scaling exponents, which after very long times crosses to the thermalized regime with normal diffusion. We corroborate our findings with analytical arguments from thermodynamics and Langevin equations.

Correlated photon pairs by Four Wave Mixing in alkali vapor for imaging application

M.M. Čurčić, D. Arsenović and B. Jelenković
Institute of Physics Belgrade, University of Belgrade, Serbia
e-mail: marijac@ipb.ac.rs

We will present our results on the generation of relative intensity difference squeezing (IDS) by Four Wave Mixing (FWM) in alkali vapors [1]. Motivated by a specific energy structure of potassium atoms and previously performed studies with different alkali atoms, Rb and Cs, we study both experimentally and theoretically generation of twin pairs – probe and conjugate by means of FWM on double-lambda scheme on D1 line in K, and their correlations. We have demonstrated and measured the squeezing level of – 6.1 dB, and investigated the dependence of gain and squeezing levels on different system parameters such as one-photon pump detuning, two-photon probe detuning, vapor temperature, cell length. We will discuss the obtained dependences and the optimal choice of parameters values, so as the advantages of K over the other alkali elements.

Having a proper theoretical model would ease the search for the optimal system parameters, especially when some specific requirements are desired by the possible application of described system. In addition to our experimental work, we have done a theoretical study and developed a quantum model for hot vapor systems based on Heisenberg-Langevin formalism, including Doppler averaging and transit time of the atoms through the interaction area. We will present the comparison of the obtained results, experimental and theoretical ones.

Finally, we will discuss the application of our quantum light source for the imaging, especially for two photon absorption (TPA), one of the most commonly used technique in bioimaging. During the last decade, taking advantages of quantum light in sensing and imaging has become a way of overcoming the limits of classical techniques, and hence method of improving sensitivity and resolution of the measurements. Entangled two-photon source by spontaneous down conversion (SPDC) in nonlinear crystal has already been shown to be a solution for overcoming photo- and thermal damaging with the common use of strong pulsed laser, and used in performing an enhanced imaging of the cells [2]. We will also comment on the advantages of FWM source of correlated photons over the SPDC.

REFERENCES

- [1] M.M. Čurčić, B.M. Jelenković, *Opt. Commun.* 533, 129301 (2023).
- [2] O. Varnavski *et al.*, *J. Phys. Chem. Lett.* 13, 2772 (2022).

Transport of cold bosonic atoms in optical lattices

I. Vasić and J. Vučićević

Institute of Physics Belgrade, University of Belgrade, Serbia

e-mail: ivana.vasic@ipb.ac.rs

Cold atoms in optical lattices provide a clean realization of the Hubbard model. While the focus of early experiments was on understanding quantum phase transitions driven by the interplay of hopping and local interactions [1], more recent experiments aim at studying quantum transport in these setups. The onset of bad-metal behavior, characterized by the resistivity linear in temperature, has been investigated recently [2,3]. While the conductivity of the fermionic version of the model has been addressed in much detail both from the theoretical and experimental perspective, far less is known about transport in the bosonic version [4]. We investigate conductivity in the strongly-interacting regime of the Bose-Hubbard model. We address the high-temperature regime and use numerically exact calculations for small lattice sizes. At weak tunneling, we find multiple peaks in the optical conductivity that stem from the Hubbard bands present in the many-body spectrum. This feature is slowly reduced as the tunneling rate gets stronger. Further, we find the regime of linear resistivity. When the interactions are very strong, the leading inverse-temperature coefficient in conductivity is proportional to the tunneling amplitude. As the tunneling becomes stronger, this dependence takes quadratic form.

REFERENCES

- [1] I. Bloch *et al.*, Rev. Mod. Phys. 80, 885 (2008).
- [2] P.T. Brown *et al.*, Science 363, 379 (2019).
- [3] J. Vučićević *et al.*, Phys. Rev. Lett. 123, 036601 (2019).
- [4] N.H. Lindner, A. Auerbach, Phys. Rev. B 81, 054512 (2010).

Experimental and theoretical study of the phase response of M_x magnetometer to modulating transversal magnetic field

M.M. Ćurčić¹, A. Milenković¹, A. Bunjac¹, T. Scholtes² and Z. Grujić¹

¹Institute of Physics Belgrade, University of Belgrade, Serbia

²Leibniz Institute of Photonic Technology, Jena, Germany

e-mail: zoran.grujic@ipb.ac.rs

We will present our results on the study of a scalar optically pumped magnetometer (OPM) [1]. More precisely, we investigate the phase response of a true scalar M_x magnetometer to the sudden changes of transversal magnetic field. As a sensing element we employ paraffin coated cell filled with Cs. A single light source is used for both pumping (polarizing) the medium and probing i.e. reading out a variation in the intensity of the resonant light due to the applied magnetic field. Pump light is circularly polarized. The wave vector and RF magnetic field that drives the spin precession are at 45° with the respect to the main static magnetic field B_0 as presented on Fig. 1. Magnetometer operates at room temperature. Set of Helmholtz coils is used for the generation of additional modulating field. The sensor head is placed inside a three layer mu-metal shielding. Changes of the magnetometer response are detected with a lock-in amplifier, which enables us to obtain in-phase and quadrature components of the transmitted probe signal.

In addition to experimental study, we did both numerical and analytical modeling of a described system. Theoretical study is based on the transient Bloch equation. Analytically, the equation is solved in rotating frame after applying a rotating wave approximation (RWA). In this manner, we were able to obtain set of simple equations describing detected signal, decomposed into in-phase and quadrature components, for comparison with experimental results and tracking of the phase evolution.

The model results show good agreement with the experiment. Being a scalar magnetometer, our sensor should not experience any changes in the measured phase depending on the orientation of the applied modulating field. However, both experimental measurements and model predictions have demonstrated this is not the case. With the main offset field in z -direction, and applied modulation in yz plane, phase of the signal shows an unexpected behavior for a scalar magnetometer. We will present obtained results, and discuss which conditions lead to the before mentioned signal abnormalities.

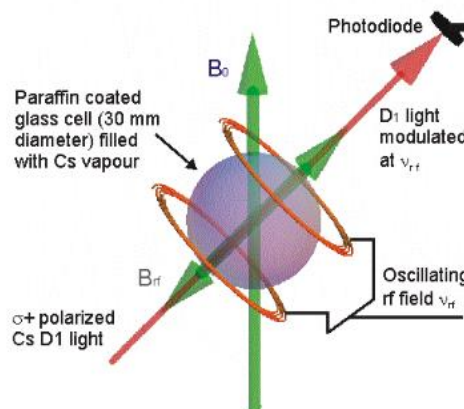


Figure 1. Schematic of the scalar M_x optically pumped magnetometer.

REFERENCES

- [1] A. Weis *et al.*, High Sensitivity Magnetometers – Magnetic Resonance Based Atomic Magnetometers, Springer, pp 361-424 (2016).

Spontaneous emission of three-level ladder-type atom coupled to one-dimensional rectangular waveguide

Lj. Stevanović and M. Perić

Department of Physic, Faculty of Sciences and Mathematics, University of Niš, Serbia

e-mail: milica.peric1@pmf.edu.rs

Coupling the quantum emitter, like an atom, to a one-dimensional waveguide provides the way of the photon propagation control in possible quantum channels [1,2]. This kind of waveguide-quantum electrodynamic system is a candidate for the application in quantum network [3] as a local quantum node playing the role of quantum switch [4] or one-photon transistor [5].

We study the spontaneous emission dynamics of the excited three-level atom in ladder configuration placed in a hollow rectangular waveguide with perfectly conducting walls. The model is based on solving time-dependent Schrödinger equation with the Hamiltonian obtained in the formalism of second quantization under the dipole and rotating-wave approximations [6]. The assumption is made that both dipole-allowed atomic transitions are coupled with transverse waveguide modes.

The effects of the atom position in the waveguide, atomic energy level separations and the orientation of atomic dipoles are discussed regarding the possible waveguide modes for the photon emission. The two cases are considered: when the two emerging photons belong to different modes and when they can be emitted in the same mode.

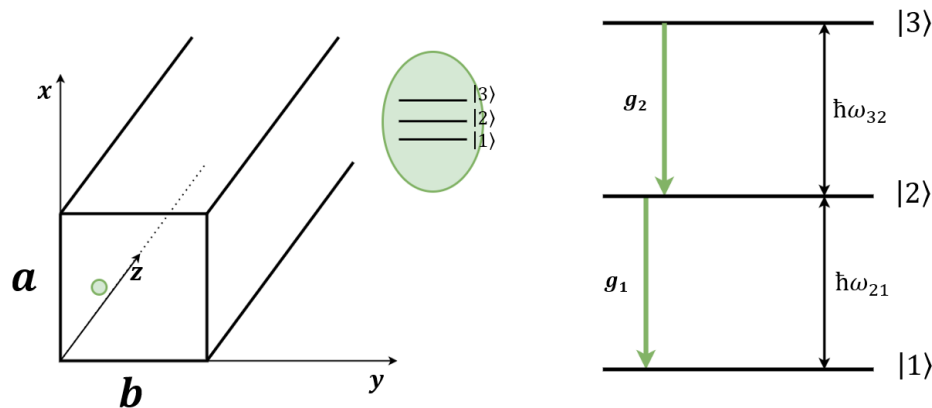


Figure 1. Three-level atom coupled to rectangular waveguide.

REFERENCES

- [1] J.T. Shen, S. Fan, Opt. Lett. 30, 2001 (2005).
- [2] Q. Li *et al.*, Phys. Rev. A 89, 063810 (2014).
- [3] H.J. Kimble, Nature 453, 1023 (2008).
- [4] L. Zhou *et al.*, Phys. Rev. Lett. 111, 103604 (2013).
- [5] D.E. Chang *et al.*, Nat. Phys. 3, 807 (2007).
- [6] H. Song *et al.*, Commun. Theor. Phys. 69, 59 (2018).

Quantized vortices in dipolar BECs when crossing the superfluid-supersolid phase transition

M. Sindik^{1,2}, A. Recati^{1,3}, S.M. Rocuzzo⁴, L. Santos⁵ and S. Stringari^{1,3}

¹*Pitaevskii BEC Center and Department of Physics, University of Trento, Italy*

²*Institute of Physics Belgrade, University of Belgrade, Serbia*

³*Trento Institute for Fundamental Physics and Applications, INFN, Italy*

⁴*Kirchhoff-Institute for Physics, Ruprecht-Karl University of Heidelberg, Germany*

⁵*Institute for Theoretical Physics, Leibniz Universität Hannover, Germany*

e-mail: marija.sindik@unitn.it

We study quantized vortices in dipolar Bose-Einstein condensates at the transition between the superfluid and the supersolid phase [1]. Recently, ultracold atomic gases have revealed unique features of supersolidity, an intriguing state of matter which presents simultaneously crystalline order and superfluidity [2-4]. However, the experimental observation of quantized vortices in these systems remains an open issue, since their observability in dipolar supersolids is largely prevented by the strong density depletion caused by the formation of droplets [5].

We propose a novel approach to the nucleation of vortices and their observation, based on the quenching of the s-wave scattering length across the phase transition. Starting from a slowly rotating, vortex-free configuration in the superfluid phase, quenching into the supersolid phase drives the vortex nucleation, due to the strong reduction of the critical angular velocity in the supersolid, as illustrated in Fig. 1. Once a vortex is created, it is robustly preserved when the condensate is brought back to the superfluid phase, where it may be readily observed. These results may have a significant impact on ongoing experiments, given that the observation of quantized vortices would constitute a key probe of the superfluid character of dipolar supersolids.

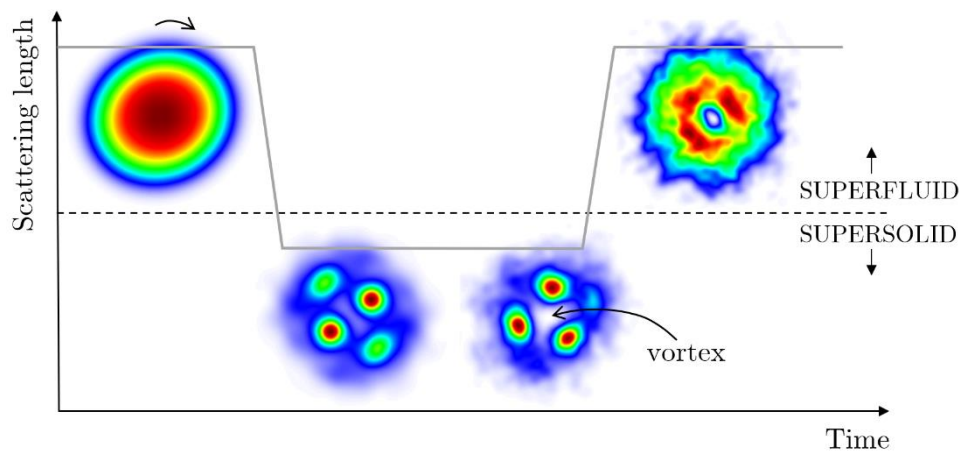


Figure 1. Step-by-step illustration of the protocol process.

REFERENCES

- [1] M. Sindik *et al.*, Phys. Rev. A 106, L061303 (2022).
- [2] L. Tanzi *et al.*, PRL 122, 130405 (2019).
- [3] F. Bottcher *et al.*, Phys. Rev. X 9, 011051 (2019).
- [4] L. Chomaz *et al.*, Phys. Rev. X 9, 021012 (2019).
- [5] A. Gallemi *et al.*, Phys. Rev. A 102, 023322 (2020).

2. Nonlinear optics

Absorption coefficients and refractive index changes in a strongly prolate and strongly oblate ellipsoidal quantum dot

V. Pavlovic and Lj. Stevanovic

Faculty of Sciences and Mathematics, University of Nis, Serbia

e-mail: vladan.pavlovic@pmf.edu.rs

Quantum dots (QDs) are nanoscale semiconductor structures that exhibit unique optical and electronic properties due to their quantum confinement effects. These properties make them highly attractive for a wide range of applications, including optoelectronics, photovoltaic, and quantum information processing. Due to quantum confinement effects, the energy levels of electrons in quantum dots become discrete, leading to size-dependent absorption spectra. Moreover, the refractive index change exhibited by quantum dots is another critical characteristic that influences their optical behavior. The refractive index represents how light propagates through a material, and any changes in this property can significantly impact the interaction of light with quantum dots.

In this paper, Optical Absorption Coefficient (AC) and Refractive Index (RI) changes of a strongly prolate and strongly oblate Ellipsoidal Quantum Dot (EQD) are investigated.

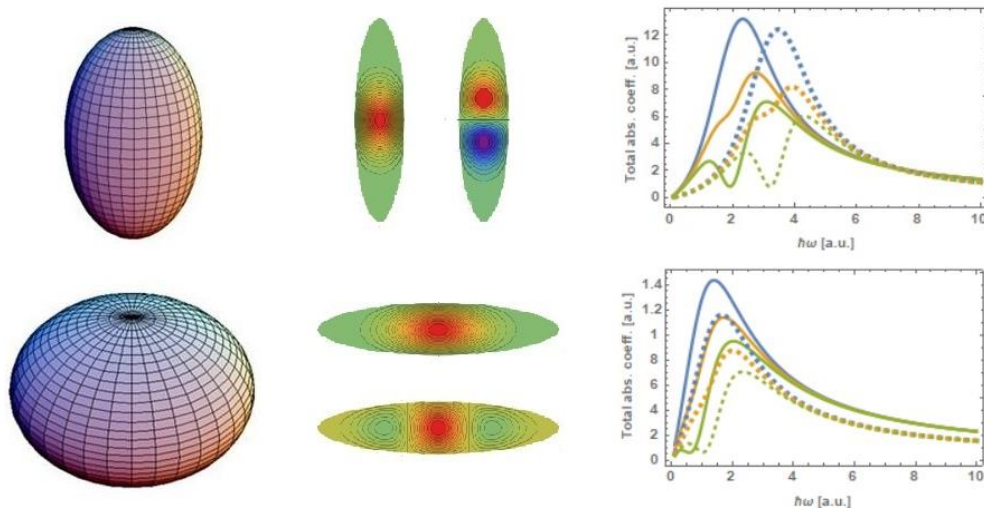


Figure 1. Strongly prolate (top) and strongly oblate (bottom) ellipsoidal quantum dot.

For a strongly prolate and strongly oblate EQD, wave function can be approximated by a suitable analytical function [1,2], where eigen energy shows good matching with numerical results. These wave functions are then used, together with density operator [3,4], given by von Neumann equation, in order to investigate the linear and the third order nonlinear optical AC and RI changes.

It is shown that the total AC and RI are strongly size dependent, and their peaks exhibit a red shift as the size increases. It is also shown that total AC and RI are dependent on ellipticity parameter, and the peaks shift toward the lower energies as ellipticity increases.

REFERENCES

- [1] D.B. Hayrapetyan, Phys. E Low-dimens. Syst. Nanostruct. 145, 115493 (2023).
- [2] D.B. Hayrapetyan *et al.*, Phys. E Low-dimens. Syst. Nanostruct. 95, 27 (2018).
- [3] E. Sadeghi *et al.*, Phys. B 406, 241 (2011).
- [4] G. Rezai *et al.*, Curr. App. Phys. 11, 176 (2011).

Impact of nonlinearity on the zero-mode lasing in optical lattices

M. Nedić, G. Gligorić, J. Petrovic and A. Maluckov

COHERENCE, Vinca Institute of Nuclear Sciences, University of Belgrade - National Institute of the Republic of Serbia

e-mail: milica.brankovic@vin.bg.ac.rs

Photonics has provided a variety of flexible and controllable systems for probing topological phenomena. Recently, the first experimental realization of a Majorana zero-mode bound at vortex-like distortion has been demonstrated in [1]. The result of the distortion is the creation of a robust mode localized in the vicinity of the vortex core.

Here, we focus on finite bipartite armchair hexagonal-shaped lattice with a vortex-like (“Kekule”) distortion [2] and study novel aspects of the zero-mode dynamics in the presence of the nonlinear lattice response and nonlinear driving [3]. We first investigate the impact of saturable Kerr nonlinearity on the properties of zero-modes [4]. The extreme robustness of zero-modes to external perturbation indicate that managing the driving parameters, saturable gain [5] and linear loss, can lead to an efficient and steady lasing regime. We examine how the nonlinearity affects the lasing efficiency, since these effects are unavoidable at higher powers. Based on the results, we propose a new topological laser realisable in a multicore optical fibre.

REFERENCES

- [1] A.J. Menssen *et al.*, Phys. Rev. Lett. 125, 117401 (2020).
- [2] C.Y. Hou *et al.*, Phys. Rev. Lett. 98, 186809 (2007).
- [3] M. Nedić *et al.*, Phys. Lett. A 477, 128893 (2023).
- [4] D. Smirnova *et al.*, Appl. Phys. Rev. 7, 021306 (2020).
- [5] S.K. Turitsyn, Opt. Express 17, 11898 (2009).

The modulation instability triggered band relaxation in photonic Chern insulator

A. Mančić¹, M. Nedić², D. Leykam³ and A. Maluckov²

¹COHERENCE, Faculty of Sciences and Mathematics, University of Niš, Serbia

²COHERENCE, Institute of Nuclear Sciences Vinča, National Institute of the Republic of Serbia, University of Belgrade, Serbia

³Center of Quantum Technologies, National University of Singapore

e-mail: sandram@vin.bg.ac.rs

Photonic lattices represent a fruitful testbed for investigating various topological phases, nonlinear phenomena, and intriguing consequences of the development of modulational instability in topologically nontrivial media, as the inter-relation between topological edge states [1], edge solitons [2] and bulk solitons [3]. They provide the possibility not only to highlight the equivalent phenomena in condensed matter systems but to go beyond them into new land of exotic nonlinearly driven topologically moderated states.

Recently, we have shown that the modulational instability of nonlinear Bloch modes could be used to probe the band topology in non-driven lattices [4]. As an extension, here, we report on the results of the study of the relaxation of the optical wave fields in nonlinear two-dimensional Chern insulators [5]. They undergo a transition from an ordered bulk state to a disordered state, triggered by the modulational instability [6]. The phenomenon of the memory loss of the initial state is related to nonlinear wave-mixing and ergodization within the gapped bands [7].

The testbed for our numerical study is two-dimensional π -flux square lattice in which we investigate the population of topological bands by the wave mixing of nonlinear Bloch waves. We tune the strength of the nonlinearity and lattice parameters in order to observe different dynamical regimes: topological transitions, stable and unstable propagation. We have found that the unstable propagation gives rise to a new quasi-steady state characterized by a convergence of certain wave field characteristics (participation ratio, Chern number, purity gap) to constant values. Next, in order to find the correspondence between this steady state and thermalized wave field we apply a grand canonical approach to calculate the effective temperature and chemical potential of the wave field. We have found that the effective temperature and chemical potential exhibit a strong k – dependence throughout the Brillouin zone. This implies the existence of a long-lived pre-thermalized regime and the absence of thermalization.

REFERENCES

- [1] B. Galilo *et al.*, Phys. Rev. Lett. 115, 245302 (2015).
- [2] D. Leykam, Y.D. Chong, Phys. Rev. Lett. 117, 143901 (2016).
- [3] Y. Lumer *et al.*, Phys. Rev. Lett. 111, 243905 (2013).
- [4] D. Leykam *et al.*, Phys. Rev. Lett. 126, 073901 (2021).
- [5] A. Mančić *et al.*, Phys. Scr. 98, 055513 (2023).
- [6] V.E. Zakharov, L.A. Ostrovsky, Physica D 238, 540 (2009).
- [7] P. Buonsante *et al.*, Phys. Rev. E 95, 052135 (2017).

Coupled vortex generator in active multi-core fibers

P.P. Beliĉev, G. Gligorić and A. Maluckov

Vinĉa Institute of Nuclear Sciences - National Institute of the Republic of Serbia, University of Belgrade,
Belgrade, Serbia

e-mail: petrab@vin.bg.ac.rs

Optical vortex is a coherent localized structure carrying energy around the pivot point. It is characterized by an optical angular momentum (OAM) mathematically described by azimuthal phase term $\exp(il\varphi)$. Here, the integer number l stands for the winding number or topological charge of the vortex [1]. Particularly interesting are vortices generated in discrete systems [2]. They are specified by quantized topological charge and exhibit inherent robustness on perturbations within the system [3].

One of the structures that support discrete vortices is multi-core fiber (MCF) [4]. Here, we study MCF structure composed of two concentric hexagonal rings, A and B (Fig. 1). Beside equal coupling constants among nearest sites of A and B ring, we also consider a presence of artificial flux (Φ) which affects coupling between sites in the A ring [5]. The presence of artificial flux does not change the topological charge of vortices, only shifts their corresponding eigenvalues. Moreover, vortex excitation in one of the rings produces a regular periodical energy exchange between A and B rings in a form of stable breathing coupled-vortex structure. In passive MCF the vortex excitation is necessary to propagate vortex through the system. However, including the saturable gain and linear loss in the MCF, the vortices of different topological charge can be excited even from the uniform background by tuning the flux value. Numerical simulations show high robustness of newly formed vortices, which offers possibility to utilize the proposed setup as highly controllable vortex generator. Moreover, this can be of particular importance in the ring array based lasers [6,7].

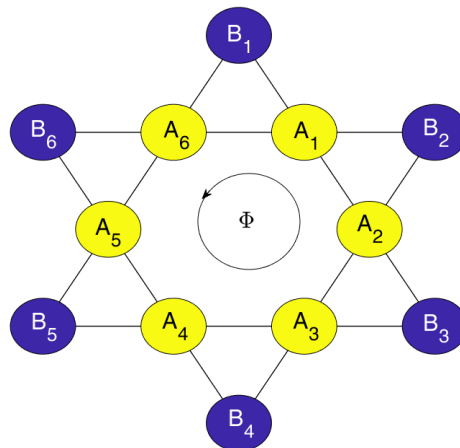


Figure 1. Schematic representation of nonlinear active MCF system with double rings A and B. Each ring has six cores. All couplings are equal (black solid lines between cores) and Φ represents artificial flux which additionally affects coupling between A sites.

REFERENCES

- [1] A. Pryamkov *et al.*, J. Eur. Opt. Soc. 17, 1 (2021).
- [2] P.P. Beliĉev *et al.*, Ann. Phys. 533, 2100108 (2021).
- [3] M. Soskin *et al.*, J. Opt. 19, 010401 (2017).
- [4] Lj. Hadžievski *et al.*, Light Sci. Appl. 4, 1 (2015).
- [5] S. Longhi, Opt. Lett. 39, 5892 (2014).
- [6] V. Dev, V. Pal, arXiv:2305.08410v1 (2023).
- [7] V. Pal *et al.*, Phys. Rev. Lett. 119, 013902 (2023).

Electric-field induced SHG (EFISHG) in graphene?

J. Woeste^{1,2}, N. Stojanovic² and M. Gensch^{1,2}

¹Technische Universität Berlin, Berlin, Germany

²Institut für Optische Sensorsysteme, DLR, Berlin, Germany

e-mail: michael.gensch@dlr.de

High harmonics generation (HHG) is a process which gives a direct insight into nonlinear properties of matter. Modern quantum materials like graphene or topological insulators attract considerable interest from scientific communities interested in the fundamental understanding of the often-exotic light-matter interactions as well as in the search for new technological applications. We mastered to study the nonlinear THz properties of such materials by means of THz emission spectroscopy e.g. single layer graphene [1]. The developed experimental set-ups allow one to determine the incident and re-emitted THz fields quantitatively with unique sensitivity levels. The results obtained for monolayer graphene can be explained by a simple thermodynamic model [1,2] and open up the technological possibility for purely electronic THz frequency synthesis within the present generation of graphene transistors operating at fundamental frequencies of a few hundred gigahertz. Recently our collaboration successfully showed that (i) the nonlinearity of graphene can be controlled over two orders of magnitude by applying moderate gate voltages in the sub-Volt regime [3] and (ii) that a specifically designed grating-graphene meta-material enables further increase in the THz nonlinearity via plasmonic field enhancement [4]. In these previous works, we have focused on studying nonlinearities of odd-order, since monolayer graphene is a centrosymmetric material, where even-order susceptibilities cancel out. As a next step we plan to investigate if an effective 2nd order nonlinearity can be efficiently generated by applying appropriate in-plane DC electric fields, thus breaking the inversion symmetry, such as what has recently been demonstrated and observed in GaAs [5]. Preparations for this experiment and its feasibility are discussed.

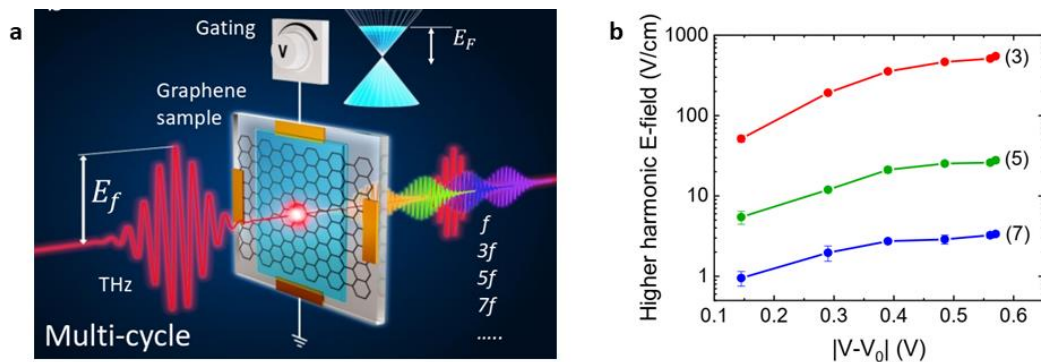


Figure 1. a) Schematics of the recent THz HHG experiment on the gated graphene sample. b) the peak electric field of the generated 3rd, 5th and 7th harmonics as a function of the gating voltage [3].

REFERENCES

- [1] H.A. Hafez *et al.*, Nature 561, 07 (2018).
- [2] Z. Mics *et al.*, Nat. Comm. 6, 7655 (2015).
- [3] S. Kovalev *et al.*, Science Adv. 7, eabf9809 (2021).
- [4] J.-C. Deinert *et al.*, ACS Nano 15, 1145 (2021).
- [5] K. Lee *et al.*, Adv. Opt. Mat. 8, 2000359 (2020).

Rogue wave clusters of the nonlinear Schrödinger equation composed of Akhmediev breathers and Kuznetsov-Ma solitons

S.N. Nikolić^{1,2}, S. Alwashahi³, N.B. Aleksić² and M.R. Belić²

¹Institute of Physics Belgrade, University of Belgrade, Pregrevica 118, 11080 Belgrade, Serbia

²Division of Arts and Sciences, Texas A&M University at Qatar, P.O. Box 23874, Doha, Qatar

³Faculty of Physics, University of Belgrade, Studentski trg 12, 11001 Belgrade, Serbia

e-mail: stankon@ipb.ac.rs

We analyze the various spatiotemporal patterns of rogue waves (RW) which may have the form of multi-elliptic clusters composed of Akhmediev breathers (AB) obtained on uniform background using the Darboux transformation (DT) scheme (Fig. 1). We solve the eigenvalue problem of the Lax pair of order n in which the first m evolution shifts are equal, nonzero, and eigenvalue dependent, while all eigenvalues' imaginary parts are close to one. We show that AB of order $n - 2m$ appears at the origin and can be considered as central rogue wave. We show that the high-intensity narrow peak, with the complex intensity distribution in its vicinity, is enclosed by m ellipses consisting of the first-order ABs. The number of maxima on each ellipse is determined by its index and solution order [1].

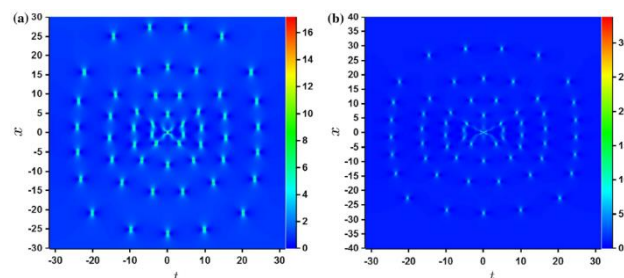


Figure 1. 2D color plots of rogue wave clusters on the uniform background having four ellipses ($m = 4$) around $n - 2m$ order rogue wave, formed at the origin of the (x, t) plane. The orders of DT and the Akhmediev breather representing the central peak are: (a) $n = 10$ with the second-order RW, and (b) $n = 11$ with the third-order RW.

We next show RW clusters composed of Kuznetsov-Ma solitons (KMS), characterized by strong intensity narrow peaks, which are periodic along the evolution axis [2]. These structures are calculated in DT scheme with commensurate frequencies when eigenvalues are greater than one (Fig. 2a). The second solution class exhibits a form of elliptical rogue wave clusters (MERWC). Similarly to AB case, the first solution class is obtained when the first m evolution shifts in the n^{th} order DT scheme are nonzero and equal. Here the high intensity peaks built on KMS of order $n - 2m$ periodically appear along the evolution axis. The central rogue waves are enclosed by m ellipses consisting of a certain number of the first-order KMS (Fig. 2b).

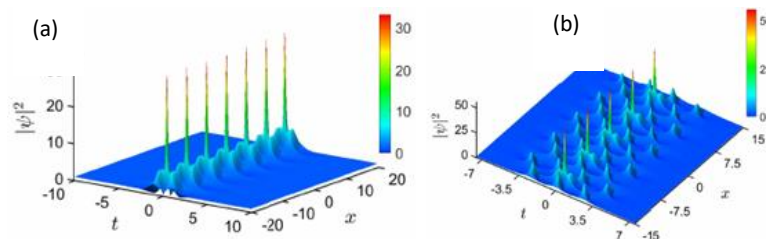


Figure 2. (a) The second-order KMS on a uniform background built from DT components with commensurate frequencies. (b) 3D intensity color plots of MERWC on the uniform background, having two ellipses ($m=2$) around the second-order central rogue waves ($n=6$).

REFERENCES

- [1] S.N. Nikolić *et al.*, *Nonlinear Dyn.* 108, 479 (2022).
 [2] S. Alwashahi *et al.*, *Nonlinear Dyn.* (2023), <https://doi.org/10.1007/s11071-023-08480-0>.

Counterpropagating rogue waves

M.S. Petrovic¹, N.B. Aleksic², A.I. Strinic^{1,2} and M.R. Belic²

¹*Institute of Physics, University of Belgrade, P.O. Box 68, 11080 Belgrade, Serbia*

²*Texas A&M University at Qatar, P.O. Box 23874, Doha, Qatar*

email: strinic@ipb.ac.rs

Extreme localized waves that suddenly appear and disappear in oceans without a trace are known as rogue waves. They are also observed in nonlinear optics, and nowadays it is accepted that rogue waves are adequately described by the cubic nonlinear Schrödinger equation (NLSE). Solutions of the cubic NLSE (Peregrine solitons, Kuznetsov-Ma breathers, Akhmediev breathers, higher order rogue waves, Fermi-Pasta-Ulam recurrent pulses...) are not rogue waves but can be used to model ones. For example, in [1,2] we used Peregrine solitons and Akhmediev breathers as inputs to demonstrate nonlinear Talbot effect from rogue waves.

It is expected that collision of two rogue waves, under some specific conditions, can produce more powerful rogue wave. Here, we investigated in details mutual interaction of two rogue waves travelling in the opposite directions.

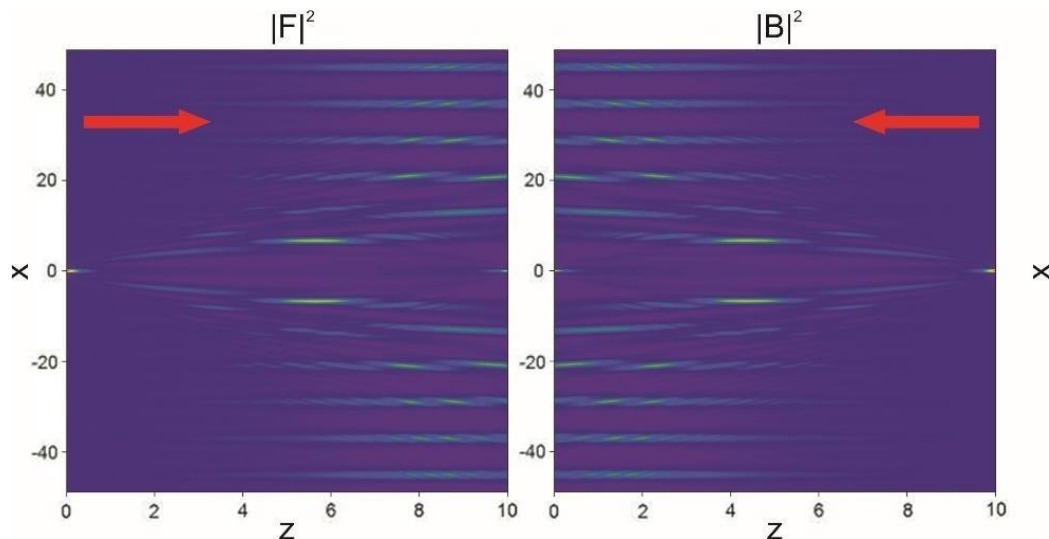


Figure 1. Counterpropagating rogue waves: input is Peregrine soliton for both forward (F) and backward (B) propagating beams.

REFERENCES

- [1] Y. Zhang *et al.*, Phys. Rev. E 89, 032902 (2014).
- [2] Y. Zhang *et al.*, Phys. Rev. E 91, 032916 (2015).

Solutions to nematic liquid crystals systems with cubic-quintic and septic nonlinearities using the Jacobi elliptic function expansion method

N. Petrović^{1,2}

¹*Institute of Physics, University of Belgrade, Pregrevica 118, 11080 Belgrade, Serbia*

²*Texas A&M University at Qatar, P.O. Box 23874, Doha, Qatar*

e-mail: nzpetr@ipb.ac.rs

Nematic liquid crystals (NLCs) are an important system for studying in nonlinear optics as these crystals allow many nonlinear phenomena to be explored due to a very large nonlinear response via the electro-optic effect [1]. In particular, spatial solitons, also known as nematicons [2], can easily be observed in NLCs and these nematicons have shown to be remarkably stable in the two transverse dimensions [3]. NLCs are generally described by a pair of interconnected nonlinear differential equations governing the behavior of the wave function of light and the angular tilt of the molecules of the crystal [4]. Of further interest is to study systems with cubic-quintic [5] and septic [6] nonlinearities in order to prevent the well-known spatiotemporal collapse of the system when there are two or more transverse dimensions [5]. Various methods have been proposed to solve the NLC system of differential equations, including the $\tan(\varphi/2)$ -expansion method [7], the modified simple equation method [8] and others [4,9].

In this work, we generalize the Jacobi elliptic function (JEF) expansion method, developed in [10] and [11], to find exact solutions to the NLC system of equations with cubic-quintic and septic nonlinearities. We apply the principle of harmonic balance to both the wave function and the angular tilt and apply matching conditions to obtain the degrees of these two functions in terms of the JEF. For the cubic-quintic nonlinearity the Jacobi function has a degree of 1, while for the septic nonlinearity it has a degree of $2/3$. Solitary and travelling wave solutions to the NLC system of equations with cubic-quintic and septic nonlinearities are obtained, both with and without chirp, which is the quadratic dependence of the phase of the solutions with respect to the transverse variables.

REFERENCES

- [1] G. Assanto *et al.*, Opt. Express 15, 5248 (2007).
- [2] G. Assanto *et al.*, Opt. Photonics News 14, 44 (2003).
- [3] M. Peccianti, G. Assanto, Phys. Rep. 516, 147 (2012).
- [4] M. Savescu *et al.*, J. Comput. Theor. Nanosci. 12, 4667 (2015).
- [5] A. Desyatnikov *et al.*, Phys. Rev. E 61, 3107 (2000).
- [6] Q. Zhou *et al.*, Chin. Phys. Lett. 39, 044202 (2022).
- [7] O.A. Ilhan *et al.*, Eur. Phys. J. Plus 135, 313 (2020).
- [8] A.H. Arnous *et al.*, Nonlinear Dyn. 88, 2863 (2017).
- [9] S. Duran, B. Karabulut, Alex. Eng. J. 61, 1695 (2022).
- [10] M. Belić *et al.*, Phys. Rev. Lett. 101, 123904 (2008).
- [11] N.Z. Petrović *et al.*, Opt. Lett. 34, 1609 (2009).

3. Optical materials

Centrosymmetric, non-symmorphic, non-magnetic, spin-orbit coupled layers without Dirac cones: a tight-binding example

V. Damljanović

Institute of Physics Belgrade, University of Belgrade, Pregrevica 118, Belgrade, Serbia

e-mail: damlja@ipb.ac.rs

It is believed that the existence of Dirac cones in the Brillouin zone (BZ) of time-reversal symmetric, two-dimensional (2D) materials with strong spin-orbit coupling (SOC) is closely connected with the presence of spatial inversion and non-symmorphic symmetry [1]. This belief is indeed confirmed in many cases published in the literature; however, a detailed group-theoretical analysis shows that this does not always hold [2]. Here we illustrate the mentioned fact by a tight-binding model from s-orbitals, on a structure that belongs to a non-symmorphic, gray, layer double group with spatial inversion. The band structure of the model consists of two double-degenerate bands touching only along a line at the BZ edge. Further, we show that neglecting SOC leads to unaltered Hamiltonian, up to numerical values of the parameters. Finally, we state some 2D materials described in the literature, with the symmetry of our model.

REFERENCES

- [1] S.M. Young, C.L. Kane, *Phys. Rev. Lett.* 115, 126803 (2015).
- [2] N. Lazić *et al.*, *J. Phys. A: Math. Theo.* 55, 325202 (2022).

Helical and square-spiral copper nanostructures: The effect of thickness and deposition conditions on the structural and optical properties

J. Potočnik, N. Božinović, M. Popović, M. Nenadović and M. Novaković
*Vinča Institute of Nuclear Sciences – National Institute of the Republic of Serbia, University of Belgrade,
Belgrade, Serbia*
e-mail: jpococnik@vin.bg.ac.rs

We have investigated the effect of thickness and deposition conditions on the structural and optical properties of nanostructured copper (Cu) thin films, deposited using e-beam glancing angle deposition. In the first series of experiments, samples were deposited in the form of helical nanostructures, to the thicknesses of 160 nm, 280 nm, 450 nm and 780 nm. The second set of the samples was fabricated in the form of zigzag and square-spiral nanostructures to a thickness of approximately 300 nm, by using different azimuthal rotations ($\varphi = 180^\circ, 90^\circ, 45^\circ, 22.5^\circ$ and 11°). Field-emission scanning electron microscopy and high-resolution transmission electron microscopy were utilized to explore morphological and structural properties, while optical studies were done using spectroscopic ellipsometry.

The results showed that for both series of the samples the deposited structures are porous with nanometer-sized particles. Detailed analyses of optical properties revealed that the thickness of the films had a significant impact on the dielectric function of Cu structures. With increasing the thickness from 160 nm to 780 nm the surface plasmon resonance (SPR) peak was shifted from 1.31 eV to 1.05 eV. Changes in SPR peak position were associated with the growth mechanism and the size of deposited nanostructures. For the second series of the samples, it was found that as the azimuthal rotation decreases, deposited nanostructures become more porous with larger number of grown arms. Optical analysis showed that the properties of the grown Cu films are greatly influenced by the deposition conditions. By decreasing the φ parameter, SPR peak was shifted from 1.19 eV to 0.75 eV, which can be correlated with the size distribution and agglomeration of Cu nanoparticles.

Luminescent lanthanide molecular materials for photonics applications

D. Mara

Institute of General and Physical Chemistry, Belgrade, Serbia

e-mail: dimitrije.mara@gmail.com

Luminescent lanthanide materials have been in use from the last decade of 19th century when the Austrian scientist Carl Auer von Welsbach has patented the light mantle called Auer mantle of Auer light [1]. From that time till now the luminescent lanthanide materials have found application in different fields of photonics from lasers, lighting, telecommunications, sensors to quantum applications [2].

Molecular luminescent lanthanide materials give wider range of the flexibility in use from the inorganic based luminescent lanthanide materials, as there is possibility of design of specific material for the application which it will be used for. Also, it is possible to introduce it into different more complex matrixes (such as sol-gels, polymers) or put them on the structured surfaces such as cavities or plasmonic structures.

Here, it will be presented short overview of some of my past, current and future research which is based on different type of luminescent lanthanide molecular materials and their applications. The first research is based on lanthanide β -diketonate complexes, second on the lanthanide hydrogen bonded organic frameworks (HOFs) and third is on the lanthanide metalorganic frameworks (MOFs) and their applications. Some of the applications which will be presented are on sensing in this case optical thermometry, lighting, telecommunications and on nonlinear optical properties such as second harmonic generation (SHG) and multiphoton fluorescence (MPF) materials which can have potential use in the quantum optics, telecommunications and computing [3,4].

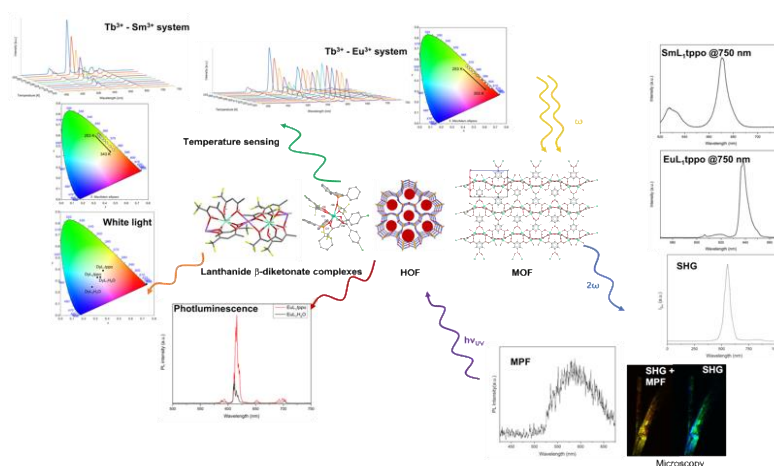


Figure 1. Linear and nonlinear optical response and applications.

REFERENCES

- [1] J.-C.G. Bunzli, I. McGill, Rare Earth Elements, Ullmann's Encyclopedia of Industrial Chemistry, American Cancer Society, pp. 1-53 (2018).
- [2] J.-C.G. Bunzli, Lanthanide Luminescence: From a Mystery to Rationalization, Understanding and Applications, Handbook of the Physics and Chemistry of Rare Earths, Chapter 287, Vol. 50, pp. 141-176. (2016).
- [3] J.F.C.B. Ramalho *et al.*, Lanthanides for the new generation of optical sensing and Internet of Things, Handbook of the Physics and Chemistry of Rare Earths, Chapter 324, Vol 61, pp. 31-128 (2022).
- [4] C. Cong, H. Ma, Adv. Opt. Mater. 9, 2100733 (2021).

Interference effect in surface modified ZnS nanoparticles / Poly (methylmethacrylate) nanocomposites

N. Romcevic¹, B. Hadzic¹, M. Curcic¹, V. Radojevic², N. Paunovic¹ and M. Romcevic¹

¹*Institute of Physics Belgrade, University of Belgrade, Belgrade, Serbia*

²*Faculty of Technology and Metallurgy, University of Belgrade, Belgrade, Serbia*

e-mail: branka@ipb.ac.rs

Surface modified ZnS nanoparticles / poly (methylmethacrylate) - (PMMA) nanocomposites were prepared by the solution casting method. The ZnS nanoparticles, as starting materials in the present study, were synthesized mechanochemically and their crystallite size was estimated as 2.3 nm. Surface modification of obtained nanoparticles was performed by 3-Mercaptopropyltrimethoxysilane.

We investigate thin samples of the nanocomposite material and of pure PMMA (about 290 μm) with strong interference effect, and corresponding thick samples, as reference. The optical properties of this material were studied by far-infrared spectroscopy. The analysis of the far-infrared reflectivity spectra was made by the fitting procedure, according to the model for a thin plate of nanocomposites in air. The dielectric function of the nanocomposites was modeled as a mixture of homogenous surface modified ZnS spherical inclusions in PMMA, by the Maxwell-Garnet formula. In the case of a PMMA thin sample, intense, well-defined interference was registered in the range of 90 to 200 cm^{-1} , while significantly weaker and less well-defined interference was registered in the range around 450 cm^{-1} . In the thin composite sample, in addition to the interference induced by sample thickness, interference induced by the existence of ZnS nanoparticles was also observed, located between TO and LO phonons of ZnS. This opens the possibility of applying nanocomposites in interferometry.

Metal ion-implanted TiN thin films: Induced effects on structural and optical properties

M. Popović¹, M. Novaković¹, D. Pjević¹, D. Vaňa², D. Jugović³ and P. Noga²

¹Department of atomic physics, Vinča Institute of Nuclear Sciences - National Institute of the Republic of Serbia, University of Belgrade, Belgrade, Serbia

²Slovak University of Technology in Bratislava, Faculty of Materials Science and Technology in Trnava, Advanced Technologies Research Institute, Trnava, Slovakia

³Institute of Technical Sciences of SASA, Belgrade, Serbia

e-mail: majap@vinca.rs

The ion implantation technique has a number of advantages over conventional methods for the improvement of thin films that offer the various possibilities of their use in different industrial and technological fields. Herein, we present the effects of metal ion implantation on the structural and optical properties of TiN thin films. TiN films of 170 nm thickness were grown by d.c. reactive sputtering on Si (100) wafers and then irradiated at 5×10^{16} ions/cm² with either Au, Ag, or Cu ions by using two different energies per each implanted metal. The results showed that as deposited TiN crystallizes in form of fcc cubic structure, with the crystallites preferentially oriented along the (111) plane. For all implanted layers the cubic crystallographic structure was preserved, but compared to as deposited TiN the crystallites were smaller and the lattice was contracted. Besides, the surface compositional analysis of as deposited sample showed the coexistence of TiN, TiO₂ and TiO_xN_y phases and this was related to the surface oxidation of the films due to the exposure to air. After implantation, the results were almost similar for all metals, showing an increase in TiO₂ contribution and the formation of pure metallic Au and Ag phases, while copper is in the Cu²⁺ state, which is attributed to Cu(II)-oxide and Cu(OH)₂. The microstructural characteristics including defect formation, changes in the crystallite size and lattice contraction, and also growth of different metallic phases during implantations were correlated with the findings of the optical characterization of the implanted films. For as deposited film we found energy gap of 2.91 eV, which was lower than the value typical for TiN. After implantation the gap was shifted to higher energies, while at the visible part of the region, additional energy levels, at photon energies below 2.9 eV were observed. Further, all implanted films showed degraded photocatalytic activity compared to as deposited TiN, among which Cu-implanted samples exhibited the best photocatalytic performances. The lower photocatalytic activity of Au and Ag-implanted films compared to Cu implantations was ascribed to larger structural defects and formation of less favorable electronic states.

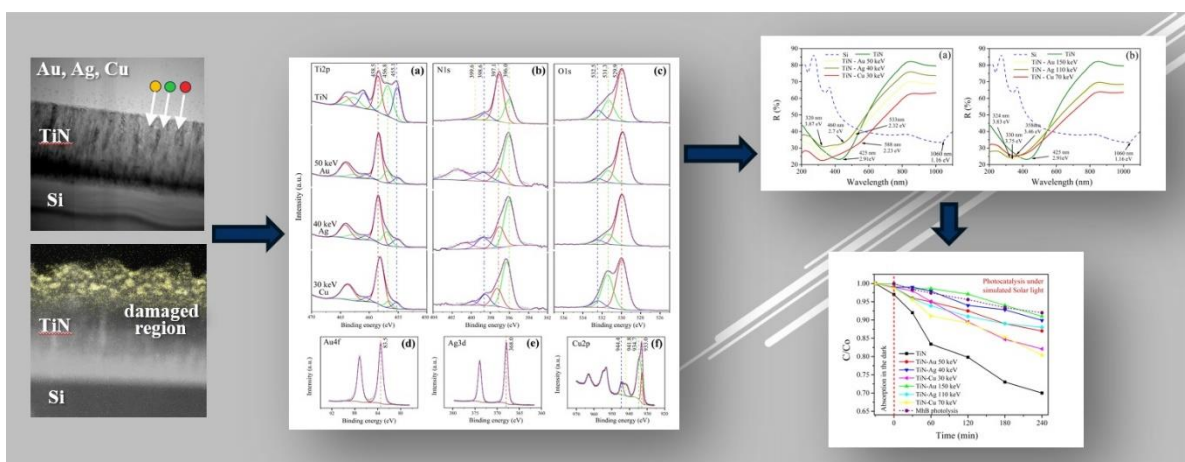


Figure 1. The results of structural, compositional and optical analyses of Au, Ag and Cu implanted TiN thin films.

Real-time fabrication of microstructures on the modified chitosan

B. Murić, S. Savić-Šević, A. Kovačević, D. Pantelić and B. Jelenković
Institute of Physics, Belgrade, Serbia
e-mail: muric@ipb.ac.rs

Chitosan is a natural polymer, partially deacetylated derivative of chitin extracted from crustacean shells, insoluble in pure water and organic solvents, but dissolves in diluted acidic solutions. Biocompatible, biodegradable and nontoxic nature of chitosan makes it a suitable polymer for various applications (biomedical, engineering, food, pharmacy, etc.) [1,2].

A simple and cheap method for preparing modified chitosan (MC) layer as ecofriendly, optically transparent, elastic, and durable material, for microstructures fabrication is presented. The anthocyanin food dye (E163) was used for MC layer sensitization makes it responsive to experimentally used blue laser light. The MC has no toxic effect, that confirmed by the biocompatibility test. The various microstructures were produced on the MC layer by direct focused laser radiation at 488 nm, with maximum output power of 100 mW, using homemade laser writing system. The fast produced concave or convex, aspheric microlenses (individual or closely packed arrays), microchannels, diffraction gratings, various complex structures etc. can be used directly, without any additional chemical processing and any waste, for a variety of applications such as: lab on a chip, medical laser, optical sensors, light-field cameras, security, biological structure, etc [3-5].

REFERENCES

- [1] A. Pellis *et al.*, Gels 8, 393 (2022).
- [2] B. Ozcelik *et al.*, Acta Biomater. 9, 6594 (2013).
- [3] S.T. Koev *et al.*, Lab. Chip 10, 3026 (2010).
- [4] R. D'Amato *et al.*, Sensors 21, 3348 (2021).
- [5] Z-Y. Hu *et al.*, Nat. Commun. 13, 5634 (2022).

Optimization of UV LED design using evolutionary algorithms

L. Leguay¹, H. Mączko², A. Schliwa¹ and S. Birner²

¹Institute of Solid-State Physics, Technical University of Berlin, Hardenbergstr. 36, 10623, Berlin, Germany

²Nextnano GmbH, Konrad-Zuse-Platz 8, 81829, Munich, Germany

e-mail: l.leguay@tu-berlin.de

In this study, we present a computational approach to optimize the design of UV-emitting LED devices based on nitride semiconductors. These devices show potential for various applications including surface sterilization, gas and disease detection, and water purification. But despite recent advances in the field, there remains a lot of room for improvement, particularly in terms of efficiency. We demonstrate that the performance of such UV LED devices can be enhanced using optimization algorithms paired with semiconductor calculation tools.

Specifically, we use the simulation software nextnano++ [1] in combination with an evolutionary algorithm [2] to optimize the design of LED nanostructures based on AlGaIn multiple quantum wells. Our findings reveal noteworthy improvements in the carrier current densities of the device with a significant increase of the theoretical internal quantum efficiency (IQE) at the target emission wavelength of 300 nm.

This work underscores the importance of ongoing research to improve the efficiency of UV LED devices and highlights the potential for optimization algorithms and semiconductor calculation tools in the development of high-performance UV LED devices with a range of practical applications.

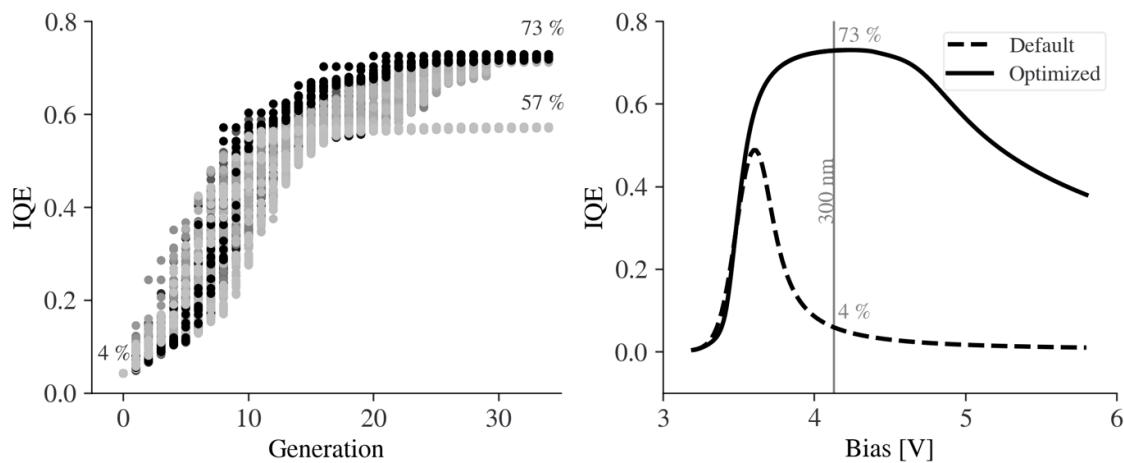


Figure 1. Evolution of the IQE through the multiple runs of the evolutionary algorithm (left) and comparison of the IQE of the default design and the optimized design (right).

REFERENCES

- [1] S. Birner *et al*, IEEE Trans. Electron Dev. 54, 2137 (2007).
- [2] H.G. Beyer, H.P. Schwefel, Nat. Comput. 1, 52 (2002).

Yellow fluorescent, water soluble N-doped graphene quantum dots: synthesis, photoluminescence and functionalization with L-Phenylalanine

Dj. Trpkov¹, D. Sredojević¹, D. Tošić¹, J. Pajović², D.K. Božanić¹ and V. Djoković¹

¹*Vinca Institute of Nuclear Sciences – National Institute of the Republic of Serbia, University of Belgrade, Belgrade, Serbia*

²*Faculty of Physics, University of Belgrade, Serbia*

e-mail: djordjet@vinca.rs

Graphene quantum dots, zero-dimensional form of graphene, have a band gap that can be controlled by changing their size, shape, edge morphology, number of layers etc. Moreover, they have various edge terminations that can be physically/chemically functionalized for numerous applications in nano electronics, biosensors, supercapacitors, and nanomedicine. In the present study, we hydrothermally synthesized nitrogen-doped graphene quantum dots (NGQD), using simple, fast synthetic route and eco-friendly chemicals, such as citric acid and urea (amine group-rich). The obtained NGQD were physically functionalized by L-phenylalanine, aromatic amino acid with interesting fluorescent properties. The hybrid NGQD-LPhe samples were characterized with UV/Vis, Raman, ATR Fourier transformed infra-red and photoluminescence (PL) spectroscopies, while their morphologies were studied by using atomic force microscopy. This work created a base for future investigations on graphene/biomolecules hybrids and their applications in fields of bioimaging and drug delivery. In addition, the experimental results were supported by DFT calculations of non-covalent stacking and hydrogen bonding interactions between NGQD and biomolecules.

Large thermally irreversible photoinduced shift of selective light reflection in hydrazone-containing cholesteric polymer systems

M. Cigl¹, A. Boychuk², V. Shibaev², V. Hamplová¹, V. Novotná¹ and A. Bobrovsky²

¹*Institute of Physics of the Czech Academy of Sciences, Prague, Czech Republic*

²*Department of Chemistry, Lomonosov Moscow State University, Moscow, Russia*

e-mail: cigl@fzu.cz

Stimuli responsive self-organized polymers are peculiar class of so-called “smart” materials demonstrating various types of mesomorphic structures easily controlled by external electric field, light or physical stimuli. In the present work we synthesized and studied a comb-shaped hydrazone-containing copolyacrylate exhibited cholesteric liquid crystalline properties with the pitch length of the helix being tuned under irradiation with light. In the cholesteric phase selective light reflection in the near IR spectral range (1650 nm) was measured and a large blue shift of the reflection peak from 1650 nm to 500 nm was found under blue light (428 or 457 nm) irradiation. This shift is related to the Z-E isomerization of photochromic hydrazone-containing groups and it is photochemically reversible. The improved and faster photo-optical response was found after copolymer doping with 10 wt % of low-molar-mass liquid crystal. In contrast to many other photochromic systems based on E-Z isomerization, the E and Z isomers of hydrazone photochromic group are kinetically stable that enable to achieve a pure photoinduced switch without any dark relaxation at any temperatures. The large photoinduced shift of the selective light reflection, together with thermal bistability, makes such systems promising for applications in photonics.

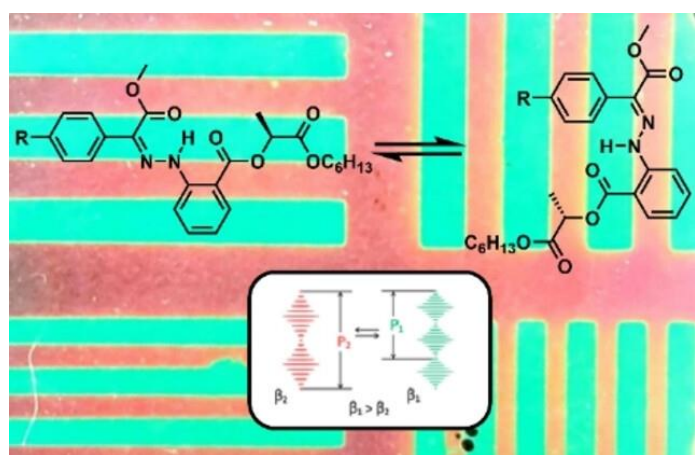


Figure 1. Hydrazone-containing copolyacrylate showing photoreversible large shift of the selective light reflection under blue and UV light irradiation.

REFERENCES

- [1] A. Bobrovsky *et al.*, *J. Mater. Chem. C* 2, 8622 (2014).
 [2] A. Boychuk *et al.*, *Chem. Phys. Chem.* 24, e202300011 (2023).

Strain-induced modulation of electronic and optical properties in hBN/group III monochalcogenide heterostructures

A. Solajic and J. Pesic

Laboratory for 2D Materials, Center for Solid State Physics and New Materials, Institute of Physics Belgrade,
University of Belgrade, Pregrevica 118, 11080 Belgrade, Serbia
e-mail: solajic@ipb.ac.rs

Van der Waals heterostructures, an intriguing class of materials composed of stacked two-dimensional layers held together by weak van der Waals (vdW) forces, have garnered significant attention in recent research. These structures exhibit a plethora of unique physics and novel effects that are absent in their constituent materials alone, rendering them highly promising for applications in modern nanodevices [1,2]. One of notable advantage lies in their remarkable manipulability – the weak nature of the vdW forces enables the easy manipulation of individual layers, offering precise control over their electronic and optical properties. This unprecedented level of control opens up a vast realm of possibilities for designing and fabricating materials with tailored characteristics, paving the way for numerous cutting-edge applications in modern nanodevices, including high performance transistors, solar cells, advanced lithium-ion batteries, and state-of-the-art light-emitting devices and photodetectors.

The application of strain provides even greater flexibility in tuning the properties of such structures, as well as exploiting them in devices such as highly precise sensors and detectors [3]. In this study, we focus on investigating novel heterostructures based on hBN and group III monochalcogenides (MX) subjected to biaxial strain. Some of them have shown exceptional potential for broad-spectrum absorbers [4], while the inclusion of hBN layer offers an excellent protection from oxidation, a common issue faced by MX materials when exposed to air. Using density functional theory, we investigate the effect of strain on their electrical and optical properties. Our findings reveal the profound impact of strain on the electronic structure, enabling precise fine-tuning of the band gap. Moreover, the absorption spectrum undergoes significant changes in response to different strain intensities, thereby enhancing specific regions of the absorption function.

REFERENCES

- [1] A.K. Geim, I.V. Grigorieva, *Nature* 499, 419 (2013).
- [2] Y. Liu, *Nat. Rev. Mater.* 1, 1 (2016).
- [3] J. Zhang *et al.*, *Phys. Chem. Chem. Phys.* 20, 17574 (2018).
- [4] A. Solajic, J. Pesic, *J. Phys. Condens. Matter* 34, 345301 (2022).

Anthocyanin-functionalized biopolymer films as pH-sensitive indicators

D. Tosić¹, R. Dojčić², D. Božanić², Dj. Trpkov¹ and V. Djoković²

¹Vinča Institute of Nuclear Sciences – National Institute of the Republic of Serbia, University of Belgrade, Mike Petrovića Alasa 12-14, 11351 Belgrade, Serbia

²Center of Excellence for Photoconversion, VINČA Institute of Nuclear Sciences – National Institute of the Republic of Serbia, University of Belgrade, Mike Petrovića Alasa 12-14, 11351 Belgrade, Serbia

e-mail: draganica@vin.bg.ac.rs

Anthocyanins are water-soluble, non-toxic flavonoid pigments, which produce the blue, red and purple color of many plants. Color change of anthocyanin extracts is a direct consequence of the transformation of their chemical structure when exposed to different pH conditions. Optical properties investigated in UV-Vis absorption and PL spectra show a clear difference between anthocyanins in acidic and in alkaline environments. Chitosan, a natural-based, non-toxic and biodegradable polysaccharide, is chosen as an ideal matrix for nanocomposites. It is proven to be a good carrier for anthocyanins, because of its ability to entrap the indicator dyes and at the same time the ability to release anthocyanins when in contact with an acidic environment.

In this research, we have developed anthocyanin-enhanced biopolymer indicator systems, which provide fast colorimetric response to alterations in pH levels of the environment. Transmittance spectra of nanocomposites show excellent light-blocking properties of the films. This opens up possibilities for advancement in future technology of smart biodegradable food packaging biomaterials. The availability of innovative and healthy materials reduces the need for using synthetic plastic in the modern food industry.

4. Biophotonics

Design of femtosecond microstructured Poly Lactic Acid temporal cellular scaffolds coated with hydroxyapatite by PLD method for bone tissue regeneration

L. Angelova¹, A. Daskalova¹, R. Mincheva², E. Filipov¹, A. Dikovska¹, M.H. Fernandes^{3,4} and I. Buchvarov⁵

¹*Institute of Electronics, Bulgarian Academy of Sciences, Sofia, Bulgaria*

²*Laboratory of Polymeric and Composite Materials (LPCM), University of Mons, Mons, Belgium*

³*LAQV/REQUIMTE, University of Porto, Porto, Portugal*

⁴*Faculdade de Medicina Dentaria, Universidade do Porto, Porto, Portugal*

⁵*Physics Department, Sofia University "St. Kliment Ohridski", Sofia, Bulgaria*

e-mail: lily1986@abv.bg

Temporary biocompatible and degradable cell scaffolds - the new tool of tissue engineering in the face of personalized medicine are emerging as one of the most powerful approaches for guided self-regeneration of injured, diseased or malfunctioning bone tissues. These structures serve as mechanically stable supporting platforms for patient's own cells attachment and proliferation and are gradually displaced by the newly formed bone tissue in an absolutely natural way. Femtosecond laser surface modification is a non-thermal and precisely controlled cell scaffold surface optimization technique, which does not change the chemical composition of the processed material, while finely tunes its topography properties, like wettability, charge, roughness and porosity. Due to its biocompatibility, biodegradability, mechanical stability and strength, Poly Lactic Acid (PLA) is gradually being established as a basic biomaterial in the design of temporary tissue engineered bone cell matrices. It represents a thermoplastic polyester of lactic acid, a natural non-toxic metabolic product, subject to carboxylic acid degradation pathway in the body. On the other hand, Hydroxyapatite (HA), the form in which calcium phosphate is naturally found in bones, is known for its osteoconductive properties and it is a key component in forming stable connection between the implants and the surrounding tissues, as it makes strong bond with them.

The aim of the present study is to create porous PLA-based temporal cellular scaffolds with specifically designed topographical orientation by means of femtosecond laser-induced microstructuring, additionally functionalized with thin layer of HA for application in bone tissue engineering. For this purpose, CPA Ti:sapphire fs laser system ($\tau = 150$ fs, $\lambda = 800$ nm, $\nu = 0.5$ kHz) was used for surface modification of PLA samples at fluence $F = 0.8$ J/cm² and scanning velocity $V = 3.8$ mm/s. A nanometric layer of HA was deposited on the patterned PLA matrices by pulse laser deposition (PLD) method for cell scaffolds surface additional functionalization. In order to monitor their complementary impact on the PLA scaffolds properties, both surface laser structuring and PLD were applied on the 2D PLA samples. Each laser processed PLA scaffold was analyzed in respect to control and laser processed surface, covered with HA. The multilevel structured scaffolds were investigated by SEM, EDX, 3D profilometer, AFM, and WCA analyses. Preliminary cell viability studies with MG-63 osteoblastic cell line were also performed. Moreover, the cellular behavior was compared with the one, seeded on Chitosan/Hydroxyapatite spin-coated fs microstructured PLA temporary cell scaffolds. Disordered spreading on smooth surfaces to a tendency of cell orientation and elongation along the laser created grooves was monitored. The results obtained show that such combined methods find application for functionalization of the bone PLA scaffolds, and can essentially improve the bioactivity properties of the as created microstructured PLA-hydroxyapatite nano designed hybrid cell matrices and their subsequent practical application in engineering of personalized bone tissue.

Non-linear excitation fluorescence imaging through two-photon laser polymerized microlenses

G. Chirico¹, M. Marini¹, R. Martínez Vázquez², R. Osellame², A. Nardini³, C. Conci³, E. Jacchetti³, D. Panzeri¹, L. Sironi¹, M. Bouzin¹, M. Collini¹, D. Inverso⁴, B.S. Kariman⁵, E. Kabouraki⁶, M. Farsari⁶, G. Cerullo⁵ and M.T. Raimondi³

¹Dept. of Physics, Università di Milano-Bicocca, Milan, Italy

²Institute for Photonics and Nanotechnologies (IFN)-, CNR Politecnico di Milano, Milan, Italy

³Dept. of Chemistry, Materials and Chemical Engineering "Giulio Natta", Politecnico di Milano, Milan, Italy

⁴Div. of Immunology, IRCCS San Raffaele Scientific Institute, Vita-Salute San Raffaele University, Milan, Italy.

⁵Dept. of Physics, Politecnico di Milano, Milan, Italy

⁶Forth- Institute for Electronic Structure and Lasers, Heraklion, Crete, Greece

e-mail: giuseppe.chirico@unimib.it

We report on methods for laser fabrication of microlenses by 2 Photon Polymerization (2PP) and their use for non-linear excitation microscopy. These lenses can help, once implanted, to reduce the spherical aberrations induced by the tissue in *in vivo* imaging.

Microlenses have already been fabricated by 2PP [1] but with too low numerical aperture to allow non-linear excitation microscopy. Therefore, up to now, no attempt has been made to use laser fabricated microlenses for non-linear excitation fluorescence microscopy of biological samples.

We show that microlenses with high numerical aperture (0.4) and large diameter (280 μm), can be fabricated with a medium throughput, about 8 minutes/lens, by limiting the 2PP fabrication to a $\approx 5 \mu\text{m}$ thick outer crust, followed by a post-development volume polymerization. This procedure leads to sufficient optical quality (roughness $\approx 80 \text{ nm}$) to use the lenses for fluorescence confocal and two-photon excitation microscopy. We report on the use of the microlenses for fluorescence non-linear excitation microscopy of cells cultures (Figure 1) and thick specimens [2].

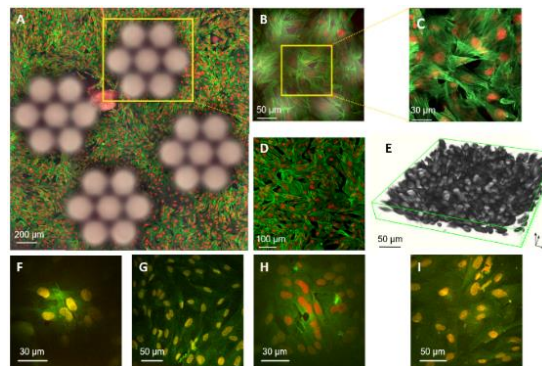


Figure 1. A: Confocal image of human fibroblasts (FITC-phalloidin, cytoskeleton and DRAQ5/Hoechst, nuclei staining). B: fluorescence confocal image through a microlenses array. C: Cropped scan area through a single microlens. D: Full field-of-view confocal microscope image of cells at the glass coverslip focal plane (20x dry objective for A-D). E: 3D reconstruction of cells through an array of microlenses. F-I: Fluorescence images of the cells under two-photon excitation ($\lambda = 800 \text{ nm}$). F: Fluorescence image through the microlenses coupled to a 20x dry objective. G: Control image through the 20x dry objective. H: Image of the cells through the microlenses coupled to a 25x water immersion objective. I: Control image through the 25x water immersion objective.

This work opens the possibility to use implanted micro-lenses for non-linear excitation of tissues, allowing the direct and continuous optical inspection of biological dynamics *in vivo*.

REFERENCES

- [1] D. Gonzalez-Hernandez *et al.*, Adv. Opt. Mater. 2300258 (2023).
 [2] M. Marini *et al.*, Adv. Fun. Mater. 2213926 (2023).

SERS-based immunosensor for sensitive detection of cancer protein biomarkers in serum

M. Kahraman¹, A.M. Saridağ¹ and I.D. Karagoz²

¹*Department of Chemistry, Gaziantep University, Gaziantep, Turkey*

²*Department of Biology, Gaziantep University, Gaziantep, Turkey*

e-mail: mskahraman46@gmail.com

Cancer is one of the most life-threatening diseases worldwide. There is a great interest to detect and monitor cancer biomarkers such as circulating proteins, cells and exosomes in serum or blood in medical diagnostics and therapies. Recently, there is a great attention on the development of simple, fast and sensitive detection methods for the circulating protein biomarkers [1]. Surface-enhanced Raman scattering is one of the promising techniques for the detection and monitoring the circulating proteins due to its sensitive and multiplexing capability [2]. SERS-based immunosensor is widely used for the medical diagnostics and detection of biological molecules, and structures. In this study, SERS-based immunosensor is developed for the detection of circulating cancer protein biomarkers such as human epidermal growth factor receptor 2 (HER2), mucin 4 (MUC 4), and prostate-specific antigen (PSA). For this purpose, layer-by-layer assembly method is used to modify natural diatomite surfaces with AgNPs to obtain SERS active platform as an immunosensor substrate. The prepared surfaces are modified with the specific antibodies to capture HER2, MUC4 and PSA antigens. Then, SERS tags are prepared having different Raman active molecules to obtain SERS signal in the presence of target proteins. Finally, SERS measurements are obtained when the sandwich form occurs. As a result of the measurements, it is possible to detect protein biomarkers down to 0.1 ng/mL. In conclusion, we developed a fast, simple, inexpensive, and sensitive method for the detection of circulating cancer protein biomarkers in serum. The developed SERS-based immunosensor can be used for the detection of circulating biomarkers.

REFERENCES

- [1] G. Wang *et al.*, *Anal. Chem.* 83, 2554 (2011).
- [2] K. Kamil Reza *et al.*, *Small* 13, 1602902 (2017).

Fabrication of flexible diatomite-based SERS active platforms

A.M. Sarıdağ and M. Kahraman

Department of Chemistry, Gaziantep University, Gaziantep, Turkey

e-mail: ayseminesaridag@gmail.com

Surface-enhanced Raman Scattering (SERS) is an emerging analytical technique used for characterization of biological and non-biological structures. Plasmonic properties of nanostructures are main factors influencing SERS performance. Thus, fabrication of plasmonic nanostructures having different plasmonic properties is a significant research interest. Recently, guided-mode resonances (GMRs) in diatom frustules have significant attention due to their potential contribution to SERS enhancement. Furthermore, there is also evidence showing that diatom frustules can be utilized in improving SERS enhancement by optically coupling the GMRs of the diatom frustules with the LSPRs of the nanostructures. In this study, inexpensive, robust, and flexible natural diatomite-based SERS platforms having different number of layers on a box tape are fabricated using layer-by-layer assembly of silver nanoparticles (AgNPs). The fabricated SERS platforms are characterized using UV-Vis spectroscopy and scanning electron microscopy (SEM). The SERS performance of the platforms was evaluated using 4 aminothiophenol (4-ATP) and rhodamine-6G. The results demonstrate that SERS performance of the platforms is dependent on the number of layers of the structures. The SERS platform having highest SERS activity can be used for the characterization of any molecules of interest.

Development of two-dimensional superresolution fluorescence microscope with structured illumination

A. Denčevski, A.J. Krmpot and M.D. Rabasović
Institute of Physics Belgrade, University of Belgrade, Belgrade, Serbia
e-mail: aleksa.dencevski@ipb.ac.rs

Structured Illumination Microscopy - SIM is a wide-field microscopy technique that enables imaging of biological samples with a lateral resolution better than the diffraction limit [1]. In this paper, we present a low-cost, custom-made superresolution fluorescent microscope which enables recording of images in two modes: epifluorescence mode and superresolution mode. Images taken in epifluorescence mode have a resolution that is slightly above the diffraction limit, while superresolution images are taken with a resolution significantly below the diffraction limit.

This microscope is basically a conventional epifluorescence microscope with the addition of specially designed diffraction grating. The excitation of the microscope is designed so that simultaneous imaging of samples at different excitation wavelengths is possible. An independent controlling system with microcontrollers was developed for this microscope. Controlling system was specifically designed to synchronously activate laser diodes, initialization of camera exposure, as well as a system for rotating diffraction grating, with the aim that biological samples are exposed to laser radiation only during image recording. On the other hand, the software of this microscope enables all users to quickly control all parts of the system as well as reconstruct recorded images. A significant application of this technique is in the recording of various biological samples [2], non-invasively, with minimal photobleaching and phototoxicity of the samples while using low laser power.

REFERENCES

- [1] M. Saxena *et al.*, Adv. Opt. Photonics 7, 241 (2015).
- [2] M. Iwai *et al.*, Plant J. 96, 233 (2018).

Smart optical assay based on novel bioorthogonal SERS nanoprobe for the β -amyloid peptide quantification

C. Dallari^{1,2}, C. Credi^{1,3} and F.S. Pavone^{1,2,3}

¹European Laboratory for Non-Linear Spectroscopy (LENS), Florence, Italy

²Department of Physics, University of Florence, Florence, Italy

³National Council of Research (INO-CNR), Sesto Fiorentino, Italy

e-mail: dallari@lens.unifi.it; caterina.dallari@unifi.it

To date, the early diagnosis will likely to be the most effective therapy for Alzheimer's disease (AD) since it can ensure timely pharmacological treatments that can reduce the irreversible impairment while delaying the AD symptoms [1]. Amyloid β -peptides ($A\beta$) are recognized as key pathological AD biomarkers present in different biological fluids, but their detection still relies on expensive or low-accuracy assays. In this context, optical detection techniques based on surface enhanced Raman spectroscopy (SERS) through advanced nanoconstructs have gained rising attention for the development of alternative methods for the targeting of $A\beta$ peptides in fluids [2]. Here, a multilayered nanoprobe constituted by bioorthogonal Raman Reporters (RRs) embedded within gold nanoparticles ($Au@RRs@AuNPs$) has been developed and successfully validated for specific detection of β -amyloid peptide ($A\beta$) in the human cerebrospinal fluid (CSF) with accuracy in the clinical range of interest, high selectivity and sensitivity down to pg/ml. These are guaranteed by the intrinsic properties of the bioorthogonal RRs working in the Raman background-free spectral region and remaining stable within the two layers of gold, a key point for quantitative SERS. Then, the selective aggregation behavior in the presence of the targeted analyte is exploited for $A\beta$ quantification considering that its concentration is proportionally reflected in Raman intensity changes. Finally, the proposed nanoplatform combines the typical speed of Raman measurements, providing high specificity and sensibility and representing a significant step ahead of the state of the art on SERS for clinical analyses.

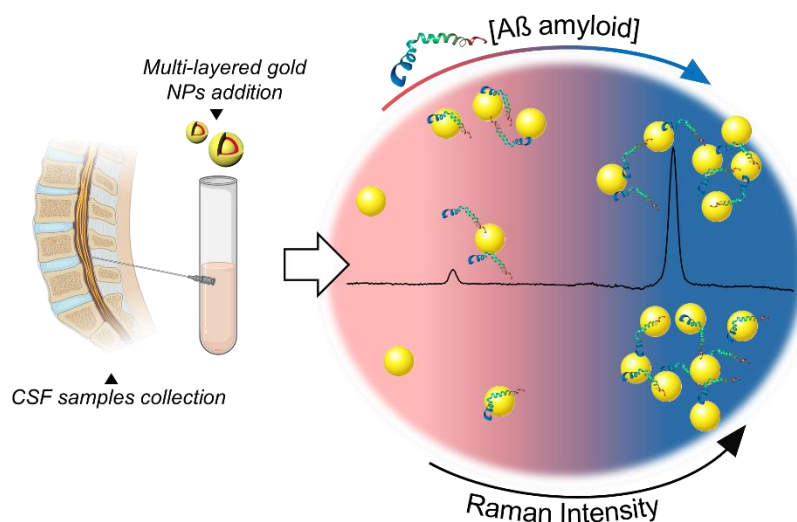


Figure 1. Graphical scheme representing the working principle of multilayered RRs@AuNPs for the early-stage detection of Alzheimer's Disease through the screening of $A\beta$ (1-42) in the cerebrospinal fluid.

REFERENCES

- [1] H. Braak, E. Braak, *Brain Pathol.* 1, 213 (1991).
- [2] L. Cheng *et al.*, *ACS Appl. Mater. Interfaces* 10, 34869 (2018).

Bioactive compounds of *Carlina acanthifolia* roots obtained by fractional extraction and their 3D fluorescence spectra

N. Petkova¹, I. Ivanov¹, E. Saralieva¹, D. Georgieva², K. Nikolova², T. Eftimov^{3,4}, G. Gentscheva⁵ and L. Vladimirova–Mihaleva⁶

¹University of Food Technologies, Plovdiv, Bulgaria

²Medical University, Varna, Bulgaria

³Université du Québec en Outaouais, Gatineau, Québec, Canada

⁴Central Laboratory of Applied Physics, Bulgarian Academy of Sciences, Plovdiv, Bulgaria

⁵Medical University, Pleven, Bulgaria

⁶Sofia University “St. Kliment Ohridski”, Sofia, Bulgaria

e-mail: kr.nikolova@abv.bg

Carlina acanthifolia. is widely used in traditional medicine due to the presence of essential oil (1-2 %) in the outer part of the roots of the plant. It is mainly used for its choleric and anti-inflammatory properties, as well as for the treatment of gastrointestinal problems. We obtain the fractions by sequential extraction with different solvents (hexane, chloroform, ethyl acetate, ethanol, and water) from carline thistles (*Carlina acanthifolia*) roots, evaluate the phytochemical compounds, and for the first time, we report here the 3D fluorescence excitation-emission spectra. The highest yield (11.02 %) was obtained by using 95 % ethanol. The highest extractive content of total phenols, flavonoids, and derivatives of economic acids was found in the ethyl acetate fraction. Three phenolic acids were detected in the ethyl acetate fraction – chlorogenic, *p*-coumaric, and sinapic acids, as chlorogenic acid was dominating among the others (16.06 mg/g extract). These fractions demonstrated the highest antioxidant potential and the fluorescent properties of the roots are related to them. The topographic view of the excitation-emission matrix (EEM) presented in Figure 1a outlines a large strong first maximum ($\lambda_{em,1} = 570$ nm for $\lambda_{ex,1} = 470$ nm) and a weaker narrower second one ($\lambda_{em,2} = 595$ nm for $\lambda_{ex,2} = 640$ nm). The emission spectrum of the main maximum is rather large at a 90 % level ($\delta\lambda_{em,1} = 60$ nm) but is observed over a narrow excitation bandwidth ($\delta\lambda_{ex,1} = 25$ nm) (Table 1). The Stokes shift $\Delta\lambda$ is around 100 nm. The energy diagram is shown in Figure 1b, with the darker areas representing the 90 % level of the larger maximum.

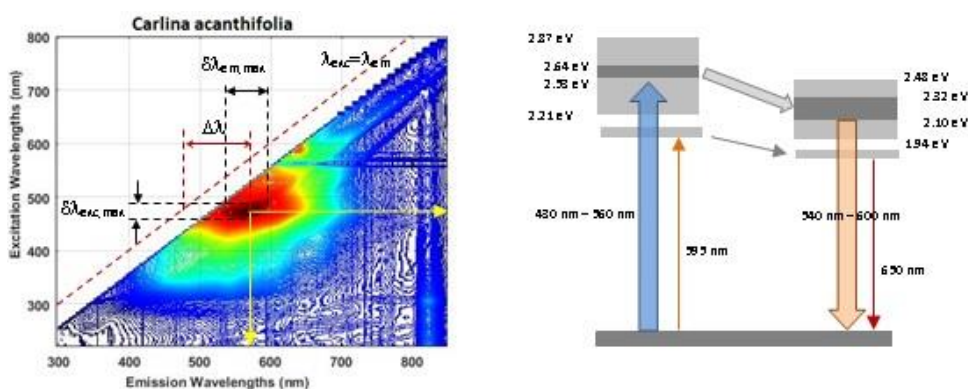


Figure 1. Fluorescence excitation-emission matrix (EEM) from *Carlina*. a) Topographic view b) Energy diagram.

Table 1. Important fluorescence maxima.

$\lambda_{ex,1}$ (nm)	$\delta\lambda_{ex,1}$ (nm)	$\lambda_{em,1}$ (nm)	$\delta\lambda_{em,1}$ (nm)	$\Delta\lambda$ (nm)	$\lambda_{ex,2}$ (nm)	$\lambda_{em,2}$ (nm)
470	25	570	60	100	595	640

Carbon quantum dots/silver based metal organic framework composites in light enhanced wound healing

I. Popović¹, A. Valenta Šobot², J. Filipović Tričković², L. Korićanac³, J. Žakula³, V. Ralić¹, A. Abu el Rub¹, M. Algarra⁴, M. Petković¹, M. Stepić¹ and M.D. Nešić¹

¹Center for Light-Based Research and Technologies COHERENCE, Department of Atomic Physics, Vinča Institute of Nuclear Sciences - National Institute of the Republic of Serbia, University of Belgrade, Belgrade, Serbia

²Department of Physical Chemistry, Vinča Institute of Nuclear Sciences - National Institute of the Republic of Serbia, University of Belgrade, Belgrade, Serbia

³Department of Molecular Biology and Endocrinology, Vinča Institute of Nuclear Sciences - National Institute of the Republic of Serbia, University of Belgrade, Belgrade, Serbia

⁴INAMAT2—Institute for Advanced Materials and Mathematics, Department of Science, Public University of Navarre, Pamplona, Spain

e-mail: ivavukicevic@vin.bg.ac.rs

In recent years researchers have developed new strategies to enhance the effectiveness of wound healing by combining nanoparticles and infra red (IR) light. For example, some studies have shown that nanoparticles can be used to enhance the absorption of near-infrared laser (NIR) light by tissues, leading to increased healing rates [1].

The influence of NIR light on proliferation, collagen production, and wound healing was tested on: keratocytes (HaCaT) and fibroblasts (MRC-5) cells that are used as model systems of human skin equivalents that comprise an epidermal and a dermal compartment of skin. Also, these cells were treated with carbon quantum dots/silver-based metal-organic framework composites (Ag-MoFs-NCDs and Ag-MoFs-SCDs), which previously showed high antibacterial activity [2], without and with laser light.

Firstly, we have found the most convenient and effective CW laser intensity (16 mW/cm^2) and illumination time (3 minutes), which is not too high and short enough to influence human cells' proliferation and metabolism positively. Additional chemical treatment with Ag-MoFs-NCDs and Ag-MoFs-SCDs results in a further increase in human cell viability. Our measurements showed that the proliferation index in laser-illuminated cells and cells treated with Ag-MoFs-SCDs was at the level of the untreated control. Furthermore, Ag-MoFs-SCDs treatment and laser illumination induced a mild, insignificant increase in cellular proliferation. On the other hand, Ag-MoFs-NCDs treatment led to a more pronounced, albeit not significant increase, in cellular proliferation, while Ag-MoFs-NCDs treatment combined with laser illumination significantly increased proliferation.

Also, we have detected a mild change in collagen level estimated by hydroxyproline assay, which may indicate a positive outcome of combined laser illumination and treatment, taking into account that after 48 hours, a change in cell's response to the treatment could be noticed. Finally, based on migration assay, we observe a complete wound closure after 48 hours in fibroblast cells treated with Ag-MoFs-NCDs and near-infrared laser light, Fig. 1.

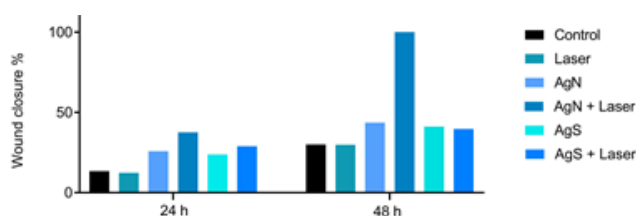


Figure 1. Percentage of wound closure after 24 hours (a) and 48 hours (b).

REFERENCES

- [1] Y. Qiao *et al.*, ACS Appl. Mater. Interfaces 10, 1 (2018).
 [2] N.A. Travlou *et al.*, Appl. Bio Mater. 1, 693 (2018).

Anti-cancer and imaging potential of fluorescent black carrot Carbon Dot nanoparticles

M.D. Nešić¹, J. Filipović Tričković², A. Valenta Šobot², J. Žakula³, L. Korićanac³, I. Popović¹, J. Soto⁴, M. Algarra⁵, V. Ralić¹, A. Abu el Rub¹, M. Matijević¹, M. Stepić¹ and M. Petković¹

¹Center for Light-Based Research and Technologies COHERENCE, Department of Atomic Physics, Vinča Institute of Nuclear Sciences - National Institute of the Republic of Serbia, University of Belgrade, Belgrade, Serbia

²Department of Physical Chemistry, Vinča Institute of Nuclear Sciences - National Institute of the Republic of Serbia, University of Belgrade, Belgrade, Serbia

³Department of Molecular Biology and Endocrinology, Vinča Institute of Nuclear Sciences - National Institute of the Republic of Serbia, University of Belgrade, Belgrade, Serbia

⁴Department of Inorganic Chemistry, Faculty of Sciences, University of Málaga, Málaga, Spain

⁵INAMAT2—Institute for Advanced Materials and Mathematics, Department of Science, Public University of Navarre, Pamplona, Spain
e-mail: maki@vin.bg.ac.rs

Carbon Dots (CDs) are biocompatible, fluorescent, water-soluble, and stable nanoparticles with a high potential to be used for vast biomedical applications [1,2]. We explore the application of CDs produced from natural sources, black carrots, as anti-cancer and imaging agents.

These nanoparticles suppress cell growth of three different cancer cell lines, cervical (HeLa), pancreatic (PANC-1), and melanoma (A375) cell lines *in vitro*. However, the cytotoxic effect against A375 cells stands out, with only 20% of viable cells left after treatment (Fig.1(a)), antimetastatic potential, and a selectivity index higher than two, which indicates that the efficacy against melanoma cells is significantly greater than the toxicity against non-malignant cells (MRC-5).

Furthermore, after the cellular uptake, green fluorescence was visible in the cytosol of A375 cells (Fig. 1 (b)). On the other hand, the DAPI stain for DNA was visible as a blue light in the cell nucleus. Moreover, cells with a higher intensity of green fluorescence in the nucleus, Fig. 1 (c) indicated with arrows, were the cells with condensed chromatin in the mitotic phase of the cell cycle (Fig. 1 (d) and (e)), which indicates that CDs interact with chromatin and that they could be used as a marker of cells mitosis and proliferation.

In summary, we have demonstrated the great anti-cancer potential of black carrot CDs, for image-guided anti-cancer therapy of melanoma that can be used to recognize cell proliferation.

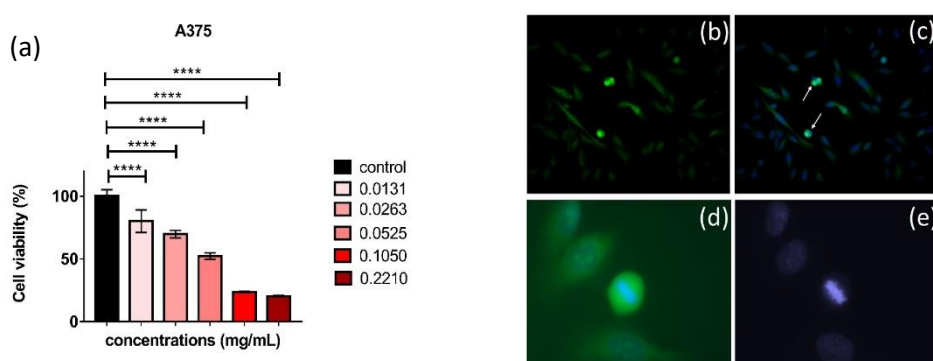


Figure 1. CDs cytotoxicity (a) and Fluorescence Microscopy image of A375 cells treated with CDs, stained with DAPI, and acquired with green (b) and merged blue and green channels (20x magnification). 100x magnified region of cell with a higher intensity of green fluorescence (d), also acquired with blue channel (e).

REFERENCES

- [1] J. Liu *et al.*, ACS Cent. Sci. 6, 2179 (2020).
- [2] H. Ehtesabi *et al.*, Microchim. Acta. 187, 150 (2020).

In search of conditions for Gd-TiO₂ activation by light irradiation in photodynamic treatment of pancreatic cancer cells

A. Abu el Rub¹, M.D. Nešić¹, J. Žakula², V. Ralić¹, M. Petković¹, I. Popović¹, M. Matijević¹, M. Radoičić³ and M. Stepić¹

¹Center for Light-Based Research and Technologies COHERENCE, Department of Atomic Physics, Vinča Institute of Nuclear Sciences - National Institute of the Republic of Serbia, University of Belgrade, Belgrade, Serbia

²Department of molecular biology and endocrinology, Vinča Institute of Nuclear Sciences - National Institute of the Republic of Serbia, University of Belgrade, Belgrade, Serbia

³Department of radiation chemistry and physics, Vinča Institute of Nuclear Sciences - National Institute of the Republic of Serbia, University of Belgrade, Belgrade, Serbia

e-mail: anamarija.abuelrub@vin.bg.ac.rs

With difficulty in early diagnosis, inaccessibility for the surgical approach, and high resistance to radio and chemotherapies, the resulting low treatment success rates are calling for new approaches in treating pancreatic cancer [1]. Photodynamic therapy (PDT), with the use of light or X-rays, is a method that has the potential to help overcome the problems that existing approaches meet [2,3]. Through activation of photo-sensitive particles with irradiation, PDT helps the production of reactive oxygen species, consequently stimulating cell death. We have synthesized and characterized Gadolinium-doped titanium dioxide nanoparticles (Gd-TiO₂ NPs) and tested them as photosensitizers on two pancreatic cancer cell lines, MIA PaCa-2 and PANC-1. Different concentrations of NP treatment, irradiation powers, and times of irradiation were trialed as parameters of activation. Cell viability was measured 48h after treatments, and although some results implied a slight decrease in the viability of treated cells, we have met difficulties in obtaining consistency in results. Statistical significance in the decrease of the viability of treated cells in most cases was not attained, suggesting that higher concentrations or irradiation power and longer illumination time might be needed to achieve a positive PDT effect with this NP system.

REFERENCES

- [1] W. Park *et al.*, JAMA 326, 851 (2021).
- [2] A.G. Niculescu, A.M. Grumezescu, Appl. Sci. 11, 3626 (2021).
- [3] W. Sun *et al.*, Theranostics 10, 1296 (2020).

Quantum sensing and imaging with entangled photons

B. Jelenković

Institute of Physics, Belgrade, Serbia

e-mail: branaj@ipb.ac.rs

Quantum correlated and entangled photons have raised increasing interest due to its important applications in sensing, imaging, security protocols. Imaging schemes based on entangled photons demonstrate increased optical resolution and sensitivity, compared to imaging with classical light. Different protocols with quantum light are being developed to take properties of entangled photons and create images with photons that have never encounter imaging object. The other photon from a pair, that has interacted with an object, can be either detected (ghost imaging, GI) or not detecting at all (quantum imaging with undetected photons, QIUP).

We present two most used methods for generating quantum correlated, energy and momentum entangled photon pairs: four-wave mixing (FWM) in alkali gases [1], and spontaneous parametric down conversion (SPDC) in nonlinear crystals.

We show advantage of using entangled photon pairs from FWM for two-photon absorption for nonlinear microscopy, in enhancing fluorescence rate by the biological sample, nearly 50 folds compared with classical (random) two-photon absorption [2]. We explain how GI harness quantum properties of photons from SPDC to go beyond quantum noise limit, an important property when imaging with low photon flux. Finally, we present the main benefits of QIUP for imaging and sensing, using highly frequency non-degenerate photon pairs from SPDC.

REFERENCES

- [1] M. Ćurčić, B. Jelenković, *Opt. Commun.* 533, 129301 (2023).
- [2] T. Li *et al.*, *Appl. Phys. Lett.* 116, 254001 (2020).

Optical skin biopsy through multispectral approach and prototype device

Ts. Genova¹, V. Mircheva¹, Al. Zhelyazkova¹, A. Markovski² and P. Troyanova³

¹*Institute of Electronics, Bulgarian Academy of Sciences, Sofia, Bulgaria*

²*Technical University of Sofia, Sofia, Bulgaria*

³*University Hospital "Tsaritsa Yoanna" - ISUL, Sofia, Bulgaria*

e-mail: ts.genova@gmail.com

A plethora of optical techniques have been researched and developed for application as a so-called "red-flag" technique for assessment of skin lesions and skin cancer. However, the implementation of those techniques in the standard clinical practice is an overwhelming challenge by itself. We have used our long-standing experience in researching the diagnostically valuable spectral peculiarities of skin lesions in order to develop a device for "optical biopsy". Additionally, it is paired with feasible algorithm for differentiation not only between cancer and healthy skin, but also between the different types of skin lesions. The differentiation is based on fluorescence spectra and diffuse reflectance spectrum of the investigated lesion and the adjacent healthy skin. The applied excitation wavelengths are 365 nm, 385 nm and 405 nm, the light source for the diffuse reflectance spectroscopy is in the range of 400-780 nm.

In this work we will evaluate the realistic clinical scope of application of a prototype device for "optical biopsy". The device and differentiation algorithm were tested in clinical environment for two years. Here by we will present the advantages, drawbacks and improvement strategies for further development towards clinical application.

Novel approach for colon cancer detection through fluorescence spectroscopy

Ts. Genova¹, Al. Zhelyazkova¹, B. Vladimirov² and N. Pankov²

¹*Institute of Electronics, Bulgarian Academy of Sciences, Sofia, Bulgaria*

²*Technical University of Sofia, Sofia, Bulgaria*

³*University Hospital "Tsaritsa Yoanna" - ISUL, Sofia, Bulgaria*

e-mail: ts.genova@gmail.com

In this work we will present the application of classification algorithm – support vector machine (SVM) and multispectral analysis (MA) for identification of diagnostically valuable autofluorescence peculiarities of colon cancer tissues *ex vivo*. The autofluorescence spectral properties of cancerous and healthy colon tissue were obtained with two techniques – excitation-emission matrices and synchronous fluorescence spectroscopy (SFS) in a broad spectrum range.

The analysis of fluorescence spectra of cancerous and healthy colon tissue through SVM algorithm and MA allowed us to determine diagnostic parameters for differentiation between cancerous and healthy tissue. The excitation wavelengths, among those applied through excitation-emission matrices, which provide greatest contrast between cancerous and healthy colon tissue were identified as 310, 340, 370 and 420 nm. For the data obtained with SFS, the spectra with offsets of 60, 90 and 120 nm delivered differentiation with accuracy of 90 %. Further, the application of MA on this data allowed recognition of cancerous and healthy colon tissue, based on its fluorescence with diagnostic accuracy up to 95 %.

Fluorescence contrast between healthy and cancerous colon tissue is based on biochemical and morphological alterations. We recognize tryptophan and collagen as endogenous fluorophores with most significant contribution for differentiation of colon abnormalities and cancer detection.

***In vivo* multiphoton imaging of a filamentous fungus *Phycomyces blakesleeanus*: the effect of small ambient temperature increase on mitochondrial morphology and lipid droplets density**

T. Pajic¹, S. Kozakijevic¹, A.J. Krmpot², M. Zivic¹, N.V. Todorovic³ and M.D. Rabasovic²

¹Faculty of Biology, University of Belgrade, Serbia

²Institute of Physics Belgrade, University of Belgrade, Serbia

³Institute for Biological Research "Siniša Stanković", University of Belgrade, Serbia

e-mail: tpajic@bio.bg.ac.rs

Mitochondrial function, and consequently cellular metabolic status and fitness of a cell, is tightly linked to the dynamic changes of mitochondrial morphology, including mitochondrial fusion, fission and mitophagy [1]. Lipid droplets (LDs) can be in close contact with mitochondria, and accumulate autophagy or mitophagy generated material during the reparatory processes [2]. The effect of increased ambient temperature on mitochondrial morphology and LDs density in living cells of the filamentous fungus *Phycomyces blakesleeanus* was investigated. For *in vivo* imaging of mitochondria and LDs multiphoton microscopy was used. Multiphoton microscopy enables 3D imaging in high resolution and reduced photodamage and photobleaching of the sample using IR ultrafast pulsed lasers. Mitochondria were stained with the vital dye Rhodamine123 (Rh123) which enters these organelles based on their membrane potential - mitochondria must be healthy/active to stain. A wavelength of 800 nm from Ti:Sa laser (160 fs pulse duration, 76 MHz repetition rate) was used for two-photon excitation of Rh123. The laser beam was focused by the Zeiss Plan Neofluar 40x1.3 objective lens and the signal was detected through a bandpass interference filter MF530/43 (ThorLabs, USA). For LDs staining a Nile Red dye was used and excited by Yb: KGW laser at 1040 nm [3]. Six morphological types of mitochondria were observed in the hyphae of this fungus: intermediate type - normal, intermediate with small semicircular tubules, tubular, elongated tubular, fragmented (small ellipsoid tubule) and fragmented with exclusively spheroid-shaped mitochondria. Changes in mitochondrial morphology were induced by a small temperature change. A 3°C increase in ambient temperature, from 22°C, had a dramatic effect on mitochondrial morphology, inducing the appearance of a predominantly tubular mitochondrial morphology. The total area percentage of mitochondria showed an increasing trend when grown at 25°C. Increasing the ambient temperature to 25°C induced a statistically significant increase in the percentage of hyphal area occupied by LDs from 2.9 ± 1.6 to 4.7 ± 2.2 (mean value and SD in percentage of hyphal area). The observed response to the small temperature increase points to the physiological adaptation of hyphal metabolism.

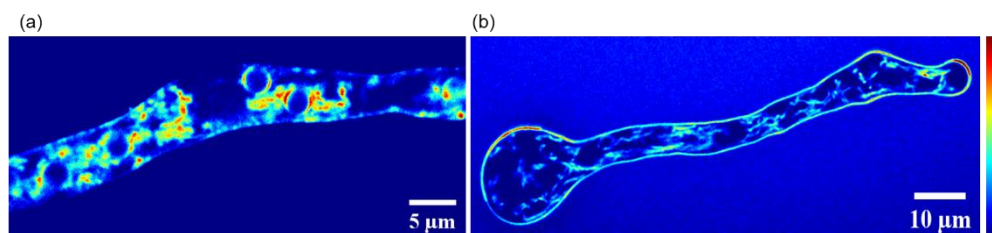


Figure 1. Two-photon images of mitochondrial morphology in *Phycomyces blakesleeanus* hyphae. (a) intermediate morphology at 22°C (b) tubular morphology at 25°C. Both hyphae were stained with 5 μ M Rh123. Intensity bar is given on the right, deep blue-lowest two photon excited fluorescence signal, deep red – highest TPEF signal.

REFERENCES

- [1] K. Ma *et al.*, Front. Cell Dev. Biol. 8, 467 (2020).
- [2] M. Long, T.G. McWilliams, Autophagy 19, 724 (2023).
- [3] T. Pajic *et al.*, Sci. Rep. 12, 18760 (2022).

Synthesis of europium-doped fluorapatite as a promising luminescent biomaterial

V. Stanic¹, M. Omerasevic¹, D. Mutavdzic², A. Mrakovic¹, Dj. Veljovic³, M. Marinovic Cincovic³ and D. Jovanovic⁴

¹*Vinca Institute of Nuclear Sciences – National Institute of the Republic of Serbia, University of Belgrade, Serbia*

²*Institute for Multidisciplinary Research, University of Belgrade, Serbia*

³*Faculty of Technology and Metallurgy, University of Belgrade, Serbia*

⁴*Faculty of Veterinary Medicine, University of Belgrade, Serbia*

e-mail: voyo@vin.bg.ac.rs

Lanthanide-doped apatite biomaterials are highly promising in medicine because of their excellent chemical and optical properties. In this study, Eu(III)-doped fluorapatite particles have been successfully synthesized by a wet method at room temperature. The characterization study from XRD showed that obtained powder is monophasic fluorapatite. Biomaterials based on fluorapatite ($\text{Ca}_{10}(\text{PO}_4)_5\text{F}_2$) doped with lanthanide elements are ideal contrast agents for a variety of biomedical applications, e.g. detection, imaging, cell tracking, and therapy [1]. Eu(III) received a great deal of interest because of several desirable properties like emission in the visible region, long luminescent lifetime, and less sensitivity to quenching by singlet oxygen [2].

REFERENCES

- [1] D.V. Milojkov *et al.*, J. Lumin. 217, 116757 (2020).
- [2] S.S. Syamchand, G. Sony, J. Lumin. 217, 190 (2015).

FEM analysis of natural photonic structures of insects in the IR band

B. Salatic¹, D. Pavlovic¹ and D. Pantelic²

¹*Institute of Physics, Belgrade, Serbia*

²*University of Belgrade, Senzor INFIZ, Institute of Physics, Serbia*

e-mail: banes@ipb.ac.rs

The cuticle plays an important role in regulating the body temperature of insects. A closer look at its structure reveals that it often has patterns on the micro and nano scale. During the interaction of electromagnetic radiation with the cuticle, these photonic structures affect the temperature of the insect depending on their size, shape and spatial arrangement. While in the visible part of the spectrum these structures behave as anti-reflection layers [1] and produce structural coloring, in the IR part of the spectrum their function can be twofold. For some insects, these structures have the role of increasing body temperature by absorbing electromagnetic radiation, while for other insects their purpose is the efficient release of excess heat radiatively into the environment [2].

Here we present a numerical model that describes the scattering of plane waves on the complex photonic structures of *Hoplia argentea* scarab beetle for the infrared spectrum of wavelengths. The FEM model is based on the SEM images of the insect elytron shown in Figure 1(a). The distance between the filaments on the top layer is 1 μm and it was a fixed value. All other dimensions such as the height and width of the filaments, the dimensions of the layers filled with air and their distance are varied and the final results of the simulation are averaged. Preliminary results indicate that this structure of the insect's elytron plays a significant role in the radiative cooling of the insect.

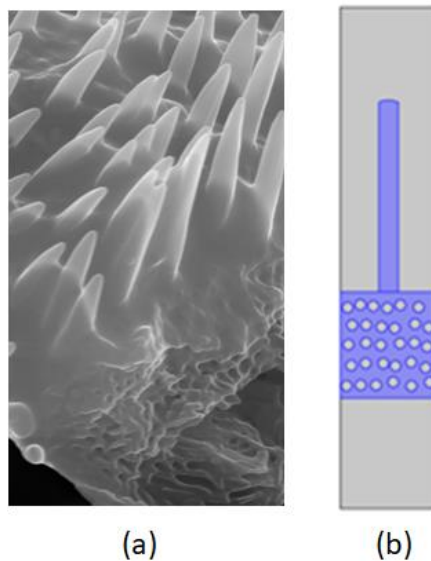


Figure 1. (a) Sem image of *H. argentea* elytron. (b) model used for FEM simulation (chitin is marked in blue, while air is gray).

REFERENCES

- [1] P. Vukusic, J.R Sambles, Nature 424, 852 (2003).
- [2] N.N. Shi *et al.*, Science 349, 298 (2015).

Dynamics of optomechanical array revealed by holography

H. Skenderović, A.M Dezfouli, D. Abramović, M. Rakić and N. Demoli
Institute of Physics, Zagreb, Croatia
 e-mail: hrvoje@ifs.hr

This work examines the possibility of making an imaging device that would use the thermophoretic effect on certain biomimetic microstructures for optical reading [1]. The microstructures are inspired by the wing scales which make butterfly wings, and a proposed imaging device would not be limited to visible light but could be sensitive in other parts of the spectrum (ultraviolet and infrared).

Due to the illumination of a butterfly wing with electromagnetic radiation, the illuminated side is slightly heated. As a result, nearby air molecules on the heated side pick up slightly more energy compared to molecules on the unheated side. This difference in energy leads to deflections which are registered by holographic method. The performance of the wings is tested by interferometric holography (setup shown in Fig. 1) using quasi-Fourier configuration.

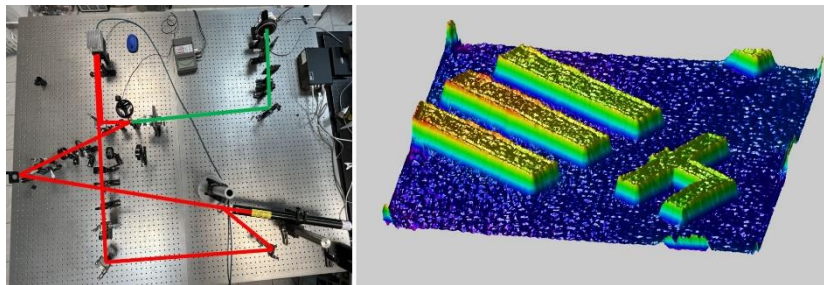


Figure 1. Left pane: holographic setup. Right panel: retrieved phase of the standard USAF target.

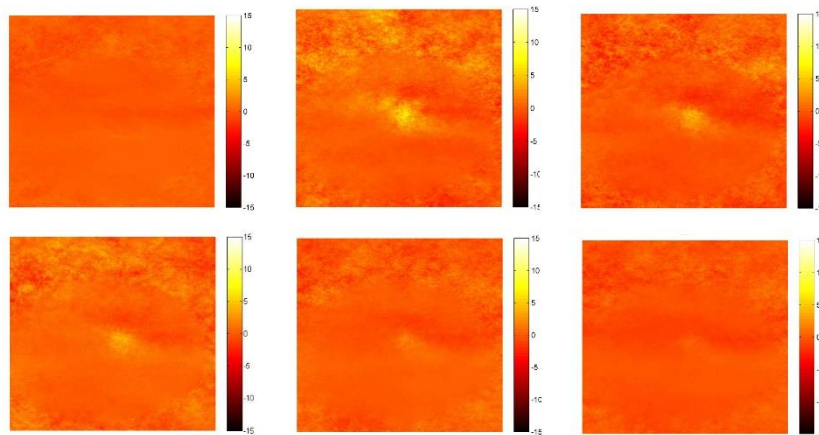


Figure 2. Time development of target upon excitation, phase image.

For probing time response of the butterfly wing, a sequence of holograms [2] was recorded upon excitation by auxiliary laser. The holograms were reconstructed and unwrapped phase image is shown in Fig. 2. Based on similar measurements dynamical and sensitivity characteristics of the wings as optomechanical array are presented.

REFERENCES

- [1] P. Atanasijevic *et al.*, *Opt. Laser Technol.* 159, 108919 (2023).
- [2] H. Skenderović, *Technical Digest Series* (Optica Publishing Group, 2022), paper M4A.1.

Functionalization of biological/bioinspired structures for multispectral surveillance

D. Pavlović¹, B. Salatić¹, H. Skenderović², M. Rakić² and D. Pantelić³

¹*Institute of Physics Belgrade, Belgrade, Serbia*

²*Institute of Physics Zagreb, Zagreb, Croatia*

³*University of Belgrade, Senzor INFIZ, Institute of Physics Belgrade, Serbia*

e-mail: danica.pavlovic@ipb.ac.rs

Infrared and other parts of electromagnetic spectrum, inaccessible to human visual perception, can be successfully applied in a wide range of applications, such as: security and surveillance, astronomy, spectroscopy, biomedicine (e.g., oncology, dermatology, dentistry), food and package inspection, non-destructive testing and process quality control, etc. [1].

The infrared part of the spectrum is important in the living world and natural, infrared photonic structures have a great biomimetic potential for passive radiative cooling [2]. Recently [3], we revealed the ability of natural nanostructured microparticles (NMPs) found on the butterfly's wings, to move and flex upon irradiation by infrared radiation. It was found that the effect is boosted through photophoresis. The resulting deformation field was imaged holographically, directly on the butterfly's wing.

We have developed additional capabilities to fabricate biomimetic structures using holographic lithography, cut NMPs and fabricate complex substrates using direct laser writing, arrange NMPs using micromanipulation and microdispensing. Biological NMPs were functionalized with respect to their shape and absorption to obtain high sensitivity and fast response time within the main IR atmospheric windows (1.5 μm , 3 – 5 μm and 8 – 13 μm). Mimetic versions of biological structures were also formed using interaction of laser radiation with multilayer foils and surfaces and holographic lithography.

REFERENCES

- [1] A. Rogalski *et al.*, Rep. Prog. Phys. 79, 046501 (2016).
- [2] N.N. Shi *et al.*, Science 349, 298 (2015).
- [3] D. Grujić *et al.*, Opt. Express 26, 14143 (2018).

A compact, holographic imaging sensor for biophotonic structures

D. Pantelic¹, D. Pavlovic², D. Grujic², B. Salatic², P. Atanasijevic³ and P. Mihailovic³

¹University of Belgrade, Senzor INFIZ, Institute of Physics, Serbia

²Institute of Physics, Belgrade, Serbia

³University of Belgrade, School of Electrical Engineering, Belgrade, Serbia

e-mail: dejanvpantelic@gmail.com

Nature is a rich source of formidable “engineering” achievements acquired through millions of years of evolution. They enable various forms of life to survive by camouflage, thermal regulation, imaging and numerous other mechanisms. Based on that, researches are looking for bioinspired and bioderived techniques, systems and devices.

A highly sensitive detection technique of infrared radiation, based on Morpho butterfly wing, was proposed [1]. A method is based on thermal dilatation of nanostructured wing scales induced by infrared radiation, and subsequent detection of spectral shift of iridescence. The method is suitable only for pointwise detection, making imaging very difficult.

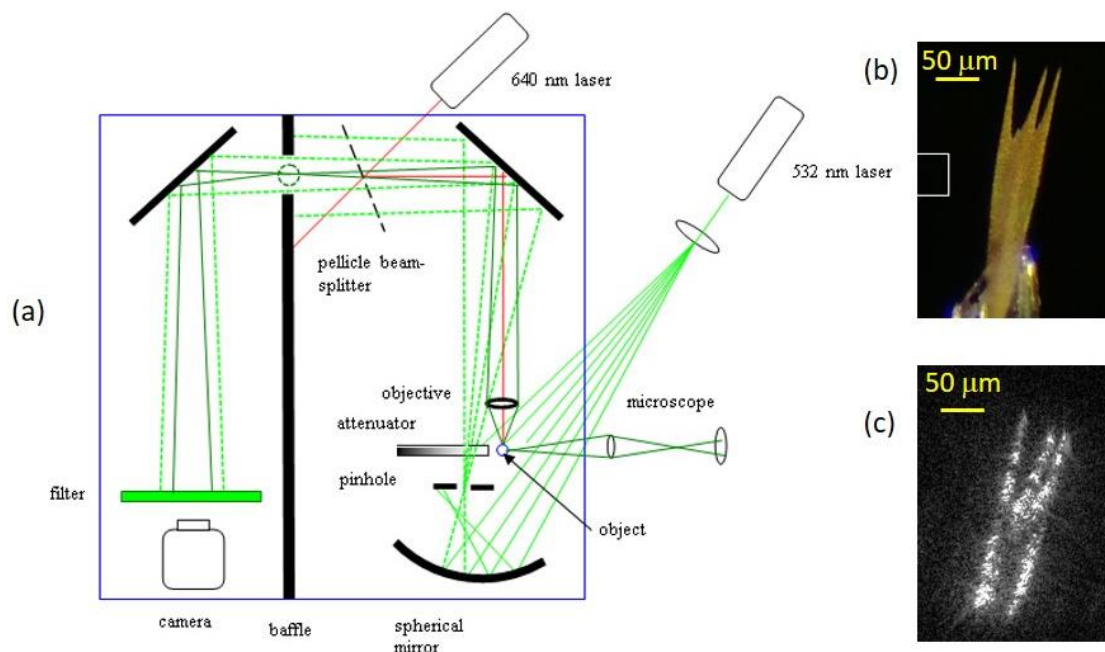


Figure 1. (a) A compact holographic imaging sensor, (b) wing scale and (c) its holographic interferogram.

Here we present further development of a compact, imaging device, based on butterfly wing scales, as an alternative to expensive thermal imaging cameras [2,3]. A system, depicted in Fig. 1(a), uses 532 nm laser as a light source for holography. A single beam is expanded and directed towards an object (butterfly wing or an individual wing scale) and a concave mirror. Light reflected from a mirror is spatially filtered and interferes with a beam reflected from an object. Interference pattern is directed towards high-speed camera using a pair of beam folding mirrors. Hologram is digitally reconstructed enabling imaging of millimeter to micron sized objects and their response to incoming radiation (Fig. 1(b, c)).

REFERENCES

- [1] A.D. Pris *et al.*, Nat. Photonics 6, 195 (2012).
- [2] D. Grujić *et al.*, Opt. Express 26, 14143 (2018).
- [3] P. Atanasijevic *et al.*, Opt. Laser Technol. 159, 108919 (2023).

Cutting edge technique for determination of spatial resolution limits of nonlinear laser scanning microscopy

M. Bukumira¹, J. Jelić¹, A. Denčevski¹, M.D. Rabasović¹, N. Vujičić², A. Senkić², A. Supina² and A. Krmpot¹

¹*Institute of Physics Belgrade, University of Belgrade, Laboratory for Biophysics, Belgrade, Serbia*

²*Institute of Physics, Center of Excellence for advanced Materials and Sensing devices, Zagreb, Croatia*

e-mail: marta@ipb.ac.rs

Microscope resolution is the shortest distance between two points on a sample that can be distinguished as separate entities. Due to the wave nature of light and the phenomenon of diffraction, it is fundamentally limited: even under theoretically ideal conditions and optical components, the microscope has a finite resolution.

In this paper, we determined the lateral and axial resolution of a nonlinear laser scanning microscope by measuring its Point Spread Function (PSF). The measurement was performed in two ways: by imaging fluorescent beads using two-photon excited fluorescence (standard method), and by using transition metal dichalcogenide monolayers of molybdenum disulfide and tungsten disulfide (cutting edge method). The monolayers - obtained by chemical vapor deposition [1], efficiently generate second harmonic (SHG) signal due to the lack of central symmetry. The monolayers were also used for determination of the lateral resolution of third harmonic generation (THG) microscopy.

Measurements were performed for different objectives and several standard excitation wavelengths, depending on the type of sample. As expected, the best resolution was obtained for the objective with the largest numerical aperture and the shortest excitation wavelength. In addition, the values obtained by the non-standard cutting edge method are closer to the theoretical values of the resolution, because the contributions of the out-of-focus signal are significantly reduced due to the two-dimensional nature of the layers. The measured PSF can be further used to deconvolve the images obtained on this microscope.

Due to its properties such as great depth of penetration of incident radiation and label-free imaging, as well as the possibility of making 3D models, our microscope is widely used in examining samples of biological origin, such as: erythrocytes [2], chitin structures [3], human colon [4], collagen, dentin, etc.

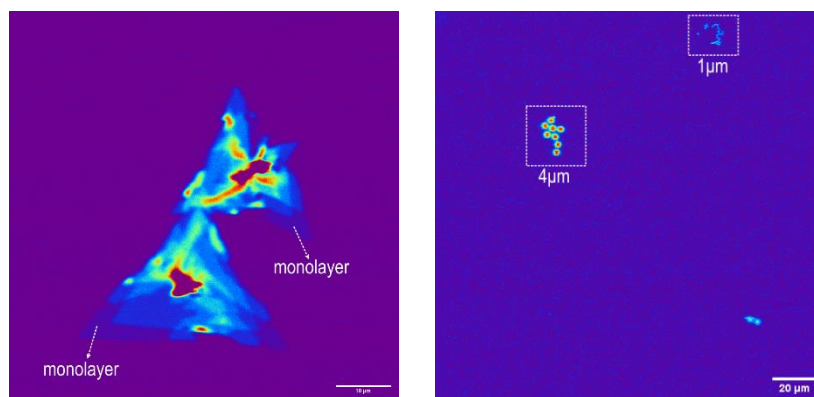


Figure 1. Left: WS₂ (mono)layers; right: fluorescent beads of different diameters (4 μm and 1 μm).

REFERENCES

- [1] A. Senkic *et al.*, *Mater. Chem. Phys.* 296, 127185 (2023).
- [2] K. Bukara *et al.*, *J. Biomed. Opt.* 22, 026003 (2017).
- [3] M.D. Rabasovic *et al.*, *J. Biomed. Opt.* 20, 016010 (2015).
- [4] S.Z. Despotovic *et al.*, *Sci. Rep.* 10, 6359 (2020).

Optical fiber curing of a dental composite: a holographic, thermographic, and Raman study

E. Novta¹, T. Lainović¹, D. Grujić², S. Savić-Šević², E. Toth³, Ž. Cvejić³, L. Blažić^{1,4} and D. Pantelić²

¹University of Novi Sad, Faculty of Medicine, School of Dental Medicine, Novi Sad, Serbia

²University of Belgrade, Institute of Physics, Belgrade, Serbia

³University of Novi Sad, Faculty of Sciences, Department of Physics, Novi Sad, Serbia

⁴Dental Clinic of Vojvodina, Novi Sad, Serbia

e-mail: evgenije.novta@mf.uns.ac.rs

The main limitation of dental resin-based composites (RBC) is shrinkage during polymer chain formation. As a consequence, at the tooth-restoration interface polymerization shrinkage stress (PSS) is generated, impairing restoration longevity. The study aimed to introduce a novel photo-activation protocol using optical fibers inserted into the RBC, for reducing PSS and guiding light directly into deeper layers of the restoration.

Tooth models with standardized cavities were filled with the RBC (Filtek™ Bulk-fill Posterior, 3M ESPE), and the proposed experimental curing was designed as follows: in the first step, two optical fibers (ϕ 1.5 mm) connected with a commercial dental LED curing unit were inserted into the filling to cure the RBC from within; in the second step, fibers were extracted, remaining voids were filled with the RBC and final conventional curing was performed with the commercial light guide positioned above the sample. As a control, conventional curing was performed on a separate group of samples (n=15 models per curing protocol). Tooth model deformation as a secondary manifestation of PSS was measured in real-time using digital holographic interferometry. Simultaneous monitoring of RBC temperature change was conducted with an infrared thermal camera. The degree of monomer-to-polymer conversion (DC) was measured immediately after curing and after 24 h of dark storage, using Raman spectroscopy (n=5 models per curing protocol; three measurements points for each sample).

Table 1. Photo-activation parameters and results.

Curing protocol	Radiant exposure (J/cm ²)	Tooth model deformation (μ m)	Temperature change ($^{\circ}$ C)	Time to reach the maximum temperature (s)	Immediate DC (%)	24 h post-cure DC (%)
Conventional	20	13.4	10.7	7.5	41.4	46.3
Experimental (1 st + 2 nd step)	14.5	8.8	6.5	8.2	33.5	38.1

The results showed a 34 % reduction of tooth model deformation using the experimental curing compared with the control. Such a finding was related to a lower temperature change (39 %), leading to a lower thermal shrinkage during the cooling process, as suggested by Palagummi et al. [1]. Furthermore, the time to reach the maximum exothermal temperature was prolonged compared with the control, allowing polymer chains to re-arrange and accommodate the volume reduction by viscous flow. Meanwhile, significantly lower immediate DC contributed to the reduction of model deformation as well. After 24 h of dark storage, the DC increased in both groups of samples as expected, but remained significantly lower for the ones cured using the experimental protocol compared with the control.

In conclusion, the proposed photo-activation using optical fibers was presented as beneficial for PSS reduction and could be easily implemented into dental clinical practice by coupling the fibers with standardized commercial light guides. However, it should be noted that measuring the irradiance of the selected light source is necessary to adequately determine exposure time since it was presented that insufficient radiant exposure (i.e. lower than suggested by the manufacturer) compromises the DC and therefore material biocompatibility and mechanics.

REFERENCES

[1] S.V. Palagummi *et al.*, Dent. Mater. 37, 1772 (2021).

Exploring the nano-scale world using a custom-made Fluorescence Correlation Spectroscopy (FCS) instrument

J.Z. Jelić¹, M.D. Rabasović¹, S. Nikolić¹, V. Vukojević² and A.J. Krmpot¹

¹*Institute of Physics Belgrade, University of Belgrade, Belgrade, Serbia*

²*Department of Clinical Neuroscience, Karolinska Institutet, Nobels väg 6, 171 77 Stockholm, Sweden*

e-mail: jovana.jelic@ipb.ac.rs

Fluorescence Correlation Spectroscopy (FCS) is a powerful and non-invasive technique for quantitative characterization of the concentration, mobility, and interactions of fluorescent/fluorescently labeled molecules *in vitro* and *in vivo* [1]. By exploiting the capabilities of a confocal microscope and time-correlated single photon counting (TCSPC), FCS offers high temporal resolution (sub-microsecond in commercially available systems, and down to picosecond time scale in custom-made instruments dedicated to the study of fast processes such as rotational diffusion of molecules and photon antibunching), diffraction-limited spatial resolution (≈ 200 nm) [2], as well as single-molecule sensitivity. Conventional FCS utilizes temporal autocorrelation analysis of fluctuations in recorded fluorescence signal caused by molecular motion through the small sample volume, often referred to as the focal volume (typically 0.2 – 1 fL) [3]. FCS enables the quantitative measurement of the concentration, translational diffusion coefficient, and interactions. Furthermore, FCS can provide insights into local microenvironments, such as viscosity or pH, or about any other molecular process related to alterations in the fluorescence signal [4]. By implementing two detection channels, conventional FCS is extended to Fluorescence Cross-Correlation Spectroscopy (FCCS) [5]. In FCCS, dual-color excitation and detection enable the monitoring of interactions and dynamics of molecules that are labeled with spectrally distinct fluorophores [5].

Here, we present our custom-made FCS system and characterize its performance using Rhodamine 110 in aqueous solutions. We show that the sensitivity and effective volume size in our home-built FCS instrument are comparable to those in commercial instruments.

REFERENCES

- [1] E. Haustein, P. Schwille, *Annu. Rev. Biophys. Biomol. Struct.* 36, 151 (2007).
- [2] The bh TCSPC Handbook 9th edition, 2021 - Becker & Hickl GmbH (becker-hickl.com).
- [3] V. Vukojević *et al.*, *Cell. Mol. Life Sci.* 62, 535 (2005).
- [4] <https://www.biophysics.org/Portals/0/BPSAssets/Articles/schwille.pdf>.
- [5] K. Bacia *et al.*, *Nat. Methods* 3, 83 (2006).

Calcium imaging of cerebellar granular neurons in culture acutely treated with cerebrospinal fluid of patients with neurodegenerative diseases

A. Laudanović¹, A. Antić¹, A. Palibrk², P. Andjus¹, Z. Stević², D. Lutz³ and M. Milošević¹

¹Center for Laser Microscopy, Institute for Physiology and Biochemistry “Jean Giaja”, Faculty of Biology, University of Belgrade, Serbia

²Neurology Clinic, Clinical Center of Serbia, School of Medicine, University of Belgrade, Serbia

³Department of Neuroanatomy and Molecular Brain Research, Ruhr University Bochum, Bochum, Germany
e-mail: andjela.laudanovic@bio.bg.ac.rs

Neurodegenerative diseases pose a significant burden to patients and their families, and many of them are diagnosed in later stages when most available treatments only alleviate the symptoms. The whole medical field is in the constant need for reliable biomarkers that would enable early diagnostics. Cerebrospinal fluid (CSF) is routinely obtained as a part of a standard diagnostic procedure. As CSF is in contact with neurons that degenerate during the disease, it is thought to contain toxic factors that influence the disease [1]. Here we implemented calcium imaging of cerebellar granular neurons in order to investigate calcium signaling evoked by CSF of patients with different neurodegenerative diseases.

Cerebellar granular neurons were isolated from 5-7 days old *Wistar* rats. Disease diagnostics and CSF sampling was conducted at the Clinic of Neurology, Clinical Center Serbia in Belgrade. Calcium transients evoked by CSF were evaluated utilizing Fluo 4-AM, a calcium-sensitive indicator that changes the intensity of fluorescence depending on the concentration of free calcium ions in the cytosol. To assess the origin of calcium influx to the cytosol, and signaling pathways involved in this process, several blockers of ion channels, receptors or enzymes were used.

CSF of patients with neurodegenerative diseases (amyotrophic lateral sclerosis, progressive supranuclear palsy, and spinal muscular atrophy type III) evoke strong calcium transients in cerebellar granular neurons, and this reaction is dose-dependent. Moreover, neurons respond to repeated CSF treatment with similar calcium transients. External calcium is necessary for the response to CSF. The amplitude and shape of the calcium transients were greatly modified by the use of lanthanum (La^{3+}), which blocks voltage-gated calcium channels [2], but also influences the connexin hemichannels [3]. Depending on the CSF sample and the type of disease, lanthanum lowered the amplitude of CSF evoked calcium transients ~30-95 %. It is interesting to note that nifedipine, which specifically blocks L-type calcium channels, negligibly influenced CSF evoked calcium transients. 2-APB, which blocks the IP_3 receptors on the endoplasmic reticulum, and ligand-gated TRP channels mostly located on the cell membrane, lowered the amplitude ~20 %. Ryanodine, a blocker of calcium channels on the endoplasmic reticulum, lowered the amplitude ~16 %. U73122, a blocker of phospholipase C, lowered the amplitude ~12 %. On the other hand, blockade of glutamate receptors (AMPA/kainate and NMDA), as well as voltage gated sodium channels, did not influence the amplitude of CSF evoked calcium transients.

Calcium imaging of CSF evoked transients in neurons could be utilized as a part of the complex analysis (ROS imaging, evaluation of inflammation, etc.) that could lead towards the complementary differential diagnostics and/or evaluation of the effectiveness of specific drugs or their combination in a patient-personalized manner.

REFERENCES

- [1] K.C. Ng Kee Kwong *et al.*, *Front. Mol. Neurosci.* 14, 647895 (2021).
- [2] R.W. Tsien *et al.*, *Annu. Rev. Biophys. Biophys. Chem.* 16, 265 (1987).
- [3] M.B. Singh *et al.*, *Cereb. Cortex* 29, 3363 (2019).

Mid-Infrared quantum scanning microscopy with visible light

J.R. León-Torres^{1,2}, J. Fuenzalida¹, M. Gilaberte¹, S. Töpfer¹, V. Gili¹ and M. Gräfe^{1,2,3}

¹Fraunhofer Institute of Applied Optics and Precision Engineering IOF, Albert-Einstein-Straße 7, D-07745 Jena, Germany

²Friedrich-Schiller-Universität Jena, Abbe Center of Photonics, Max-Wien-Platz 1, D-07745 Jena, Germany

³Institute of Applied Physics, Technische Universität Darmstadt, Schloßgartenstraße 6, D-64289 Darmstadt, Germany

e-mail: josue.ricardo.leon.torres@iof.fraunhofer.de

A label-free quantum scanning imaging system is presented, capable of detecting in the visible regime, while illuminating with undetected light in the Mid-IR region by exploiting the phenomenon of induced coherence [1] and the quantum correlations of photon-pairs generated by Spontaneous Parametric Down Conversion (SPDC) Laser scanning microscopy (LSM) is the workhorse for modern life-science, it allows to get new insights into a variety of biological processes. LSM together with illumination in the mid infrared region (Mid-IR) permits to map the chemical composition of samples to a space frame. However, low-light observations in the Mid-IR spectrum are still challenging and a limiting factor for a faster development.

In this work a highly non-degenerated entangled photon-pair is created through SPDC when a pump photon interacts with a PPKTP non-linear crystal. The SPDC process can take place in the forward or backward direction, creating two probability amplitudes of photon-pair generation. In the forward direction, the idler photon ($\lambda_i=2400$ nm) is reflected by a dichroic mirror and directed towards the sample [2]. The MIR photon illuminates the sample, while the VIS photon is used for reconstructing the object, by using a single pixel detector.

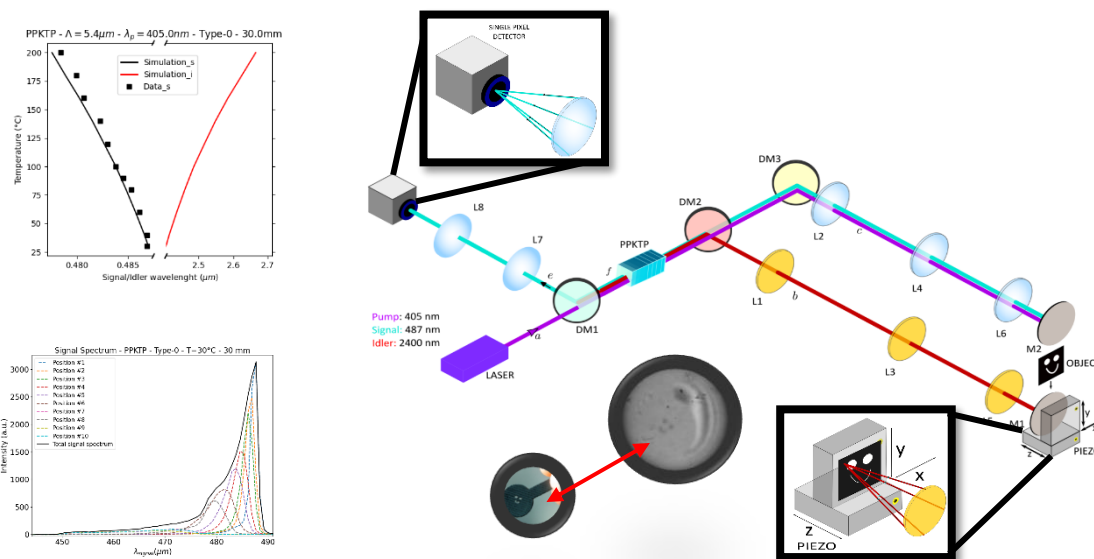


Figure 1. Experimental setup, quantum imaging with undetected photons. Pump and signal photons in the VIS spectrum and idler in the Mid-IR spectrum. Idler photon is used to probe the sample, different functional groups in the fingerprint region (2.5- 12 μm) will absorb the illumination light, while the signal photon is detected.

REFERENCES

- [1] X.Y. Zou *et al.*, Phys. Rev. Lett. 67, 318 (1991).
- [2] M.G. Basset *et al.*, Laser Photonics Rev. 15, 202000327 (2021).

Fluorescent products upon heme degradation as potential biomarkers: Understanding their formation via Hemoglobin oxidation

M.D. Radmilović¹, I.T. Drvenica², M.D. Rabasović¹, V.Lj. Ilić² and A.J. Krmpot¹

¹*Institute of Physics, Belgrade, Serbia*

²*Institute for Medical Research, National Institute of Republic of Serbia, University of Belgrade, Serbia*

e-mail: mihajlor@ipb.ac.rs

Formation of a fluorescent products was observed upon hemoglobin (Hb) treatment with H₂O₂ [1]. This study explores the formation mechanism of fluorescent products resulting from hemoglobin (Hb) treatment with hydrogen peroxide (H₂O₂), as well as the generation of similar fluorescent molecular species upon Hb interaction with 730 nm ultrashort laser pulses [2]. Our previous publication has shown a correlation between Two-photon Emission Fluorescence (TPEF) intensity of erythrocytes and Hb distribution inside them [3]. By comparing TPEF intensity changes and spectra properties, we observed immediate and intense TPEF emission upon H₂O₂-treated Hb excitation, contrasting with the gradual increase observed in the Hb thin film. The TPEF intensity remained unaffected by the number of exposures to 730 nm ultrashort laser pulses, confirming photodegradation of Hb during the formation of fluorescent products and reaching plateau. Additionally, we investigated the photophysical properties of Protoporphyrin IX (PpIX), a structural component of the heme functional group, during its interaction with 730 nm ultrashort laser pulses. Furthermore, erythrocytes treated with Tert Butyl Hydrogen Peroxide (TBHP) were examined to understand how in vitro-induced oxidative stress correlates with observed fluorescence. The TPEF spectrum of H₂O₂-treated Hb thin film closely matched that of Hb thin film treated with ultrashort laser pulses, erythrocytes, and the PpIX layer. Significantly different flow cytometry signals from erythrocytes treated with TBHP indicate the potential of flow cytometry as a methodology for tracking oxidation status in large cell populations.

REFERENCES

- [1] E. Nagababu, J.M Second, *Biochem. Biophys. Res. Commun.* 247, 592 (1998).
- [2] M.D. Radmilović *et al.*, *Int. J. Biol. Macromol.* 244, 125312 (2023).
- [3] K. Bukara *et al.*, *J. Biomed. Opt.*, 22, 026003 (2017).

5. Devices and components

High-power diffraction-limited laser systems with variable output characteristics oscillating in visible spectral range on atomic copper self-terminating transitions for advanced material microprocessing

I. Kostadinov, K. Temelkov, S. Slaveeva and G. Yankov

Metal Vapor Lasers Laboratory, Georgi Nadjakov Institute of Solid State Physics, Bulgarian Academy of Sciences, 72 Tzarigradsko Chaussee, 1784 Sofia, Bulgaria
e-mail: temelkov@issp.bas.bg

Though the copper (Cu) vapor laser is characterized with unique features and has remained the most powerful laser source in the visible spectral range ($\lambda=510.6$ nm and $\lambda=578.2$ nm) so far [1], the enormous technological difficulties in the laser tube development and operation have inspired and justified the development of low-temperature version of this perspective laser, such as Cu halide vapor lasers [2]. Though the continuous development of these lasers toward the design of compact reliable sealed-off lasers is quite successful, the competing with the solid state lasers operating in the visible spectral region via second harmonic generation is far from over. Commercial solid state lasers produced by leading laser companies usually delivers TEM₀₀ Gaussian laser beam, i.e. beam propagation factor M^2 is well in the range between 1.05 and 1.3, while metal vapor lasers produce partially or near diffraction-limited laser radiation (up to 90 % of the laser output is diffraction-limited) with a record-low $M^2 = 1.3$ [3], due to the short laser pulse and a small number of cavity round-passes. It necessitates the development of master oscillator – power amplifier (MO–PA) laser systems using unstable cavity configuration and spatial filtering. The MO–PA system based on the atomic Cu bromide (CuBr) vapor laser is well established as a laser source used for precise micromachining in the industry for drilling, cutting, scribing, marking, welding, etc. of various materials. Though the development and operation difficulties, the atomic Cu vapor laser has unsurpassable advantages over the Cu halide lasers, namely lasing stability, higher laser pulse energy at the same average output power, two-time shorter laser pulse, the possibility to operate with small-bore laser tubes (the aperture smaller than 4 mm), etc. New considerably improved MO–PA laser systems delivering diffraction-limited high-power laser radiation ($M^2 = 1$) at the atomic copper 510.6 and 578.2 nm lines are developed and investigated. As a master oscillator (MO), laser characteristics of CuBr vapor MO operating with a negative branch unstable resonator and small-bore Cu vapor MO oscillating with a flat-flat stable cavity are compared. In order to increase considerably the output parameters, two CuBr vapor laser tubes with a significantly enhanced active volume are compared as a power amplifier (PA). Various designs of the laser systems, namely single- and double-pass PAs, matching telescopes with different magnifications M are realized. The highest beam quality achieved so far with laser systems oscillating on the metal self-terminating transitions is confirmed by precise measurement of the threshold average output power for volumetric optical breakdown at different focusing distances f and a known breakdown threshold I_{th} . Laser radiation with both record-high average output power and beam quality is obtained. Precise microprocessing of various materials, such as stainless steel, silicon and optical grade fused quartz is accomplished. Using an aspheric lens with a focusing distance of 2 cm for the laser beam focusing, spherical aberrations are overcome and a crater diameter and a channel width of about 2 μ m are achieved. Microcutting with multi-contour trepanning and wobbling is also realised.

REFERENCES

- [1] R.P. Hackel, B.E. Warner, Proc. SPIE 1859, 120 (1993).
- [2] S. Gabay *et al.*, IEEE J. Quantum Electron. 13, 364 (1977).
- [3] M.J. Withfold *et al.*, Prog. Quantum. Electron. 28, 165 (2004).

Interband cascade lasers: advantages of bulk AlGaAsSb claddings

B. Petrović¹, A. Bader¹, F. Hartmann¹, R. Weih², F. Jabeen¹ and S. Höfling¹

¹Julius-Maximilians-Universität Würzburg, Physikalisches Institut, Lehrstuhl für Technische Physik, Am Hubland, 97074 Würzburg, Germany

²Nanoplus Nanosystems and Technologies GmbH, Oberer Kirschberg 4, D-97218 Gerbrunn, Germany
e-mail: borislav.petrovic@physik.uni-wuerzburg.de

Interband cascade lasers (ICLs) are mid-infrared emitting devices used for gas-sensing applications in environmental protection, medicine, and military applications. In the 3-7 μm wavelength range, ICLs have the lowest threshold current densities and also have significantly higher characteristic temperatures compared to type-I laser diodes. This is crucial for portable devices operating in continuous wave (CW) regime. Cladding materials of low refractive index and high thermal conductivity are important for the optical confinement and heat dissipation.

We have grown ICLs emitting at 4.9 μm with AlGaAsSb bulk and AlSb/InAs superlattice claddings (Figure 1a) and we characterize and contrast the lasers' figures of merit. P-I-curves (Figure 1b) and temperature dependent measurements (Figure 1c) show improved device operation for ICLs with bulk claddings in comparison to the usually employed superlattice claddings. The improvement of threshold current density can be attributed to lower refractive index of AlGaAsSb cladding [1]. In support to the result, we have simulated optical mode confinement factor throughout both ICL structures and noted it's increase of 10.3 % in the active region of ICL with AlGaAsSb claddings.

Higher thermal conductivity of the bulk compared to superlattice (7 W/m·K to 1-3 W/m·K) claddings [2] and higher characteristic temperature contribute to enhancement in operation in CW.

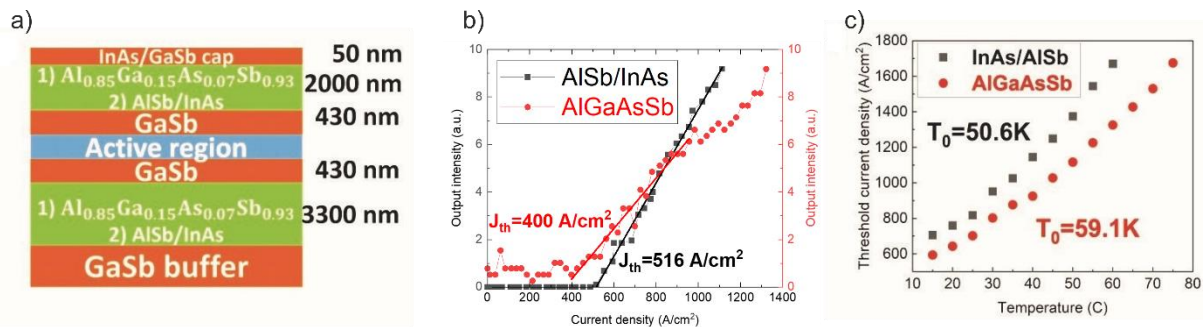


Figure 1. a) Layer structure with 1) bulk and 2) superlattice claddings, b) P-I characteristics, c) characteristic temperatures.

REFERENCES

- [1] R. Weih *et al.*, Opt. Mater. Express 3, 10 (2013).
[2] T. Borca-Tasciuc *et al.*, IEEE J. Appl. Phys. 9, 92 (2002).

Dependence of transport parameters on interface composition diffusion and doping segregation in longitudinal optical phonon, bound to continuum and hybrid THz quantum cascade laser designs

N. Stanojević^{1,2}, A. Demić³, N. Vuković¹, D. Indjin³ and J. Radovanović¹

¹School of Electrical Engineering, University of Belgrade, Serbia

²Vlatacom Institute of High Technologies, Belgrade, Serbia

³School of Electronic and Electrical Engineering, University of Leeds, UK

e-mail: novakstanojevic1@gmail.com

Quantum cascade lasers (QCLs) are semiconductor lasers with emission frequencies ranging from the mid-IR to the THz part of the spectrum, that can be designed by varying layer thicknesses and composition [1]. Due to the unique THz light emission of QCLs, many designs have been developed, the most important of which are the Longitudinal Optical Phonon (LO), Bound to Continuum (BTC), and Hybrid designs [2]. These devices are created at high temperatures by molecular beam epitaxy (MBE) making them prone to diffusion of added barrier material that leads to interface composition diffusion which can have a prominent effect on QCL operation [3]. Doping segregation, that is the diffusion of the charged dopants, which affects the doping profile, and Hartree term in the total effective potential energy is also present in real QCLs. In this contribution, we investigate the dependence of transport parameters such as material gain, current density, and emission frequency in the negative differential resistance (NDR) point in the three most common THz QCL designs that are stated above, on interface diffusion and doping segregation. The NDR point defines the maximum current density at which the QCL can operate, while the operation starts at material gain equal to the threshold value. The transport of these devices was modeled using the density matrix formalism which takes into account quantum coherence effects thus adequately describing resonant tunneling through the injection barrier [4]. The finite difference method was then used for the numerical solving of Fick's law to model both composition diffusion and doping segregation.

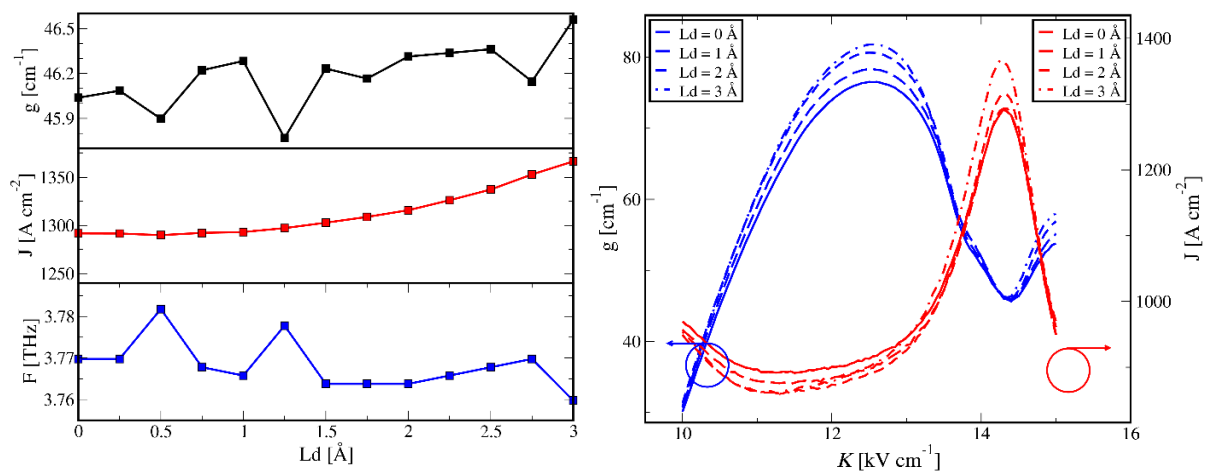


Figure 1. Effect of interface diffusion on transport parameters in NDR point (left), and on material gain and current density versus external bias (right) in a LO design quantum cascade laser.

REFERENCES

- [1] J. Faist *et al.*, Science 264, 553 (1994).
- [2] B.S. Williams, Nat. Photon. 1, 517 (2007).
- [3] Li Wang *et al.*, Appl. Phys. Express 16, 032007 (2023).
- [4] A. Demić *et al.*, IEEE Trans. Terahertz Sci. Technol. 7, 368 (2017).

Investigation of intersubband transitions in wide bandgap oxide quantum well structures for optoelectronic device applications

A. Atić^{1,2,3}, N. Vuković^{2,3} and J. Radovanović^{2,3}

¹*Vinča Institute of Nuclear Sciences – National Institute of the Republic of Serbia, University of Belgrade, Belgrade, Serbia*

²*School of Electrical Engineering, University of Belgrade, Serbia*

³*Centre for Light-Based Research and Technologies COHERENCE, Belgrade, Serbia*

e-mail: atic@vin.bg.ac.rs

There has been a surge of interest in recent years for the advancement of wide bandgap oxides such as zinc oxide (ZnO), magnesium oxide (MgO), gallium oxide (Ga₂O₃), etc. [1,2]. These materials have gained significant attention due to their distinctive characteristics and properties which are promising for the development of high-performance optoelectronic devices for applications in the domains of sensing, communications, and imaging. More specifically, Ga₂O₃ has wide bandgap energy of approximately 4.8 to 4.9 electron volts (eV), thus exhibiting exceptional transparency to ultraviolet (UV) radiation while displaying opaqueness to visible light [3]. On a parallel note, ZnO shows exemplary optical and electrical properties, including a high exciton binding energy and substantial oscillator strength [4]. Of particular significance is the exploration of intersubband transitions within multiple quantum well (MQW) structures, which offers a promising path for efficient light absorption and emission in the mid-infrared to terahertz spectral range.

In this contribution we will numerically simulate the absorption spectra of the wide bandgap oxide MQW structures, adapting the approach for treating the light-matter interaction suitable when the depolarization field is the dominant many-body contribution, and discuss the potential applications in optoelectronic devices, specifically mid-infrared detectors, quantum cascade lasers, and modulators.

REFERENCES

- [1] J.Y. Tsao *et al.*, Adv. Electron. Mater. 4, 1600501 (2018).
- [2] A.V. Osipov *et al.*, Coatings 12, 1802 (2022).
- [3] J.E. Lyman, S. Krishnamoorthy, J. Appl. Phys. 127, 173102 (2020).
- [4] T. Makino *et al.*, Appl. Phys. Lett. 76, 3549 (2000).

Multiport splitters based on waveguide arrays

K. Bugarski^{1,2}, P. Vildoso^{3,4}, M. Stojanovic¹, A. Maluckov¹, G.Z. Mashanovich^{2,5}, R.A. Vicencio^{3,4} and J. Petrovic¹

¹Vinca Institute of Nuclear Sciences - National Institute of the Republic of Serbia, University of Belgrade, Serbia

²School of Electrical Engineering, University of Belgrade, Serbia

³Departamento de Física, Facultad de Ciencias Físicas y Matemáticas, Universidad de Chile, Chile

⁴Millenium Institute for Research in Optics - MIRO, Chile

⁵Optoelectronics Research Centre, University of Southampton, UK

e-mail: kolja.bugarski@vin.bg.ac.rs

Conventional designs of multiport splitters rely on concatenation of directional couplers or multimode interference [1,2]. However, the splitters show a considerable insertion loss and fast bandwidth drop with the number of ports. Inverse nanodesigns enable broad-bandwidth semiconductor splitters, however, at high fabrication and design costs [3,4].

In this work, we present fast and low-cost inverse designs of multiport splitters with near-zero insertion loss and respectable bandwidth. Designs are based on adjustments of the separations or lengths of waveguides composing a linearly coupled waveguide array.

By tailoring the separations to achieve self-imaging of the input light pattern, a series of $1 \times N$ splitters can be achieved prior to the revival [5,6]. To demonstrate the technique, the power splitters were fabricated in a borosilicate wafer by femtosecond laser writing method [7]. The splitters show zero insertion loss within the experimental error, bandwidth of 20–60 nm around a wavelength of 640 nm and low imbalance < 0.5 dB [8]. Their footprint scales exponentially with the waveguide separation, which can be reduced to the limit of mode confinement. The footprint reduction is particularly pronounced in waveguides with high refractive index contrast, such as those in SOI, where we design the splitters with the footprint as small as $6 \mu\text{m}^2$.

The proposed splitters offer new possibilities for path-entanglement generation, multipath interferometry on chip and spatial mode multiplexing.

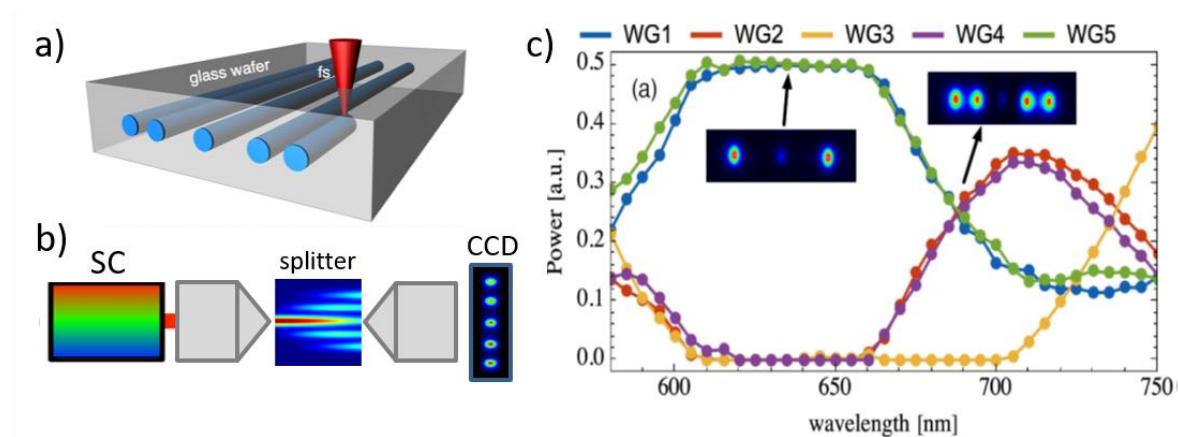


Figure 1. (a) Femtosecond laser writing technique. (b) Splitter testing setup and output light intensity recorded on CCD. (c) Demonstration of the splitter multifunctionality.

REFERENCES

- [1] J. Wang *et al.*, Science 360, 285 (2018).
- [2] L.B. Soldano, E.C. Pennings, J. Lightwave Technol. 13, 615 (1995).
- [3] H. Xie *et al.*, IEEE Photon. J. 10, 1 (2018).
- [4] A.Y. Piggott *et al.*, Sci. Rep. 7, 1 (2017).
- [5] J. Petrovic, Opt. Lett. 40, 139 (2015).
- [6] J. Petrovic *et al.*, J. Opt. Las. Technol. 163, 109381 (2023).
- [7] D. Guzmán-Silva *et al.*, Phys. Rev. Lett. 127, 066601 (2021).
- [8] P. Vildoso *et al.*, Opt. Express 31, 12703 (2023).

Optical interconnects and filters based on waveguide arrays

J. Krsic¹, M. Stojanovic¹, K. Bugarski^{1,2}, N. Stojanovic³, A. Maluckov¹, P. Veerman⁴ and J. Petrovic¹

¹Vinca Institute of Nuclear Sciences - National Institute of the Republic of Serbia, University of Belgrade, Serbia

²School of Electrical Engineering, University of Belgrade, Serbia

³Deutsches Zentrum für Luft- und Raumfahrt (DLR), Berlin, Germany

⁴Portland State University, Oregon, US

e-mail: mirjana.stojanovic@vin.bg.ac.rs

Rapidly increasing demand for higher data bandwidths has motivated exploration of new communication channels based on spatially multiplexed in-fibre and on-chip coupled light guides [1]. However, the conventionally used periodically arranged coupled waveguides display complicated light propagation patterns, ranging from quasiperiodic to nearly chaotic. Taking a different approach, we spectrally engineer interwaveguide coupling to instigate self-imaging of the input light state at the array output and thus enable construction of novel high-fidelity interconnects [2]. Simple implementation via modulation of the interwaveguide separations makes these interconnects realizable in all fabrication platforms.

Moreover, the wavelength dependent self-imaging opens up possibilities for construction of new multiplexing devices [3]. Here, we present designs of band-pass filters and dichroic splitters for VIS and NIR and propose the strategies for selection of their central wavelengths and bandwidths.

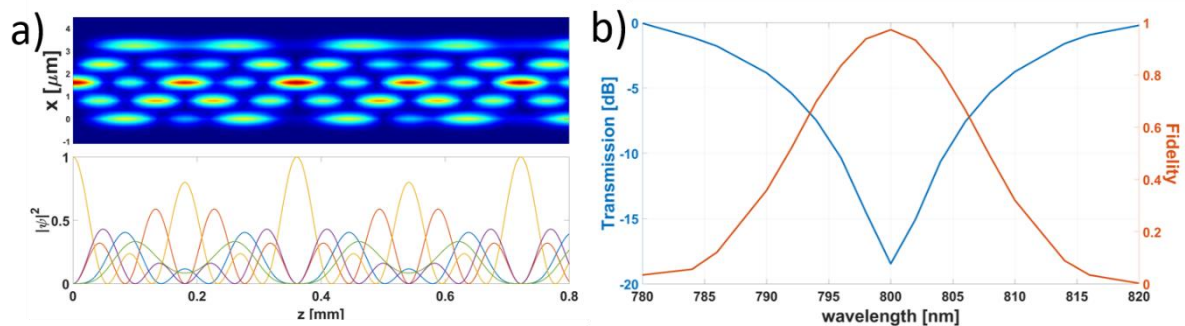


Figure 1. a) Self-imaging in a SiN array composed of 5 waveguides. b) Transmission and fidelity of transfer after the 1st revival period at $z = 0.36$ mm [3].

REFERENCES

- [1] B.J. Puttnam *et al.*, *Optica* 8, 1186 (2021).
- [2] J. Petrovic, J. Veerman, *Ann. Phys.* 392, 128 (2018).
- [3] J. Petrovic *et al.*, *J. Opt. Las. Technol.* 163, 109381 (2023).

Photo-electronic security device based on photonics integrated circuits

C. Cid-Lara^{1,2,3} and R.A. Vicencio^{1,2}

¹Departamento de Física, Facultad de Ciencias Físicas y Matemáticas, Universidad de Chile, Chile

²Millenium Institute for Research in Optics – MIRO, Chile

³Departamento de Ingeniería Eléctrica, Facultad de Ciencias Físicas y Matemáticas, Universidad de Chile, Chile

e-mail: c.cid.l@outlook.com

Photonics chips or Photonic integrated circuits (PIC) are mainly based on waveguide lattices phenomena and have been widely studied on several fields such as computing [1], neural networks training and inference [2], analogies of physical systems [3], and microfluidics [4]. But real applications face substantial limitations due to the utilization of expensive equipment such as lasers, cameras and optics in a controllable environment.

We propose and test a photonic chip having an array-like pattern to encode binary information (users definition) that can be reconstructed through automatic image processing on free space after illumination. This detection can produce a triggering signal of opening/closing into a given actuator. We created a low-budget device capable of detecting binary patterns of femtosecond-written waveguide lattices in borosilicate. Our system only requires a LED, a lens, a microcontroller, and a cheap CCD camera. We also propose scalability to more complex systems, having improved security protocols, like encrypting information in the form of flat bands states [5].

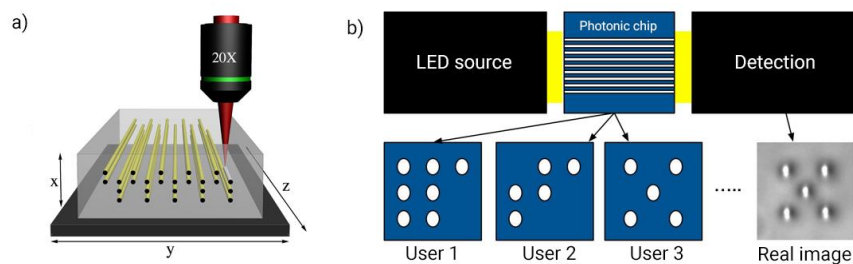


Figure 1. (a) Femtosecond laser writing technique. (b) Diagram of the photo-electric system.

As shown in Fig. 1 (b) we encode users as a binary matrix (in this figure 3x3) inside the photonic chip, so it can be detected through a CCD camera once it is illuminated with a LED. The detection is made through image processing in a Raspberry Pi Zero W and OpenCV python library in real time with high specificity.

REFERENCES

- [1] M. Nakajima *et al.*, *Commun. Phys.* 4, 20 (2021).
- [2] F. Ashtiani *et al.*, *Nature* 606, 501 (2022).
- [3] D. Román-Cortés *et al.*, *Sci Rep* 11, 21411 (2021).
- [4] I. Rodríguez-Ruiz *et al.*, *Anal Chem.* 88, 6630 (2016).
- [5] R.A. Vicencio *et al.*, "Control system and procedure for controlled access by means of an optical device based on flat bands" US20180210150A1.

The influence of injection barriers on performance of organic solar cells studied by drift-diffusion model with transport layers

T. Pavlicevic¹, J. Gojanovic² and S. Zivanovic³

¹*School of Electrical Engineering, University of Belgrade, Serbia*

²*School of Electrical Engineering, University of Belgrade, Serbia*

³*Institute for Micromanufacturing, Louisiana Tech University, Ruston, LA 71272 USA*

e-mail: pavlicevictedora@gmail.com

Organic solar cells (OSCs) are prospective technology because they are inexpensive, lightweight, flexible, and ideal for roll-to-roll large-scale processing. An impressive improvement in their power conversion efficiency (PCE) has been achieved in the past few years with the PCE reaching a certified value of 19.2% [1]. However, an adequate and comprehensive theoretical model which would explain the progress so far and indicate the direction of future performance improvement is still missing.

Along the path of further PCE improvement, the main goal is to achieve the best possible absorption, photogeneration, and transport of charge carriers in the active layer (AL), as well as to reduce recombination losses in it. However, contact phenomena which include effects of transport layers (TLs) have turned out to be very important and influential in OSCs [2]. The amount of the photogenerated electrons and holes that are brought to the corresponding electrodes as well as the efficiency of their extraction is strongly dependent on TLs. In contrast, the drift-diffusion models (DDMs) used for modeling the OSCs do not consider the existence of TLs [3].

Here, the DDM that includes the Poisson equation and continuity equations for electrons and holes was used. The domain was divided into three subdomains corresponding to the hole transport layer (HTL), AL, and electron transport layer (ETL) and each layer is described with its electrical and optical material parameters. The absorption profile was described by the Beer-Lambert law and photogeneration was assumed to take place only in the AL. The mobilities of electrons and holes were taken to be constant in each layer, and a reduced Langevin recombination was assumed. The Dirichlet boundary conditions (BCs) at TL/electrode interfaces were used. The BCs include the effect of injection barriers (IBs) through thermionic electron and hole concentrations [4]. The system of equations was solved with use of the finite difference discretization improved by Scharfetter and Gummel approach and the Newton algorithm.

The TLs have the role to reduce IBs between the AL and electrodes, thus, it is important to apply exact values for the hole and electron IBs in the DDM. It is expected that lowering the IBs leads to a higher PCE, which was verified using our model. We also simulated the current density-voltage (J-V) characteristics for the ITO/P3HT:PCBM/Al solar cell (structure without TLs) and the ITO/PEDOT:PSS/P3HT/LiF/Al solar cell in which PEDOT:PSS is the HTL and LiF is the ETL. The simulated J-V curves for the ITO/P3HT:PCBM/Al device without taking into account IBs (zero IBs) and including IBs were compared to the experimental J-V curve taken from [5]. A better agreement with the experiment was obtained when the IBs were included. The same was done for the ITO/PEDOT:PSS/P3HT/LiF/Al solar cell. In this case, the model which doesn't include IBs reproduced the experimental J-V curve, taken from [6], better. This was taken as evidence of the electrodes Fermi level pinning in the considered device.

REFERENCES

- [1] J. Wang *et al.*, Adv. Mat. 7, 2301583 (2023).
- [2] X. Li, Ph.D. dissertation, Fac. of Sci. and Engr., Linköping Univ., Norrköping, [Online] (2023).
- [3] D. Li *et al.*, Adv. Sci. 7, 1901397 (2019).
- [4] A. Khalf *et al.*, Opt. Quantum Electron. 52, 121 (2020).
- [5] M.I. Algazzar, Ph.D. dissertation, Univ. of Wisconsin, Milwaukee, [Online] (2014).
- [6] M. Wang *et al.*, ACS Appl. Mater. Inter. 2, 2699 (2010).

Characterization and performance evaluation of a dual loop Sagnac interferometer as sensing system for intrusion location detection

M. Vasiljević Toskić¹, J.S. Bajić¹, L. Manojlović² and B. Batinić¹

¹University of Novi Sad, Faculty of Technical Sciences, Department of Power, Electronic and Telecommunication Engineering, Novi Sad, Serbia

²Zrenjanin Technical College, Zrenjanin, Serbia

e-mail: markovt@uns.ac.rs

The importance of securing critical areas such as airports, military bases, and power plants has driven the development of optical fiber-based sensors, aiming to meet the requirements for long-range sensitivity, robustness, reliability, and simplicity in detecting unwanted intrusions and disturbances. However, the limitations associated with cost, continuity, and reliability in traditional intrusion detection methods emphasize the significance of advancing sensor technologies in this field. Due to their high sensitivity to vibrations and temperature discrimination, optical fiber interferometers employing the Sagnac loop configuration have proven to be effective methods for distributed intrusion detection and localization [1,2].

In this paper, the modification of an optical system based on the Sagnac interferometer is investigated, building upon the concepts presented in the previous research. Various aspects of the proposed sensing system are presented in previous research, including system topology, operational principles, mathematical relationships, hardware configuration, and signal processing software [3]. The testing approach is enhanced by the integration of two devices: mini-shaker Type 4810 and Red Pitaya STEMLab 125-14 board for the detailed characterization and performance validation of the sensor system. By integrating the mini-shaker Type 4810 into the optical system, controlled vibrations are generated, allowing for a comprehensive characterization of the sensor system's response to stimuli of various frequencies, amplitudes, and patterns. Utilizing the Red Pitaya STEMLab 125-14 board for the light source excitation and as data acquisition device simplifies the experimental setup, offering a cost-effective and efficient solution for performance validation.

This proposed experimental setup allows for the precise assessment of the system's sensitivity, stability, reliability and overall performance.

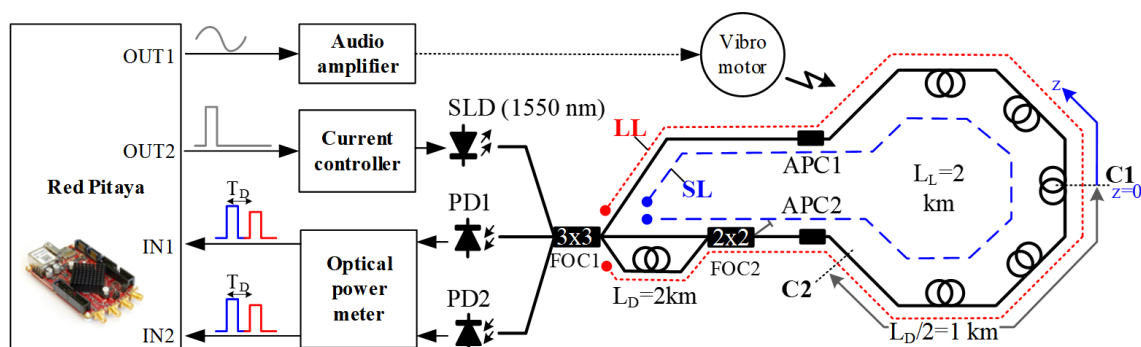


Figure 1. Experimental setup used in this work.

REFERENCES

- [1] G. Sun *et al.*, IEEE Photon. Technol. Lett. 19, 2027 (2007).
- [2] G. Sun *et al.*, IEEE Photon. Technol. Lett. 24, 587 (2012).
- [3] M. Vasiljevic Toskić *et al.*, VIII International School and Conference on Photonics pp. 125 (2021).

6. Optical communications

Free-space OAM wave transmission: a short dipole modeling study

A.Ž. Ilić¹, J.Z. Trajković¹, S.V. Savić² and M.M. Ilić²

¹Institute of Physics Belgrade, University of Belgrade, Serbia

²School of Electrical Engineering, University of Belgrade, Serbia

e-mail: andjelijailic@ieee.org

Orbital angular momentum (OAM) multiplexing is, since recently, considered to be one of the key technology enablers for enhancing wireless and free-space optical communications channel capacity, whether implemented separately or in combination with existing multiplexing techniques. The OAM wave generation systems have been a topic of a number of recent publications. The actual possibilities and limitations of the free-space OAM wave transmission have also been investigated in several studies, e.g. [1-4]. The results have pointed out the most probable utility of the free-space OAM waves for short-range transmission distances that are on the order of magnitude of the Rayleigh distance. However, there are just a few in-depth investigations into the properties of such short-range OAM wave transmission. Here we report on the recently proposed use of the short (Hertz) dipole method customized for the detailed analysis of the OAM waves [5]. Employing that method and focusing on the uniform circular antenna arrays (UCA), as a very representative example of easily reconfigurable discrete OAM wave sources, we studied the properties of the short-range transmission at different frequencies, for different UCA electrical sizes, and different distances from the source plane [5]. Guidelines for using the proposed methodology and the obtained results in the future designs of free-space communication systems employing OAM multiplexing were provided.

As expected, short (Hertz) dipole modeling proved highly efficient and versatile in an investigation of electrically large discrete OAM EM wave sources. A general framework of combining the short dipole method with full-wave numerical EM modeling for the analysis of arbitrary antenna arrays or other OAM wave radiating structures was also presented.

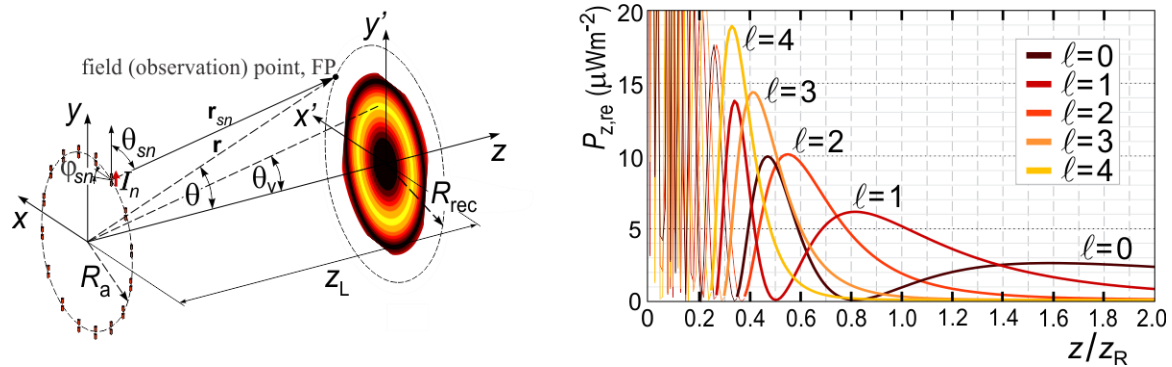


Figure 1. Short (Hertz) dipole modeling, computationally efficient for electrically large discrete EM wave sources (plot on the left). The vortex angle, θ_v , corresponds to the OAM EM field maximum. The link distance is denoted as z_L . Dependence of the axial Poynting vector for $x=0$, $y=R_{\text{rec}}=z_L \tan(\theta_v)$, on the distance from the source plane, z , is plotted on the right (R_{rec} represents the radius of receiving UCA). The Rayleigh distance is denoted as z_R . The optimal receiving distance, i.e., link range, corresponds to the axial coordinates of OAM EM field maxima.

REFERENCES

- [1] A.F. Morabito *et al.*, IEEE Antennas Propag. Mag. 60, 59 (2018).
- [2] A. Sawant *et al.*, IEEE Wirel. Commun. 28, 90 (2021).
- [3] A.E. Willner *et al.*, J. Opt. 18, 074014 (2016).
- [4] A.Z. Golubović *et al.*, Int. J. Electron. Commun. (AEÜ) 165, 154643 (2023).
- [5] A.Ž. Ilić *et al.*, accepted for publication in J. Phys. A: Math. Theor.

OAM mode quality comparisons for discrete EM radiating sources

J.Z. Trajković¹, A.Ž. Ilić¹, S.V. Savić², N. Maletić³, E. Grass^{3,4} and M.M. Ilić²

¹Institute of Physics Belgrade, University of Belgrade, Serbia

²School of Electrical Engineering, University of Belgrade, Serbia

³IHP – Leibniz-Institut für innovative Mikroelektronik, Frankfurt (Oder), Germany

⁴Humboldt-Universität zu Berlin, Berlin, Germany

e-mail: jelena.trajkovic@ipb.ac.rs

Electromagnetic (EM) waves carrying the orbital angular momentum (OAM) are currently being considered for use in optical wireless communications, as well as wireless communications at terahertz and millimeter wave frequencies [1,2]. The apertures radiating with their entire surfaces, often used in the optical domain, produce very high quality OAM EM waves. However, partial radiating apertures and discrete OAM wave sources, considered here, facilitate OAM source reconfiguration as well as multiplexing of different OAM modes through a single aperture. Moreover, at terahertz and millimeter wave frequencies, powering and phasing of discrete OAM EM wave sources often becomes increasingly more complex and costly, especially for a very large number of elements of radiating antenna arrays. Therefore, it is of interest to use low-cost, low-profile, efficiently powered and phased antenna arrays consisting of a limited number of elements, while optimizing the OAM mode quality.

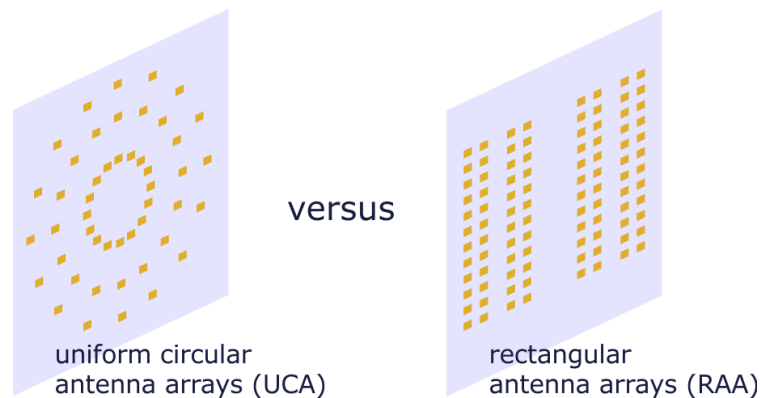


Figure 1. Uniform circular antenna arrays (UCA) are often used to produce the OAM EM waves at millimeter wave frequencies. Rectangular antenna arrays (RAA) could offer some additional flexibility to the designer; however, the calculation of the RAA element phase shifts is more complex, and additional optimization might be required to attain similar OAM mode quality in comparison with the UCA.

Utilization of uniform circular antenna arrays (UCA) as discrete OAM EM wave sources has been successful in the millimeter wave frequency band; phasing of the UCA is quite straightforward and symmetrical antenna arrangements are advantageous from the OAM mode quality viewpoint. However, the OAM EM wave sources for use in wireless communications have to be electrically large [2,3], to allow the desired system performance. From that point of view, either uniform or non-uniform rectangular antenna arrays (RAA) provide additional flexibility to the designer and could benefit from the well-developed theory and implementation methods of conventional antenna arrays [4]. We compare the OAM mode quality of different antenna array arrangements at millimeter wave frequencies to define the prerequisites for the RAA for attaining high wireless data transfer performance.

REFERENCES

- [1] A.E. Willner *et al.*, *J. Opt.* 18, 074014 (2016).
- [2] A.Z. Golubović *et al.*, *Int. J. Electron. Commun. (AEÜ)* 165, 154643 (2023).
- [3] A.Ž. Ilić *et al.*, *J. Phys. A: Math. Theor.* 56, 255701 (2023).
- [4] Y.H. Cho, W.J. Byun, *Electron. Lett.* 55, 503 (2019).

7. Laser spectroscopy and metrology

An upgrade of the primary length standard of Republic of Serbia

Z.D. Grujić¹, M.G. Nikolić¹, S. Zelenika² and M.D. Rabasović¹

¹*Institute of Physics Belgrade, University of Belgrade, Photonica Center, Pregrevica 118, 11080 Belgrade – Zemun, Serbia*

²*Directorate of Measures and Precious Metals, Mike Alasa 14, 11158 Belgrade, Serbia*

e-mail: rabasovic@ipb.ac.rs

We have performed upgrade of the electronics for frequency stabilization of the primary length standard of Republic of Serbia. The standard is red HeNe laser at 633 nm. The stabilization is done by standalone electronics based on Arduino microcontroller. We have used off-the-shelf electronics components, thus, setup is simple and inexpensive. The stabilization electronics is connected to the computer via USB port. The purpose of the computer is only to communicate with the user, not to perform stabilization, thus, the computer can be easily replaced in case of failure. Namely, the previous version of the standard, based on the computer, broke down because the computer broke down, and the repair was not cost effective.

The stabilization procedure is very well known [1]. Namely, the saturation spectroscopy of the I₂ vapor has been used. Back mirror is scanned at frequency f , and the signal of the laser power at $3f$ is detected. Digital lock-in detection is used to improve signal-to-noise ratio. Also, we have developed analog electronics to improve performances of the setup.

We achieved very good results despite using cheap and simple components. E.g. we have reached fractional frequency difference equal to $3.1 (25.3) \times 10^{-12}$.

REFERENCES

[1] https://www.bipm.org/documents/20126/41549560/M-e-P_I2_633.pdf/c4c25f25-ae65-e05d-402a-9bfc84c715c3.

Combined spectroscopic approach for the characterization of pigments used in prehistoric pottery from the region of Western Bulgaria

V. Tankova¹, V. Atanassova¹, V. Mihailov¹ and A. Pirovska²

¹*G. Nadjakov Institute of Solid State Physics, Bulgarian Academy of Sciences, Sofia, Bulgaria*

²*Department of Prehistory, Archaeological Museum "Maritza-Iztok", Radnevo, Bulgaria*

e-mail: vanitankova@gmail.com

This research is concerned with spectroscopic characterization of red and brown pigments used for decoration of Early-Neolithic pottery from the settlement of Buhovo and Galabnik, Western Bulgaria. For determining the elemental and mineral composition of the pigments two complementary analytical techniques are applied – Laser Induced Breakdown Spectroscopy (LIBS) and Fourier Transformed Infrared Spectroscopy in Attenuated Total Reflectance mode (ATR-FTIR). The LIBS analysis provides information on elemental composition of pigments and based on the detected elements a semi-quantitative analysis was performed. A statistical method Principal Component Analysis (PCA) was applied on the obtained semi quantitative data in order to classify the objects and to cluster the sherds with similar elemental composition of the decorations. To complement the results from LIBS measurement and identify the minerals in pigments, an ATR-FTIR was applied. On the basis of the results from LIBS and FTIR analysis assumptions about production technology and the raw materials used for manufacture of painted motifs were made. Conclusions on the possible trade routes between the cultures in this specific region and the nearby areas during the Neolithic were drawn.

Fluorescence spectroscopy and sucrose presence in onion genotypes after long-term storage

L. Vladimirova-Mihaleva¹, M. Mihalev², V. Slavova³, G. Pevicharova³, S. Genova³ and V. Boteva³

¹*Sofia University "St. Kliment Ohridski", Faculty of Physics, Department of Optics and Spectroscopy, 5 James Bourchier Blvd., 1164 Sofia, Bulgaria*

²*Technical University Sofia, Faculty of Mechanical Engineering, Department of PEMI, 8 Kliment Ohridski Blvd., 1000 Sofia, Bulgaria*

³*Maritsa Vegetable Crops Research Institute, Department of Plant Breeding, 32, Brezovsko shosse St., 4003 Plovdiv, Bulgaria*

e-mail: mmihalev@tu-sofia.bg

Onion is of great importance for the national economy and the nutrition of the population. It is available in the market fresh and after different periods of storage. For this reason, research on the storage process is of considerable interest. The aim of the study was to determine the presence of sucrose both by chemical analysis and by fluorescence in different onion genotypes stored for 3, 6 and 9 months. Portable equipment with applicability in local conditions was used. A decrease of water content in the bulbs with increase of storage duration was established. An effect of irrigation during the onion growth on the intensity of the spectra was observed. The spectra at different sucrose concentrations were obtained. A practical coincidence of the fluorescence peaks of the onion genotypes stored for different periods and the pure sucrose peaks was found. The results of the experiments will be a good basis to create algorithms to optimize the time for analysis of the total sugars (sucrose) and to get quick information about the quality of the onion genotypes during the breeding, cultivation and storage.

Measurement of the heading error of a free alignment precession magnetometer

Z.D. Grujić¹, M. Ćurčić¹, A. Milenković¹, J. Hinkel² and T. Scholtes²

¹*Institute of Physics Belgrade, Serbia*

²*Leibniz Institute of Photonic Technology, Jena, Germany*

e-mail: zoran.grujic@ipb.ac.rs

Optically pumped magnetometers (OPMs) have proved competitive sensitivities, robustness, and low cost with respect to competition, but their performance for high accuracy applications is not well studied. Optimization of an all optical free spin precession (FSP) magnetometer [1] has shown possible high accuracy of a such device. But, in unpublished investigations that followed that work it emerged that FSP magnetometer suffers from a heading error two orders of magnitude larger than its sensitivity. Then an investigation on applicability of Free Alignment Precession (FAP) produced by linearly polarized light was started.

We studied Larmor frequency measured simultaneously by two linearly polarized beams, in a spherical cesium cell with antirelaxation coating. If frequencies measured by those beams are different and function of the angle between their polarizations a heading error is detected. The experimental setup allows arbitrary mutual orientations of magnetic field $B_0 \approx 1.58 \mu\text{T}$ and directions of polarizations of light beams.

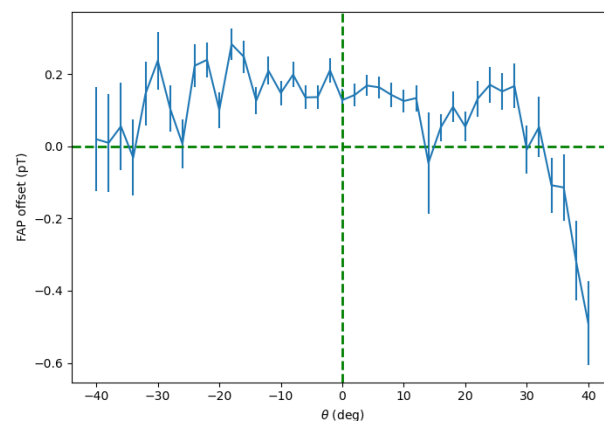


Figure 1. Measurement of the heading error of a FAP magnetometer. Direction of the B_0 and polarization direction of one of probe beams was fixed while we varied the polarization direction of the second probe beam.

In this particular case (see Fig. 1), the heading error is below 1 pT, thus at least six orders of magnitude below B_0 . Further investigation is under way.

REFERENCES

[1] Z.D. Grujić *et al.*, Eur. Phys. J. D 69, 135 (2015).

8. Ultrafast optical phenomena

Femtosecond laser spectroscopy for exploration of space

Y. Ha^{1,2}, O. Gueckstock³, G. Kourfakas⁴, J. Petrovic⁵, M. Rabasovic⁶, A. Krmpot⁶, T. Seifert^{3,7}, R. Pan⁸,
A. Denker³, T. Kampfrath^{3,7}, N. Stojanovic¹ and M. Gensch^{1,2}

¹German Aerospace Center (DLR), Institute of Optical Sensor Systems, Rutherfordstr. 2, 12489 Berlin, Germany

²Technische Universität Berlin, Strasse des 17. Juni 135, 10623 Berlin, Germany.

³Department of Physics, Freie Universität Berlin, Arnimallee 14, 14195 Berlin, Germany

⁴Helmholtz-Zentrum Berlin, Hahn-Meitner Platz 1, 14109 Berlin, Germany

⁵Vinča Nuclear Research Institute, Mike Petrovića Alasa 12-14, 11351, Beograd, Serbia

⁶Institute of Physics Belgrade, Pregrevica 118, 11080 Belgrade, Serbia

⁷TeraSpinTec GmbH, Lüneburger Str. 26, 10557 Berlin, Germany

⁸DESY, Notkestraße 85, 22607 Hamburg, Germany

e-mail: nikola.stojanovic@dlr.de

Space agencies around the world have the exploration of solar system bodies in the focus of their activities for decades already. The search for traces of life and to a better understanding of the geology of planets, moons and asteroids motivates these explorations. Our (DLR institute for Optical Sensor Systems (DLR-OS)) contribution to this topic is the development of spectroscopic sensors for material identification. DLR-OS is developing a wide range of spectroscopic sensors that reach from passive infrared spectrometers for remote sensing employed on orbiters to active laser spectroscopies such as NIR spectroscopy, Raman spectroscopy or Laser-Induced Breakdown Spectroscopy that are employed on robotic lander missions. Space, weight and power restrictions as well as robustness against harsh environmental conditions are inherent prerequisites for space missions and lead to specific design solutions for these instruments. Driven by emerging technology of space ready short-pulsed (femtosecond) lasers [1,2], we are introducing the new topic of time domain spectroscopies to space exploration. In this work, we present our first results on coherent phonon and THz time domain spectroscopies on space relevant minerals.

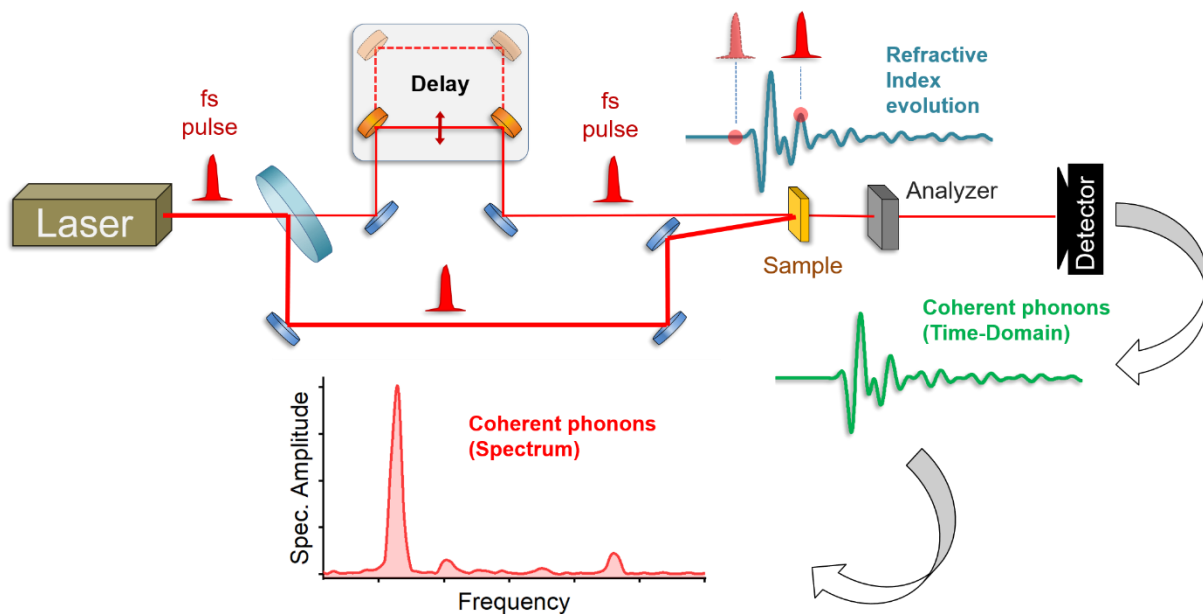


Figure 1. Scheme of Time-Domain Coherent Phonon Spectroscopy setup.

REFERENCES

- [1] J. Lee *et al.*, *Sci. Rep.* 4, 5134 (2014).
[2] M. Lezius *et al.*, *Optica* 3, 1381 (2016).

9. Laser - material interaction

Preparing the bioactive surface of Ti/Zr/Ti system by femtosecond laser pre-patterning of substrate

N. Božinović¹, V. Rajić¹, K. Savva², J. Potočnik¹, E. Stratakis² and S. Petrović¹

¹Vinča Institute of Nuclear Sciences - National Institute of the Republic of Serbia, University of Belgrade, Belgrade, Serbia

²Institute of Electronic Structure and Laser (IESL), Foundation for Research and Technology (FORTH), N. Plastira 100, Vassilika Vouton, 70013 Heraklion, Crete, Greece

e-mail: nevena.bozinovic@vin.bg.ac.rs

The experimental study of the dynamic femtosecond laser substrate pre-patterning of the Ti/Zr/Ti thin film system is reported. The design of surface patterning with the micrometer features in the form of spikes is investigated in order to improve the arrayed surface structures for biomedical applications. Femtosecond laser pulses were used to acquire black silicon surfaces decorated with conical structures (spikes) on crystalline silicon surfaces under 6.5×10^2 mbar of SF₆ environmental atmosphere. After irradiation, the silicon surface exhibits high aspect ratio spikes, which have conical shapes of about 2 μm height, 40° angle opening, 13×10^6 cm⁻² density that remains approximately uniform across the processed area. Results show that the base of the induced conical structures has an elliptical shape with a major (long) and minor (short) axis on the horizontal plane. It is revealed that the orientation of the long axis of the ellipsis is polarization-dependent with the long axis oriented always perpendicularly to the electric field of the laser beam. Spike formation has been attributed to a complex mechanism initiated by partial material melting and subsequent capillary wave formation driven by surface tension gradients within the molten region. Ion sputtering was used to create unique composite thin films on pre-patterned Si substrates that consist of two layers of Ti and subsurface layer of Zr on the interface of titanium. The total thickness of the deposited composite in Ti/Zr/Ti form was 300 nm. The composition, surface morphology and wetting properties were analyzed by scanning electron microscopy (SEM-EDS), profilometry and wettability measurements.

The formation of micro-patterns with spikes array of composite Ti/Zr/Ti thin film systems was used to observe the effects of morphology on survival, adhesion and proliferation of the MRC-5 cell culture line. To determine whether Ti/Zr/Ti thin films have a toxic effect on living cells, an MTT assay was performed. The relative cytotoxic effect as a percentage of surviving cells showed that there was no difference in cell number between the Ti/Zr/Ti thin films and the control cells. There was also no difference in the viability of the MRC-5 cells.

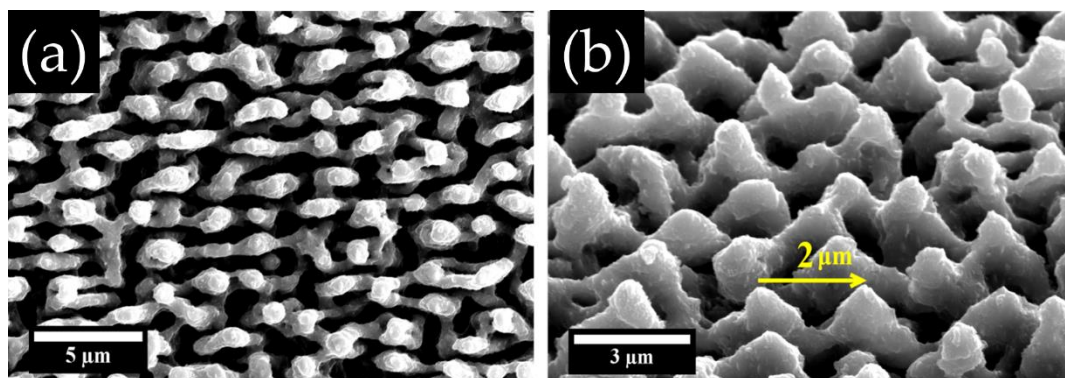


Figure 1. FESEM micrograph of conical spikes produced on Si (100) by femtosecond laser pulses in SF₆ at a pressure of 6.5×10^2 mbar viewed from the normal incident angle (a) and planar view (b). The distance between spikes was noted with a yellow arrow.

Selective ablation and laser induced periodical surface structures (LIPSS) produced on (Ni/Ti) nano layer thin film with ultrafast laser pulses

S. Petrović¹, B. Gaković¹, C. Siogka², D. Milovanović³ and G. Tsididis²

¹Vinča Institute of Nuclear Sciences - National Institute of the Republic of Serbia, University of Belgrade, Belgrade, Serbia

²Institute of Electronic Structure and Laser (FORTH), Heraklion, Greece

³Institute of General and Physical Chemistry, Belgrade, Serbia

e-mail: spetro@vin.bg.ac.rs

Nano layer thin films (NLTF), composed of alternating layers of various materials, are widely used in modern nanotechnology. Ultrafast lasers for processing is a precise non-contact method. Single pulses can be used to remove NLTF from the substrate or to accurately and selectively ablate one or more layers of the film's surface. Selective ablation can only be achieved at specified values of the laser beam's properties for a given material [1-3]. On practically any material, a laser beam can be used to produce the universal phenomena known as "laser-induced periodic surface structures" (LIPSSs). These structures are created by exposing the sample's surface to multi-pulse irradiation and have a variety of applications [4,5].

The interaction of ultrafast laser pulses with nickel/titanium (Ni/Ti) thin film was investigated. The NLTF, composed of ten alternating Ni and Ti layers, was deposited on silicon (Si) substrate by ion-sputtering. A single and multi-pulse irradiation was done in air with focused and linearly polarized laser pulses (wavelength 1026 nm and pulse duration 170 fs). For achieving selective ablation, the single pulse energy was gradually increased from near the ablation threshold to a level that completely removed the NLTF. The pulse energy for LIPSS creation was close to the ablation threshold of the NLTF. The laser induced morphology and the elemental composition changes were examined with microscopy, optical profilometry and energy dispersive X-ray spectroscopy. To interpret the experimental observations, theoretical simulation has been performed to explore the thermal response of the NLTF after irradiation with single laser pulses.

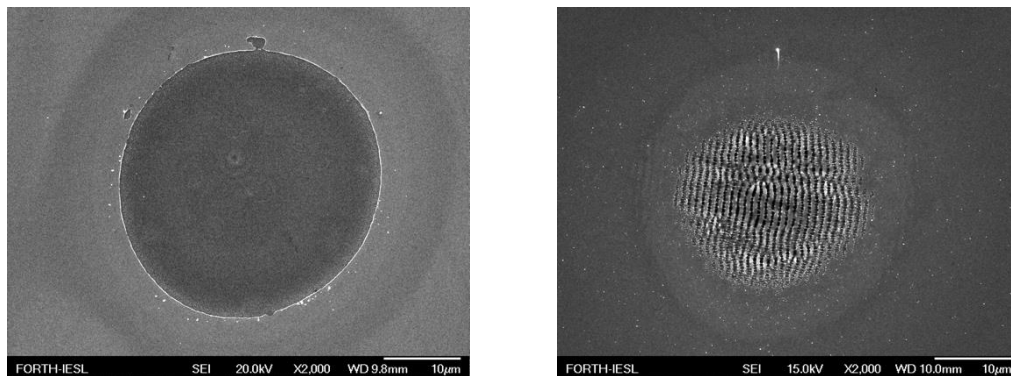


Figure 1. SEM micrographs of (Ni/Ti) surface after single pulse ablation of the first Ni layer at fluence of 0.2 J/cm² (left), and LIPSS formation after 10 pulses at 0.08 J/cm² (right).

REFERENCES

- [1] C. Wu, L.V. Zhigilei, *Appl. Phys. A* 114, 11 (2014).
- [2] B. Gaković *et al.*, *J. Appl. Phys.* 122, 223106 (2017).
- [3] B. Gaković *et al.*, *Eur. Phys. J. D* 75, 288 (2021).
- [4] S. Petrovic *et al.*, *Eur. Phys. J. D* 75, 304 (2021).
- [5] J. Bonse, S. Gräf, *Laser Photonics Rev.* 14, 2000215 (2020).

Experimental demonstration of vectorial spin-orbital Hall effect of light

A. Porfirev¹, S. Khonina¹, A. Ustinov¹, N. Ivliev¹ and I. Golub²

¹Image Processing Systems Institute of RAS—Branch of the FSRC “Crystallography and Photonics” RAS, Samara, Russia

²School of Advanced Technology, Algonquin College, Ottawa, Canada
e-mail: porfirev.alexey@gmail.com

Spin-orbital Hall effect of light is known as a one of the most prominent effects due to breaking the symmetry of a light field. It is obtained when an asymmetric light beam possessing spin or orbital angular momentum (SAM or OAM) is tightly focused and the effect is manifested in a shift of barycenter/center of gravity of light in the transverse focal plane. Here, we investigate asymmetric beams shifted from the optical axis. An asymmetric input beam with SAM and/or OAM will obviously have a non-uniform input angular momentum (AM) with transverse and longitudinal components [1,2]. Since the AM components depend on electric field components, the focal plane electric field distribution has to reflect the presence of AM and thus has to differ from the symmetrical focal plane distribution exhibited when focusing a linear polarized asymmetric input beam. This is achieved by shifts of the barycenters of the field components in the focus in order to produce the required AM components.

There are materials that can be used for direct visualization of the longitudinal component of light. For example, our recent studies have shown the high sensitivity of azobenzene molecules to this component of laser radiation [3]. In this work, we experimentally demonstrated, for the first time, to the best of our knowledge, the spin-orbit Hall effect of light upon tight focusing in free space. We have shown that in spin-orbital Hall effect of light upon tight focusing of an asymmetric beam, different Cartesian components in the focus are shifted, perpendicular to the symmetry breaking axis by different amounts and in different directions (see Fig. 1). These findings elucidate the Hall effect of light and may broaden the spectrum of its applications.

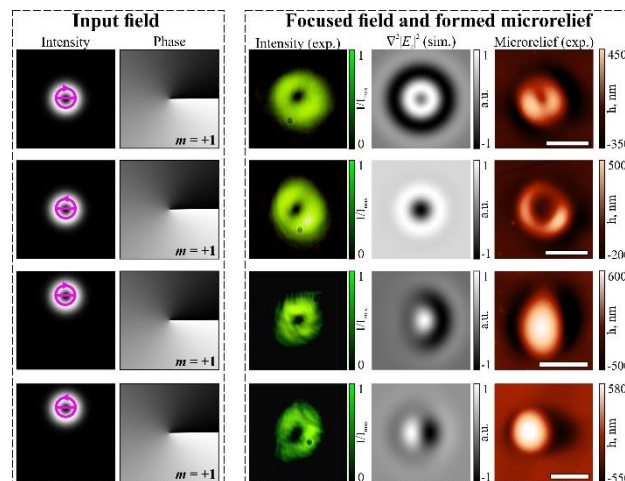


Figure 1. Laser patterning of an azopolymer thin film with right- and left-handed circularly polarized on- and off-axis OV beams of ± 1 order.

REFERENCES

- [1] K. Bliokh *et al.*, Phys. Rev. A 82, 063825 (2010).
- [2] W. Zhu, W. She, Opt. Lett. 39, 1337 (2014).
- [3] A. Porfirev *et al.*, Sci. Rep. 12, 1 (2022).

Structured laser beams: generation and applications

D. Porfirev^{1,2}, A. Porfirev^{1,2}, S. Khonina^{1,2} and S. Karpeev^{1,2}

¹Samara National Research University, Samara, Russia

²Image Processing Systems Institute of RAS—Branch of the FSRC “Crystallography and Photonics” RAS, Samara, Russia

e-mail: dporfirev@gmail.com

In recent years, structured laser beams with a complex distribution of intensity, phase, and polarization are increasingly used in different fields of modern science – optical manipulation, communication, microscopy, laser material processing, etc. In the field of optical manipulation, structured laser beams are effectively used for the realization holographic optical tweezers - modifications of the conventional optical tweezers, for the invention of which Arthur Ashkin was awarded the Nobel Prize in Physics in 2018. The use of structured laser beams made it possible to shape complex optical traps for the rotation of micro-objects [1], moving them along predetermined complex three-dimensional trajectories [2], and also for the realization of the so-called tractor beams [3]. In the field of laser material processing, structured laser beams are widely used for direct one-step fabrication of various unique one-, two-, and even three-dimensional microstructures.

In this work, we demonstrate the use of diffractive optical elements and their combinations with polarizing elements, such as q -plates and depolarizers for generation of structured laser beams with the desired amplitude, phase and/or polarization. The generation of multi “bottle” optical beams, multi-spiral laser beams, hybrid cylindrical vector beams, and arrays of non-uniformly polarized laser beams are demonstrated. The proposed approaches made it possible to realize advanced optical manipulation - trapping and guiding of multiple particles in space (see Fig. 1). In addition, we used the generated laser beams for realization of precision laser processing of polarization-sensitive materials (such as azopolymer thin films and nano-multilayer structures based on chalcogenide glasses) and demonstration of spiral-shaped mass transfer, polarization-sensitive multi-beams patterning, and direct fabrication of different types of surface relief gratings (see Fig. 2).

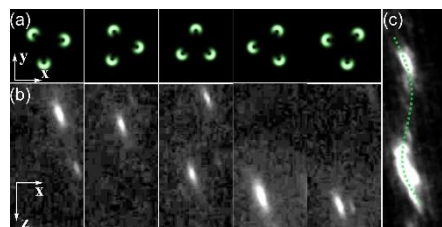


Figure 1. Laser guiding of a light-absorbing particle in air with a rotating laser beam: (a) transverse intensity distributions of the beam, (b) motion stages of the guided particle, (c) particle trajectory.

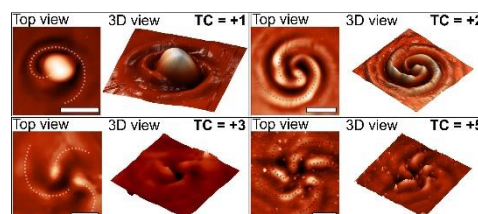


Figure 2. Multi-spiral laser patterning of azopolymer thin films: profiles of the microstructures fabricated with circularly polarized multi-spiral light fields.

REFERENCES

- [1] M. Padgett, R. Bowman, *Nat. Photonics* 5, 343 (2011).
- [2] J.A. Rodrigo, T. Alieva, *Optica* 2, 812 (2015).
- [3] S. Sukhov, A. Dogariu, *Phys. Rev. Lett.* 107, 203602 (2011).

Carbon dots nanoparticles as an effective gate for PDT

M. Algarra¹, M.D. Nešić², J. Soto³, M. Stepić², A. Urrutia⁴, J.J. Imas⁴, T. Dučić⁵ and M. Petković²

¹INAMAT². Public University of Navarra, Campus de Arrosadía Pamplona, Spain

²Vinca Institute of Nuclear Sciences – National Institute of the Republic of Serbia, University of Belgrade, Belgrade, Serbia

³Dept Physical Chemistry, Faculty of Science, University of Málaga, Málaga, Spain

⁴ISC, Public University of Navarra, Campus de Arrosadía Pamplona, Spain

e-mail: manuel.algarra@unavarra.es

The promising strategy for targeted cancer treatment is to employ light as an external activator of a drug accumulated in tumor tissue. This approach is so-called photodynamic therapy (PDT) and can be used for diagnostic purposes. A photosensitizer, molecular oxygen, and laser light are the three significant components of Type II PDT, and the mechanism is the catalysis of the production of reactive oxygen species that lead to the oxidative damage of cellular molecules inducing cancer cell death [1]. Fluorescent carbon dots (CDs), spherical nanoparticles with size < 10 nm that can function as bioimaging agents and photosensitizers, have demonstrated significant potential in cancer theranostics [2]. Here, we have created Nitrogen co-doped carbon dots (N-CDs) surface decorated with organometallics compound, based on the Ru complex (Ru@N-CDs) [3,4] that were active in inducing biomolecular changes in ovarian cancer cell line upon illumination. Upon illumination, the most significant structural changes occurred in ovarian cancer cells and were detected in the protein region; we postulate interference with signaling pathways involved in regulating cancer cell growth and tumor progression.

However, the limitation of light is the depth of penetration through the tissues, which prevents significant therapeutic effects on deep tumors. A strategy to overcome this is to use optical fibers that have coatings fabricated from the N-CDs, thus developing a so-called lab-on fiber system. The light propagating through the fiber [4] can activate the overall coating on the optical fiber surface with the presence of Ru@N-CDs. We hypothesize that the activation by the light results in the locally increased ROS production combined with enhanced release of the Ru complex from the surface, similar to the Ru@TiO₂ NCS [5].

Our preliminary results demonstrate a high potential of the lab-on-fiber system in therapy against ovarian cancer that can resist traditional chemotherapeutic approaches.

REFERENCES

- [1] J.H. Correia *et al.*, *Pharmaceutics* 13, 1332 (2021).
- [2] T. Dučić *et al.*, *J. Coll. Interf. Sci.* 623, 226 (2022).
- [3] M.D. Nešić *et al.*, *Chem. Biol. Interact.* 360, 109950 (2022).
- [4] A. Urrutia *et al.*, *Laser Photonics Rev.* 13, 1900094 (2019).
- [5] M.D. Nešić *et al.*, *J. Photochem. Photobiol. A: Chem.* 347, 55 (2017).

All PM, 14 W, 2.8 GHz intra-burst repetition rate Yb-doped fiber laser

E. Hasar and P. Elahi

Department of Physics, Bogazici University, Istanbul, Turkey
e-mail: emre.hasar@boun.edu.tr

Ultrafast fiber lasers operating in burst mode enable new possibilities in laser-material processing, especially in high-precision thermal-damage-free ablation [1]. The Burst of ultra-fast pulses draws attention as a new technique for ablation-cooled material removal [2]. Ultrafast pulse trains in the burst are used to ablate the target material diverging from the processing region before the residual heat is delivered by the previous pulses [3].

We present the development of an all polarization maintaining (PM), high-power, ultra-high repetition rate, burst-mode Yb-doped fiber laser system with an average power of 14 W to achieve ablation-cooled material processing. We first developed the mode-locked oscillator, which generates about two ps-long pulses at an 89 MHz repetition rate. We used a cascade of 50/50 couplers and generated pulses at a 2.89 GHz repetition rate. Using three amplifier stages, all consisting of double-clad 10/125 fibers, we achieved 14 W output average power. We employed an acousto-optic modulator (AOM) after the first amplifier to generate a burst. The developed laser can be operated in both uniform and burst modes. Using a pair of 1200 line/mm compressor grating and after decompressing the pulses, we achieved about 760 fs long pulses at approximately 140 nJ pulse energy. We then investigated the micromachining of silicon and metals at different pulse energies and the number of pulses.

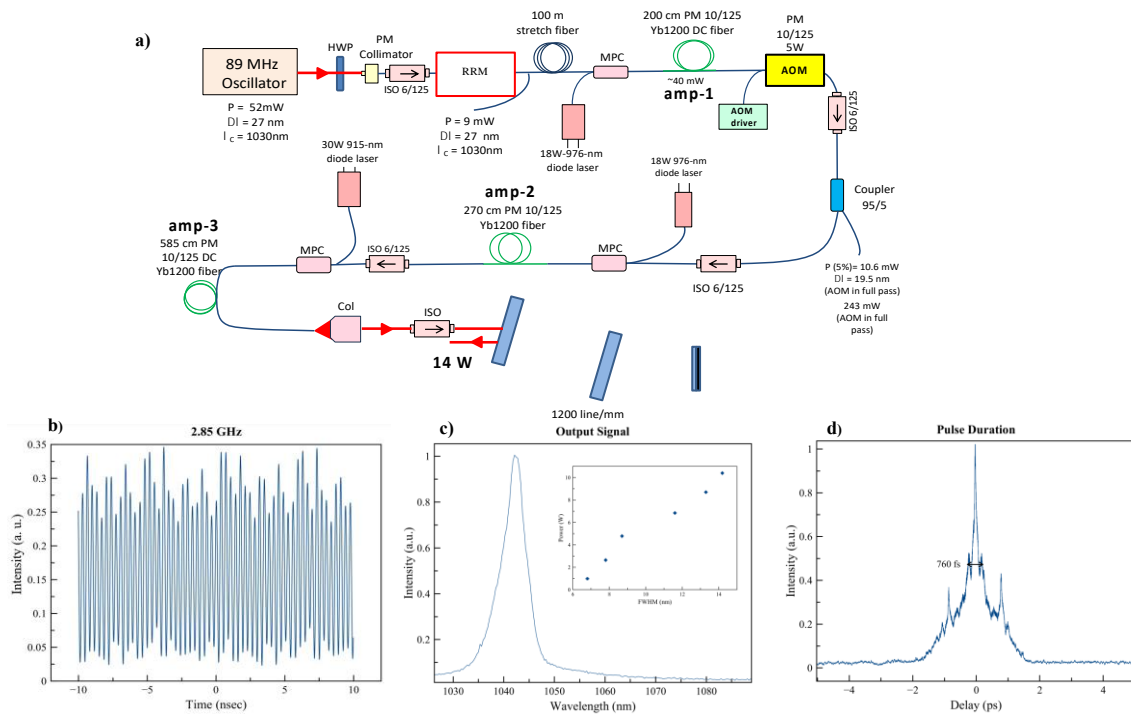


Figure 1. (a) Schematic setup of the developed laser system, (b) Intra-burst repetition rate at 2.8 GHz, (c) Output optical spectrum at full power (inset: FWHM changing by power), (d) Measured autocorrelation of the compressed pulses at 140 nJ individual pulse energy.

REFERENCES

- [1] H. Kalaycioglu *et al.*, IEEE J. Sel. Top. Quantum Electron. 24, 8800312 (2018).
- [2] C. Kerse *et al.*, Nature 537, 84 (2016).
- [3] P. Elahi *et al.*, Conference on Lasers and Electro-Optics Pacific Rim (Optica Publishing Group), paper s1710 (2017).

The analysis of the influence of optical absorbance on photothermally induced surface temperature variations in a thin sample of high optical transparency

M. Nesic¹, M. Popovic², S. Galovic¹, V. Miletic³ and Lj. Kostic⁴

¹Vinca Institute of Nuclear Sciences – National Institute of the Republic of Serbia, University of Belgrade, Belgrade

²Institute of Physics – National Institute of the Republic of Serbia, University of Belgrade, Belgrade

³Faculty of Philosophy – Pale, University of East Sarajevo, Sarajevo

⁴Faculty of Sciences and Mathematics – Department of Physics, University of Nis, Nis

e-mail: mioljub.nesic@vin.bg.ac.rs

In transmission gas-microphone photoacoustics, in order to protect the microphone and improve the Signal to Noise Ratio of the experiment, a thin non-transparent layer is applied on the surface of the sample. When the applied layer is not illuminated – the incident light is passed through the sample, instead, and all the transmitted radiation is absorbed at the non-illuminated side of the system – optical absorption properties of the sample are preserved in the recorded photoacoustic response [1-3].

Thermoelastic component of photoacoustic response is based on the integral of temperature distribution in the sample. However, in the described configuration, the amplitude ratio and the phase difference of surface temperature variations can notably influence the direction and the intensity of the thermoelastic movement of the sample, thus modifying the induced photoacoustic response.

Herein, the analysis of surface temperature variations is done, aimed at the prediction of thermoelastic component of the induced photoacoustic response, and the sensitivity of the described model to the alterations of optical absorption coefficient is analyzed and discussed.

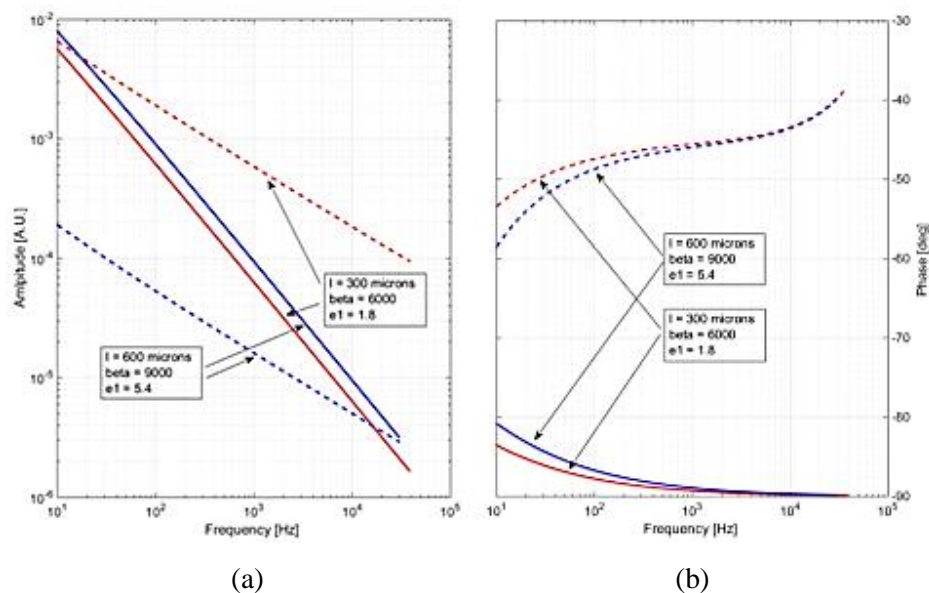


Figure 1. The influence of different values of absorbance (e_l) on amplitude (a) and phase (b) of surface temperature variations of the examined sample (illuminated side given in full, backside in dotted lines) [3].

REFERENCES

- [1] M.N. Popovic *et al.*, Opt. Quantum Electron. 50, 1 (2018).
- [2] V.V. Miletic *et al.*, J. Appl. Phys. 133, 075101 (2023).
- [3] V.V. Miletic *et al.*, Facta Univ. - Ser. Physics, Chem. Technol. 20, 67 (2022).

Interaction of ns laser with 316L-NiB stainless steel obtained by powder metallurgy – morphological effects and LIBS analysis

J. Stasic¹, M. Trtica¹, M. Kuzmanovic², J. Savovic¹, J. Ruzic¹, M. Simic¹, X. Chen³ and D. Bozic¹

¹Vinca Institute of Nuclear Sciences - National Institute of the Republic of Serbia, University of Belgrade, Belgrade, Serbia

²University of Belgrade, Faculty of Physical Chemistry, Belgrade, Serbia

³School for Mechanical and Electrical Engineering, Wenzhou University, Wenzhou City, PR China

e-mail: jelsta@vinca.rs

Austenitic stainless steel 316L finds a number of applications including filtration technology, nuclear industry, biomedicine, etc. Powder metallurgy (PM) allows obtaining the desired structure of the material, from full density to highly porous one, and PM technology most often comprises pressing and sintering steps. Gravity sintering, applied in this work, i.e. liquid phase sintering where the pressing step is excluded, is enabled by adding small amount of boron or its compound [1]. The addition of NiB lowers the sintering temperature by formation of eutectics (liquid phase), and also enhances mechanical properties (tensile strength, hardness) and corrosion resistance of 316L steel [2]. The aim of this work was to examine the surface behavior of PM-obtained 316L-NiB exposed to conditions of high heat fluxes by employing nanosecond laser pulses (TEA CO₂ laser emitting at 10.6 μm, fluence ~14 J/cm², intensity ~40 MW/cm²), which is reported scarcely in literature [3]. Simultaneously with irradiation in vacuum, plasma formed by laser irradiation above the sample surface was analyzed using LIBS (Laser Induced Breakdown Spectroscopy). Namely, small amount of boron (1 wt.% of NiB contains 83 wt.% of Ni and 17 wt.% of B) is not easily detected in gravity sintered sample and one of the techniques of choice could be the LIBS. For comparison purposes, 316L sample without NiB was also examined. Laser-irradiated surfaces were analyzed using SEM connected to EDX device. The damage was superficial, with intense melting in the central part of the irradiated spot, Fig. 1(a). LIBS analysis, Fig. 1(b), has shown successful in detecting the presence of boron in the 316L-NiB stainless steel, with low estimated limit of detection of 32 ppm.

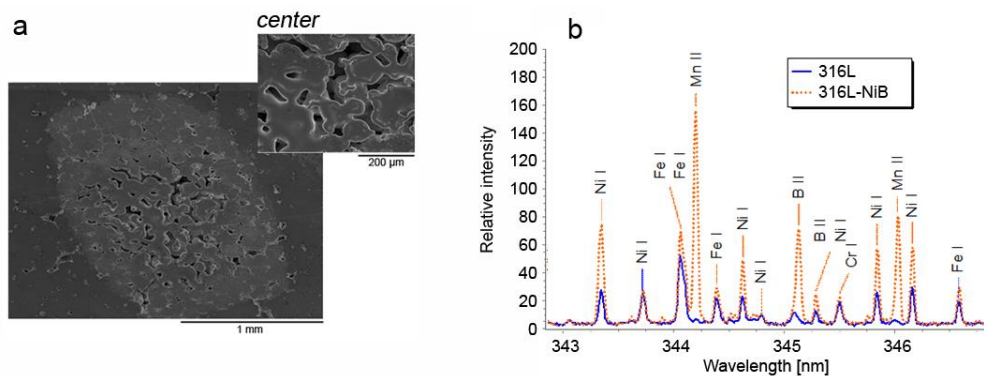


Figure 1. (a) 316L-NiB irradiated by 300 ns pulses (inset - central part); (b) corresponding LIBS spectra.

REFERENCES

- [1] D. Bozic *et al.*, *Sci. Sint.* 48, 293 (2016).
- [2] E. Bayraktaroglu *et al.*, *BioMed. Mater. Eng.* 22, 333 (2012).
- [3] N. Farid *et al.*, *Nucl. Fusion* 54, 012002 (2014).

ns-Laser – titanium interaction: hydrogen ambience

M. Trtica and J. Stasic

VINCA Institute of Nuclear Sciences - National Institute of the Republic of Serbia, University of Belgrade,
Belgrade, Serbia

e-mail: etrtica@vinca.rs

Interaction of a pulsed, ns-laser operating at 10.6 μm with a titanium target in hydrogen ambience was studied. In general, interaction in this type of environment is scarcely studied; however it can be of great importance. Titanium and its alloys show excellent physical and chemical properties and for these reasons they are attractive for aero-space and marine engineering, medicine, nuclear problematics, etc. Some phenomena, especially the action of thermal flux on a material, within fission/fusion reactor for example, can be simulated by ns-laser [1,2]. The Ti-surface variations at high TEA CO_2 laser energy density/fluence of $\sim 20 \text{ J/cm}^2$ and intensity of $\sim 60 \text{ MW/cm}^2$ were investigated in this work. Irradiation was carried out at a reduced H_2 atmosphere of $\sim 200 \text{ mbar}$ [3]. The energy absorbed from the laser beam is partially converted to thermal energy, which generates a series of effects, such as melting, vaporization of the molten material, shock waves, etc. Also, it should be mentioned that irradiation was accompanied by generation of plasma in front of the target. The following titanium target surface changes and phenomena were observed: (i) the damages were only on a superficial level (Fig. 1B) with depth $\leq 2 \mu\text{m}$; (ii) appearance of pores on the grain boundaries in the central irradiated zone (Fig. 1A). The cracking effect is visible as well in this zone. In the main, all changes can be attributed to the extra-fast heating and cooling process; (iii) in the peripheral zones similar features were registered, while the transition between irradiated and non-irradiated region is sharp.

It can be concluded from this study that the reported laser fluence and intensity, in hydrogen ambience, effectively modified the titanium target. The created surface structures generally could be acceptable in cases where high roughness is required, while for some applications in nuclear technologies additional studies should be done (in this context, the presence of H_2 in fusion reactor materials is not desirable [3]).

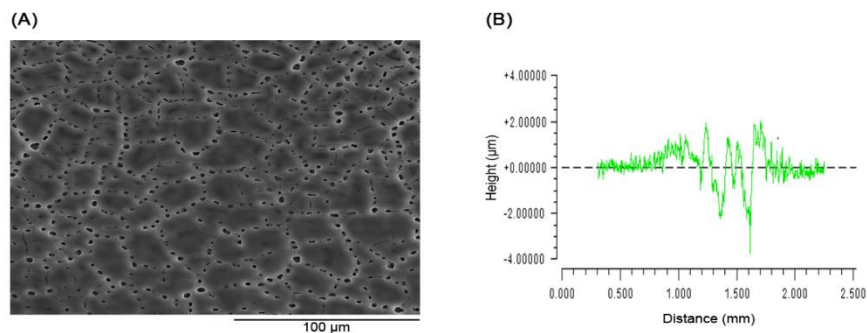


Figure 1. (A) SEM analysis of Ti-target in H_2 ambience; (B) 2D profilometry; (Irradiation after 300 laser pulses).

REFERENCES

- [1] M. Trtica *et al.*, Appl. Surf. Sci. 258, 2741 (2012).
- [2] N. Farid *et al.*, Nucl. Fusion 54, 012002 (2014).
- [3] M. Trtica *et al.*, The paper ref. no. 246-22 (title: LIBS Hydrogen Isotopes Detection: Significance in Nuclear/Fusion Technology) - accepted for publication in ZhPS (Russian version), 91, January-February (2024).

10. Optical metamaterials and plasmonics

All-dielectric optical metasurfaces for sensing of substances with identical real parts of refractive index

M. Obradov, Z. Jakšić, I. Mladenović, M. Rašljčić Rafajilović and D. Vasiljević Radović
 Centre of Microelectronic Technologies, Institute of Chemistry, Technology and Metallurgy – National Institute of the Republic of Serbia, University of Belgrade, Njegoseva 12, 11000 Belgrade, Serbia
 e-mail: marko.obradov@ihtm.bg.ac.rs

Metasurfaces are one of the most attractive research fields in recent years, in no small measure due to their use as refractometric sensors with unparalleled sensitivity, enabling sensing of even single atoms or molecules. This sensitivity is rooted in their ability to localize electromagnetic fields in volumes orders of magnitude below the diffraction limit. This is achieved by special geometry and refractive index contrast of metasurface nanocomposites. A plethora of both conductive (metals, TCO, graphene, MXenes...) and dielectric (oxides, semiconductors) materials can be used, all of them bringing different functionalities which further enhance the freedom of design when tailoring metasurfaces [1]. However, the fundamental sensing mechanism is practically identical across all platforms and is based on the spectral shift of transmission or reflection due to a difference in the values of the real parts of refractive index between analyte and the environment.

Here we propose an alternative approach, the use of exceptional capabilities of optical metasurfaces in transforming optical space to sense analytes with identical real parts of refractive index but different imaginary parts (losses). This is becoming increasingly important with the need to detect airborne viruses [2]. We propose a metasurface formed by cruciform openings in a thin silicon layer on a SiO₂ substrate, as shown in Fig. 1a. The structure is suspended in the air. For our FEM simulation we used measured values for Si and SiO₂ refractive index taken from literature [3,4]. The electric field distribution and its circular power flow, both at a wavelength of 630 nm, are shown in Fig. 1b. We gradually increase the imaginary part of the refractive index in the cruciform openings, starting with the lossless case, while maintaining the real part of refractive index equal to unity (air). The dispersive properties that depend on the value of the imaginary part are shown in Fig. 1c. The circular power flow that increases the optical path, the field localization and intrinsically low losses of the structure in the visible range all cause that adding even the smallest volumes of analyte with slightly increased optical absorption in comparison to the metasurface significantly reduces transmission through the structure, despite the exceptionally low structure thickness.

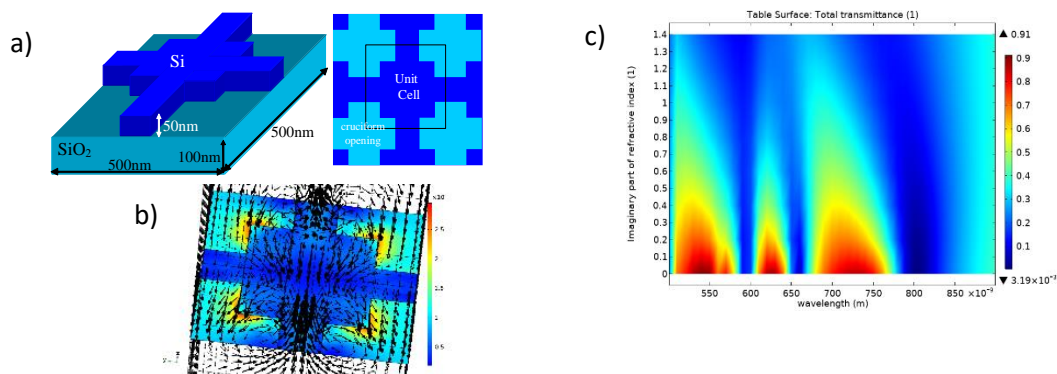


Figure 1. a) Unit cell of an all-dielectric Si on SiO₂ metasurface; b) Electric field distribution and circular power flow at a wavelength of 630 nm; c) Transmission dispersion depending on the material losses (imaginary part of refractive index) in the cruciform openings.

REFERENCES

- [1] B.I. Karawdeniya *et al.*, Chem. Rev. 122, 14990 (2022).
- [2] M. Amin *et al.*, Carbon 176, 580 (2021).
- [3] D. E. Aspnes, A. Studna, Phys. Rev. B 27, 985 (1983).
- [4] L.V. Rodríguez-de Marcos *et al.*, Opt. Mat. Exp. 6, 3622 (2016).

Electron energy loss spectroscopy of multilayered structures: Theoretical aspects and the role of graphene-insulator distance

I. Radović¹, A. Kalinić¹, L. Karbunar² and Z.L. Mišković³

¹*Department of Atomic Physics, "VINČA" Institute of Nuclear Sciences - National Institute of the Republic of Serbia, University of Belgrade, Belgrade, Serbia*

²*School of Computing, Union University, Belgrade, Serbia*

³*Department of Applied Mathematics, and Waterloo Institute for Nanotechnology, University of Waterloo, Waterloo, Ontario, Canada*

e-mail: iradovic@vin.bg.ac.rs

Electron energy loss spectroscopy (EELS) is a commonly used experimental technique for investigating electronic and plasmonic properties of materials, including van der Waals (vdW) materials [1]. Following Ref. [2] we derive a general expression for the effective dielectric function of multilayered structures made of two-dimensional (2D) vdW materials separated by insulating layers, in terms of the dielectric functions of the insulating layers and the 2D response functions of the vdW sheets, so the EEL spectrum of such structures may be deduced and compared with the available experimental data.

In our previous publications [3-5] we investigated the effects of plasmon-phonon hybridization in graphene-insulator-graphene heterostructures. In all those publications we assumed a zero gap between graphene and insulator to simplify calculations. In this work we assign for the first time a finite gap size between graphene and insulator, and apply the general expression for the effective dielectric function of multilayered structures to the case of graphene-insulator-graphene composite. The energy loss function (the imaginary part of the negative value of the inverse dielectric function) is shown for the cases of graphene-insulator-graphene composite systems with and without the finite gap size between graphene and insulator in order to study the role of graphene-insulator distance on the hybridization between the Dirac plasmons in graphene layers and the Fuchs-Kliwer phonons in both surfaces of the insulator slab. The response function of each graphene is obtained using the dynamic polarization function of graphene within the random phase approximation for its π electrons described as Dirac's fermions. The response of the insulator layer is described by a dielectric function consisting of several Lorentzian terms.

REFERENCES

- [1] A.A. Govyadinov *et al.*, Nat. Commun. 8, 95 (2017).
- [2] Ph. Lambin *et al.*, Phys. Rev. B 32, 8203 (1985).
- [3] V. Despoja *et al.*, Phys. Rev. B 96, 075433 (2017).
- [4] V. Despoja *et al.*, Phys. Rev. B 100, 035443 (2019).
- [5] A. Kalinić *et al.*, Phys. Rev. B 106, 115430 (2022).

Plasmon-phonon hybridization in drift-current biased supported graphene

I. Radović¹, A. Kalinić¹, L. Karbunar² and Z.L. Mišković³

¹*Department of Atomic Physics, "VINČA" Institute of Nuclear Sciences - National Institute of the Republic of Serbia, University of Belgrade, Belgrade, Serbia*

²*School of Computing, Union University, Belgrade, Serbia*

³*Department of Applied Mathematics, and Waterloo Institute for Nanotechnology, University of Waterloo, Waterloo, Ontario, Canada*

e-mail: zmiskovi@uwaterloo.ca

In our previous publications [1-4] we studied the effects of plasmon-phonon hybridization in graphene supported by an insulating substrate [1], as well as in graphene-insulator-graphene composite systems [2-4]. In this work we investigate the hybridization between the Dirac plasmon in graphene layer biased with a drift electric current and the surface optical phonon modes in the insulating substrate. The dielectric function of the system is written in terms of the response function of graphene and the bulk dielectric function of the substrate. The response function is expressed in terms of a nonlocal conductivity of graphene. The intraband conductivity of graphene is obtained using the Boltzmann theory [5-6], whereas the effects of high-energy interband electron transitions are accounted for by using a linear function of frequency for the imaginary part of the interband conductivity [7]. The conductivity with a drift current is evaluated using the Galilean Doppler shift model [8,9]. The energy loss function (the imaginary part of the negative value of the inverse dielectric function) is presented for three different values of the drifting velocities of electrons showing the effects of the drift velocity on the plasmon-phonon hybridization.

REFERENCES

- [1] T. Marinković *et al.*, *Plasmonics* 10, 1741 (2015).
- [2] V. Despoja *et al.*, *Phys. Rev. B* 96, 075433 (2017).
- [3] V. Despoja *et al.*, *Phys. Rev. B* 100, 035443 (2019).
- [4] A. Kalinić *et al.*, *Phys. Rev. B* 106, 115430 (2022).
- [5] I. Radović *et al.*, *Phys. Rev. B* 77, 075428 (2008).
- [6] T.A. Morgado, M.G. Silveirinha, *Nanophotonics* 11, 4929 (2022).
- [7] Z.L. Mišković *et al.*, *Radiat. Eff. Defects Solids* 178, 54 (2023).
- [8] T.A. Morgado, M.G. Silveirinha, *Phys. Rev. Lett.* 119, 133901 (2017).
- [9] T.A. Morgado, M.G. Silveirinha, *Phys. Rev. Lett.* 123, 219402 (2019).

Terahertz transmission through metal-insulator-metal cavity arrays infiltrated by liquid crystals

G. Isić¹, D.C. Zografopoulos² and B. Vasić¹

¹*Institute of Physics Belgrade, University of Belgrade, Belgrade, Serbia*

²*Consiglio Nazionale delle Ricerche, Istituto per la Microelettronica e Microsistemi, Roma, Italy*

e-mail: isicg@ipb.ac.rs

Standard liquid crystal (LC) cell designs, ubiquitous in modern optical devices, cannot simply be scaled up for terahertz frequencies due to limitations associated with the physics of LC switching (for example, terahertz cells would be orders of magnitude slower than optical LC cells [1]). For narrow bandwidth applications, LC cells involving a resonant response of leaky eigenmodes, e.g. in metal-insulator-metal cavity arrays [2], have been found promising [3]. We have previously found that such arrays are interesting for tuning various properties of the reflected beam, including amplitude modulation [4], polarization conversion [5] and beam steering [6].

In this work, we examine terahertz transmission through an array of metal-insulator-metal cavities infiltrated by liquid crystals. The addition of another radiative decay channel for the cavity array eigenmodes (the one corresponding to the transmitted beam), complicates considerably the reflection and transmission spectra. We discuss the applicability of the temporal-coupled mode theory model [7] for understanding the resonant response, the typical amplitude modulation depth that can be expected and its dependence on materials and geometrical parameters.

REFERENCES

- [1] N. Vieweg *et al.*, *J. Infrared Millimeter Terahertz Waves* 33, 327 (2012).
- [2] Y. Todorov *et al.*, *Phys. Rev. Lett.* 102, 186402 (2009).
- [3] S.A. Jewell *et al.*, *Mol. Cryst. Liq. Cryst.* 494, 320 (2008).
- [4] G. Isić *et al.*, *Phys. Rev. Appl.* 3, 064007 (2015).
- [5] B. Vasić *et al.*, *Nanotechnology* 28, 124002 (2017).
- [6] B. Vasić *et al.*, *IEEE J. Sel. Top. Quantum Electron.* 26, 7701609 (2020).
- [7] S. Fan, W. Suh, *J. Opt. Soc. Am. A* 20, 569 (2003).

Ellipsometric Study of Interactions of Erufosine with Solid-supported by Metasurfaces Lipid Films

D. Georgieva¹, M. Tanovska¹, V. Vassilev¹, R. Tzoneva², M. Berger³, M. Rahmani⁴, D. Neshev⁴ and L. Vladimirova-Mihaleva¹

¹*Sofia University "St. Kliment Ohridski", Faculty of Physics, Department of Optics and Spectroscopy, 5 James Bourchier Blvd., 1164 Sofia, Bulgaria*

²*Bulgarian Academy of Sciences, Institute of Biophysics and Biomedical Engineering, Sofia, Bulgaria*

³*German Cancer Research Center, Toxicology and Chemotherapy Unit, Heidelberg, Germany*

⁴*The Australian National University, Research School of Physics, ARC Centre of Excellence for Transformative Meta-Optical Systems (TMOS), Canberra, ACT 2601, Australia*

e-mail: vladimirova@phys.uni-sofia.bg

It is well known that cell membranes are responsible for the interaction of cells with the environment. For this reason, the sensory systems of the cells are concentrated into them. The process of transporting drugs across the cell membrane is intricate and challenging to comprehend due to its dynamic nature. In this work, we present spectral ellipsometry as an optical technique by which we can study the interaction of the anticancer drug erufosine with a lipid model system mimicking the cell membrane. Erufosine (EPC3) is a novel ether-lipid alkyl-phosphocholine showing high efficacy in vitro and in vivo tumour models. Lipid films are composed of phosphatidylcholine, cholesterol and sphingomyelin. In our study, we utilize metamaterial surfaces to support the lipid films. Our metasurfaces are fabricated from amorphous silicon on glass by electron beam lithography and subsequent etching. Such metasurfaces have been used in various biological research areas, such as the chemical composition of liquids, biosensors for biomolecular recognition, and the detection of cancer cells [1,2]. Studies conducted at different cholesterol concentrations show that the ellipsometric angle Δ increases with the growth of the cholesterol in the system. A peak shift into higher wavelengths is observed. The obtained data show that with the growth of the concentration of erufosine in the system, the ellipsometric angle Δ also increases. The results display the ability of the lipid layer's reorganization upon interaction with the anticancer agent. The presented study confirms that metasurfaces can be used as an efficient sensor platform for the determination of the action of drugs on the cell membranes.

REFERENCES

- [1] R. Melik *et al.*, Opt. Express 18 (2010).
- [2] J.F. O'Hara *et al.*, Opt. Express 16 (2008).

Rosette based metamaterial for circularly polarized terahertz waves manipulation

D.B. Stojanovic¹, U. Ralevic², Y. Demirhan³, G. Aygun³ and L. Ozyuzer^{3,4}

¹*Vinca Institute of Nuclear Sciences-National Institute of Republic of Serbia, University of Belgrade, Belgrade, Serbia*

²*Institute of physics, University of Belgrade, Belgrade, Serbia*

³*Department of Physics, Izmir Institute of Technology, Izmir, Turkey*

⁴*Teknoma Technological Materials Industrial and Trading Inc., Izmir, Turkey*

e-mail: dankas@vin.bg.ac.rs

Metamaterials that respond resonantly in interaction with the terahertz (THz) electromagnetic waves are significant for the achievement of diverse optical functionalities in THz spectral range [1]. Also, they are virtually desirable platforms for investigating chiral effects which rise due to different interaction of metamaterials with left and right circularly polarized light [2,3]. Light polarization is an important feature of electromagnetic waves and manipulation of polarization plays pivotal role in various areas such as communications, imaging and sensing. One of potential applications of the THz metadevices is for protein quality control in the biotechnology or food industries [4].

Chiral properties of metamaterial can be modified via different external influences, such as by changing the interlayer twist angle, adding a dielectric spacer, or modulating its thickness. Twisting or rotating achiral layered structures in parallel planes enables engineering of the extrinsic chirality and consequential optical performance. For example, the twist angle from counterclockwise rotation of an upper layer with respect to the one under it, leads to a left-handed stacking geometry [5]. In this study, we performed numerical simulations of the metamaterial structure in terahertz frequency range, 0.25-0.75 THz. The numerical simulations were done for the case of two parallel gold rosettes on sapphire substrates in which we analyzed the influence of rotating one rosette with respect to the another on chiral properties. Two geometries of the rosette based structures were studied. First geometry is based on resonator which consists of two same parallel rosettes and the second one of two parallel rosettes, but one of them is trimmed.

REFERENCES

- [1] M. Tonouchi, *Nat. Photonics* 1, 97 (2007).
- [2] D.B. Stojanović *et al.*, *J. Phys. D: Appl. Phys.* 51, 045106 (2018).
- [3] Z. Wang *et al.*, *Nanotechnology* 27, 412001 (2016).
- [4] Z. Zhang *et al.*, *Biomed. Opt. Express* 13, 209 (2022).
- [5] Z. Han *et al.*, *Adv. Mater.* 35, 2206141 (2023).

11. Machine learning in photonics

Remote temperature sensing using upconverting phosphor and artificial neural networks

M.S. Rabasovic, M.G. Nikolic and D. Sevic
 Institute of Physics, Belgrade, Serbia
 e-mail: majap@ipb.ac.rs

In this study we analyze possibilities of using artificial neural networks (ANN) for modeling the temperature sensing curve of a thermophosphor.

For machine learning analysis of data and ANN model we have used Solo+Mia software package (Version 9.1, Eigenvector Research Inc, USA). Experimental results were obtained using experimental setup presented in detail in [1,2]. Upconverting material was excited at 980 nm by using pulsed laser diode. Usual, conventional way is to use intensity ratios of spectral lines for determining the calibration curves for remote temperature sensing [3-5]. Based on thus obtained data we have trained the neural network to recognize temperature of sample based on its luminescence spectrum. For training we have used 69 measured spectral points between 525 nm and 560 nm, so the neural network has 69 input nodes.

Temperature sensing calibration curve of $\text{Y}_2\text{O}_2\text{S}:\text{Er}^{3+}, \text{Yb}^{3+}$ is shown in Figure 1 (a). Structure of ANN used to model the temperature sensing characteristics of nano phosphor is shown in Figure 1 (b). ANN predictions, shown in Figure 1 (c) imply reliable estimation of temperature using ANN shown in Figure 1 (b).

The artificial neural network provides quick and strait answer when questioned with data of samples heated to unknown temperatures. This kind of approach is very versatile, and, if needed, improved by other machine learning approaches and deep learning [6,7].

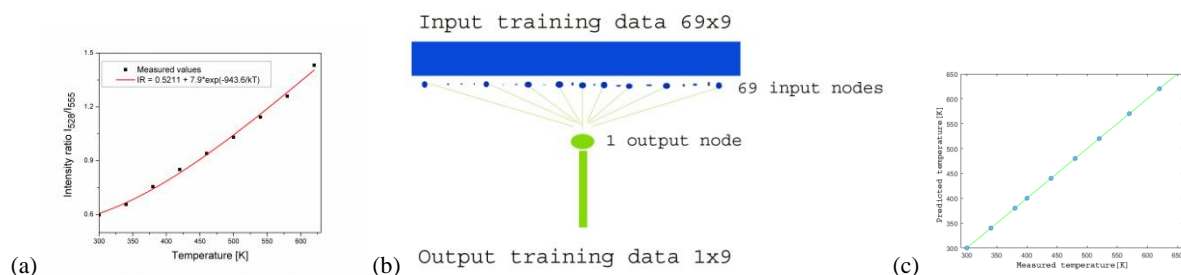


Figure 1. (a) Temperature sensing calibration curve of $\text{Y}_2\text{O}_2\text{S}:\text{Er}^{3+}, \text{Yb}^{3+}$. (b) Structure of ANN used to model the temperature sensing characteristics of nano phosphor. (c) Plot of predicted temperatures vs measured temperatures from training set.

REFERENCES

- [1] D. Sevic *et al.*, Opt. Quantum Electron. 52, 232 (2020).
- [2] D. Sevic *et al.*, J. Phys. D: Appl. Phys. 53, 015106 (2020).
- [3] D. Jaque, F. Vetrone, Nanoscale 4, 4301 (2012).
- [4] C.D.S. Brites *et al.*, Nanoscale 4, 4799 (2012).
- [5] M. Aldén *et al.*, Prog. Energy Combust. Sci. 37, 422 (2011).
- [6] M.S. Rabasovic *et al.*, Adv. Space Res. 71, 1331 (2023).
- [7] M.S. Rabasovic *et al.*, Contrib. Astron. Obs. Skalnat Pleso 50/3, 1 (2022).

Reverse sigmoid-like nonlinearity in Fabry-Perot injection-locked lasers

P. Atanasijević, M. Banović, J. Crnjanski, M. Krstić, P. Mihailović, S. Petričević and D. Gvozdić
 School of Electrical Engineering, University of Belgrade, Serbia
 e-mail: petarat@etf.bg.ac.rs

The increasing demand for faster, more efficient computing propelled the field of neuromorphic photonics to unforeseen extents. A variety of approaches to generation of much needed nonlinearities were proposed, while still evolving all-optical solutions remain the most promising way to achieve scalability [1]. Contrary to their monotonically increasing equivalents, the examples of decreasing nonlinearities, such as the reverse sigmoid are rarely encountered in proposed solutions [2].

In this research, we experimentally realize an all-optical nonlinear unit based on an injection-locked Fabry-Perot laser diode, exploiting its dispersive bistability [3]. An input optical pulse train with 5 ns pulse widths, 128 ns periods and increasing amplitudes is injected near the slave laser's $m = +2$ side mode (positive side modes correspond to shorter wavelengths), with a controlled frequency detuning of -12.7 GHz (negative value corresponding to red shift). Positive/negative pulses are applied depending on the initial state of the slave laser, free-running or injection-locked (Fig. 1 a) and b), respectively). The central mode of the free-running slave laser's spectrum is filtered using a bandpass optical filter and monitored as the unit's output using a photodiode. The nonlinear input-output dependence exhibits a reverse sigmoid-like trend, influenced by injection-locking parameters, as well as slave laser's operating conditions. Furthermore, different nonlinearities are achieved depending on the slave laser's initial state, as shown in Fig. 1. Typical 50 % sigmoid thresholds are achieved for peak input optical powers of about 100 μW , corresponding to pulse energies of 0.5 pJ. Presented nonlinearity provides a promising alternative route to current trends in neuromorphic photonics.

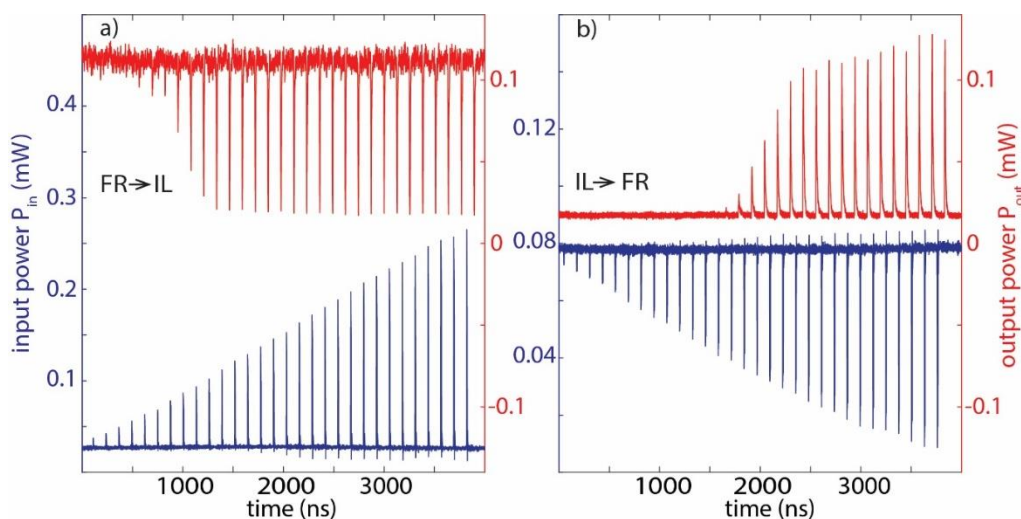


Figure 1. Input (blue) and output (red) pulses of the proposed nonlinear unit, for different initial states of the slave laser: a) free-running (FR), and b) injection-locked state (IL).

REFERENCES

- [1] G. Dabos *et al.*, Opt. Mater. Express 12, 2343 (2022).
- [2] A.N. Tait *et al.*, Phys. Rev. Appl. 11, 064043 (2019).
- [3] J.V. Crnjanski *et al.*, Opt. Lett. 46, 2003 (2021).

Low-cost raspberry Pi based imaging system for analysis of Fiber Specklegram Sensors

L. Brestovacki, M. Golubovic, J. Bajic, A. Joža and V. Rajs

University of Novi Sad, Faculty of Technical Sciences, Department of Power, Electronic and Telecommunication Engineering, Novi Sad, Serbia

e-mail: lenkabrestovacki@uns.ac.rs

Fiber optic sensors are becoming highly popular due to their multiplexing capability, compactness, and electromagnetic field immunity [1]. For determining strain and stress impact especially promising are Fiber Specklegram Sensors (FSS) regarding their high sensitivity and possibility of low-cost implementation in electronics [2-4]. In this paper, one low-cost imaging system for FSS based on Raspberry Pi is presented. The aim of this research is to investigate the influence of mechanical deformations on specklegram by comparing referent specklegram (when the fiber is not deformed) and specklegram taken for deformed fiber. In Figure 1 the experimental setup of the proposed system for analysis of Fiber Specklegram Sensors is presented. A spatially coherent light source emits light waves with different but constant phases of the same frequency and amplitude through a 50 μm multimode (MM) optical fiber. Due to modal interference, one may notice a speckle pattern as the light modes propagate. Since high intensity of light can cause sensor saturation, the attenuator is required for decreasing light intensity. Mechanical deformation made in this experiment can vary the angle and intensity of force. By manually making deformations it is observed that the geometrics of speckles are different for different deformations. For extracting information on the activity of the tested sample of the recorded light intensity distribution is used a statistical approach. Statistical analysis is almost mandatory for the study of dynamic speckle phenomena [5]. Therefore, the use of machine learning for tracking feature changes is proposed.

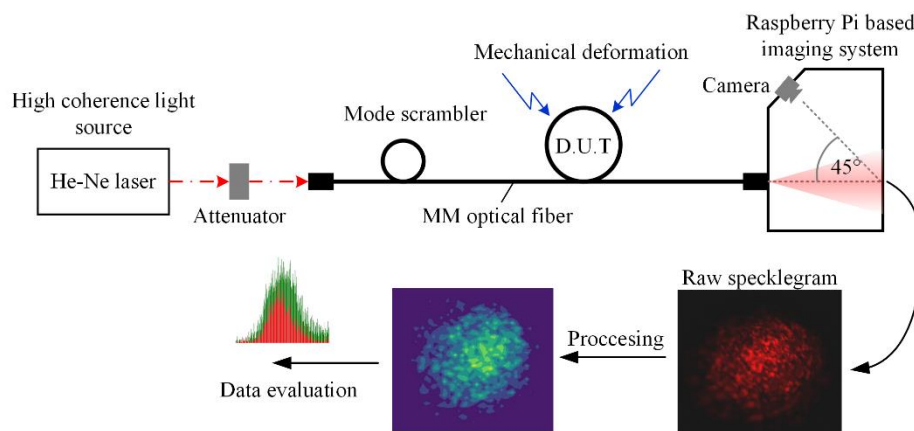


Figure 1. Experimental setup used in this work.

For taking images Raspberry Pi camera module v2 NoIR is used, while image processing is performed on Raspberry Pi model 3, 1GB.

REFERENCES

- [1] A.G. Leal-Junior *et al.*, IEEE Sens. J. 20, 569 (2019).
- [2] E. Fujiwara *et al.*, Opt. Eng. 57, 116107 (2018).
- [3] L. Rodriguez-Cobo *et al.*, Sens. Actuator. A-Phys. 203, 341 (2013).
- [4] E. Fujiwara *et al.*, IEEE Sens. J. 17, 951 (2016).
- [5] P. Etchepareborda *et al.*, Appl. Opt. 49, 3753 (2010).

12. Other topics in photonics

Revealing non-equilibrium dynamics by holography: The case of Briggs-Rauscher reaction

M. Pagnacco¹, M. Simovic Pavlovic², A. Radulovic³, B. Bokic⁴, D. Vasiljevic⁴ and B. Kolaric^{4,5}

¹University of Belgrade, Institute of Chemistry, Technology and Metallurgy, Njegoseva 12, Belgrade, Serbia

²University of Belgrade, Faculty of Mechanical Engineering, Kraljice Marije 16, Belgrade, Serbia

³University of Belgrade, Institute of General and Physical Chemistry, Studentski trg 12/V, Belgrade, Serbia

⁴University of Belgrade, Institute of Physics, Photonics Center, Pregrevica 118, Belgrade, Serbia

⁵Micro- and Nanophotonic Materials Group, University of Mons, Place du Parc 20, 7000 Mons, Belgium

e-mail: simovicmarina99@gmail.com

In this study, the interferometric (holographic) approach is used to unveil the dynamics of the phase transition, e.g., the formation of solid iodine in the Briggs-Rauscher (BR) non-equilibrium system. Subsequently, after deterministic oscillatory dynamics this system undergoes random transition from state I (low iodide and iodine concentration) to state II (high iodide and iodine concentration, with the formation of solid iodine) [1].

The observed interferometric pattern of dark and bright lines known as fringes is applied to monitor the changes in BR dynamics as a function of time. The pattern abruptly changes at the point of the phase transition.

The power of holography is related to its ability to see the rise of the phase transition directly. At the same time, other methods, such as potentiometry (often used in non-equilibrium studies), are limited by secondary processes such as adsorption and electrode passivation. The holography opens the way to reveal nanoscale dynamics with minimal disturbances in various non-equilibrium systems [2].

REFERENCES

- [1] M.C. Pagnacco *et al.*, J. Phys. Chem. A 122, 482 (2018).
- [2] M. Simovic-Pavlovic *et al.*, J. Vis. Exp. 181, e63676 (2022).

Using Laser-Induced Fluorescence technique for interdisciplinary natural sciences school experiment

L. Zaharieva¹, M. Stoyanova², V. Dimova², V. Deneva¹, Ts. Genova¹, A. Markovski³, L. Antonov¹ and C. Andreeva^{1,2}

¹*Institute of Electronics, Bulgarian Academy of Sciences, Sofia, Bulgaria*

²*Faculty of Physics, Sofia University "St. Kliment Ohridski", Sofia, Bulgaria*

³*Faculty of Automatics, Technical University of Sofia, Bulgaria*

e-mail: zaharievalidia@gmail.com

The requirements laid down in modern education strengthen the role of experimental methods, research tasks, integrative processes, digital competence and students' skills for independent acquisition of knowledge. These elements of the learning process find their specific place in natural science education.

According to the European Reference Framework for Lifelong Learning, physics is directly related to the following key competence: building of "mathematical competence and competence in science, technology and engineering" [1]. Often the subjects of mathematics and physics are neglected in the education on chemistry and biology, leaving a gap that needs a scientifically sound, but at the same time interesting and life-related bridge to be built.

In the current work, we will present the possibility of making a connection between physics, chemistry and biology (through food technology) and information technology through the application of the research method when conducting an educational physics experiment.

More specifically, we will demonstrate the application of Laser-Induced Fluorescence (LIF) method, with the main focus on the characterization / identification of organic materials like honey and its adulterations. The goal is for students to see the possible applications of this method when working with food, medicinal and cosmetic products. As described in [2], the radiation from the laser with a wavelength of 405 nm is fed to a cuvette holder, in which cuvettes with the samples are placed. Transverse fluorescence is collected using the collimator and fed by fiber to the spectrometer connected to a computer for visualization and post-processing of the data.

The inspiration for this work came from a problem given at the European Olympiad on Experimental Sciences (2021), where the participating students had to process data obtained in a scientific laboratory [3]. In our work we go a step further and show how such experiment can be made feasible in any standard school with very affordable educational-grade equipment.

The obtained results will help in the development and use of STEM centers and programs in schools, they will also contribute to the better understanding of the interdisciplinary connections between physics and biology, they will also raise the students' interest in natural sciences education and support the professional education of students, future biologists, chemists, doctors, etc.

REFERENCES

- [1] Official Journal of the European Union 61, C 189/01 (2018).
- [2] N.M. El-Biale *et al.*, Aust. J. Basic Appl. Sci. 7, 132 (2013).
- [3] <https://u-szeged.hu/gyakorlo-honlap/menu-vertikalis/day-1>.

One dimensional SP lattices based on photonic molecules

D. Román-Cortés^{1,2}, G. Cáceres-Aravena^{1,2}, B. Real^{1,2} and R.A. Vicencio^{1,2}

¹*Departamento de Física, Facultad de Ciencias Físicas y Matemáticas, Universidad de Chile, Santiago, Chile.*

²*Millennium Institute for Research in Optics - MIRO*

e-mail: rvicencio@uchile.cl

The development of the femtosecond laser writing technique has revolutionized the fabrication of waveguide arrays and photonic lattices due to its simplicity and versatility. Different configurations on different dimensions are possible by simply coding the X, Y and Z positions of waveguides inside a glass material [1]. However, the natural vertical ellipticity of fabricated waveguides is a major challenge that can be overcome by tuning the vertical distances among waveguides for compensating the coupling constants. However, when having the need of, for example, exciting different modes (orbitals) on single waveguides, this vertical orientation destroys the degeneracy and vertically oriented states are the ones obtained experimentally [2]. This decreases the available experimental possibilities for studying more complex interactions on lattices [3].

In this work, we use the femtosecond laser writing technique and study the effect of writing two very close waveguides, such that they can be treated as an effective wider waveguide or “photonic molecule” [4]. We demonstrate that different higher order states can be excited depending on the excitation wavelength, and that the vertical restricted dipoles of single waveguides [2,3] can be oriented now, for example, horizontally. This can be thought as a simple spatial rotation but has very important consequences when studying lattice dynamics on non-trivial configurations. To demonstrate this effect, we fabricate one of the simplest inter-orbital lattice configurations: a one-dimensional alternating SP lattice. We study the excitation of a zero-momentum Gaussian beam (using a spatial light modulator image technique) and observe maximum diffraction of two well defined escaping lobes. This is in strong contrast with standard 1D lattices where for zero momentum the energy does not transport through the system. In addition, we also found that for a small non-zero detuning in between S and P modes, the 1D lattice can be mapped onto an effective diamond lattice that exhibit flat band and topological properties which strongly affect the expected dynamics of this otherwise trivial lattice.

REFERENCES

- [1] A. Szameit *et al.*, Opt. Express 13, 10552 (2005).
- [2] D. Guzmán-Silva *et al.*, Phys. Rev. Lett. 127, 066601 (2020).
- [3] G. Cáceres-Aravena *et al.*, Phys. Rev. Lett. 128, 256602 (2021).
- [4] M. Bayer *et al.*, Phys. Rev. Lett. 81, 2582 (1998).

Wave-packets induced by the radiation of an atom coupled to the continuum in photonic lattices

B. Real^{1,2}, D. Guzmán-Silva^{1,2} and R.A. Vicencio^{1,2}

¹Departamento de Física, Facultad de Ciencias Físicas y Matemáticas, Universidad de Chile, Chile

²Millennium Institute for Research in Optics - MIRO, Chile

e-mail: bastianreal71@gmail.com

The generation of an input wave-packet with well-defined momentum and energy is an experimental challenge when exciting photonic lattices. So far, most of the experimental techniques lie in externally modulating a beam via, for instance, spatial light modulators [1]. Despite these progresses, an optically integrated control of wave-packets is needed to excite desired eigenstates, which could facilitate concatenate photonic operations.

In this work, we exploit the analogy of an atom decaying into a continuum using waveguide arrays [2,3], to generate wave-packets with precise momenta. A metastable atom and the continuum are simulated respectively by a single waveguide and a 1D tight-binding lattice [2], which are weakly coupled, as schematized in Fig. 1(a). The temporal decay and radiation are mapped into the spatial propagation along the waveguides facilitating the detection at given “times”. Experimentally, we fabricate a waveguide weakly coupled to a 1D photonic lattice using the femtosecond laser writing technique [4]. We excite the waveguide atom and, after 3 cm of propagation, we detect the radiation in the 1D lattice has a specific momentum (see Fig. 1(b)-(c)). When placing an adjacent SSH lattice in the nontrivial topological phase, the wave-packet with wave-vector center in $\pi/2$ (and thus zero energy) excites precisely one of its edge state, exhibiting light intensity only on A sites, as shown in Fig. 1(d).

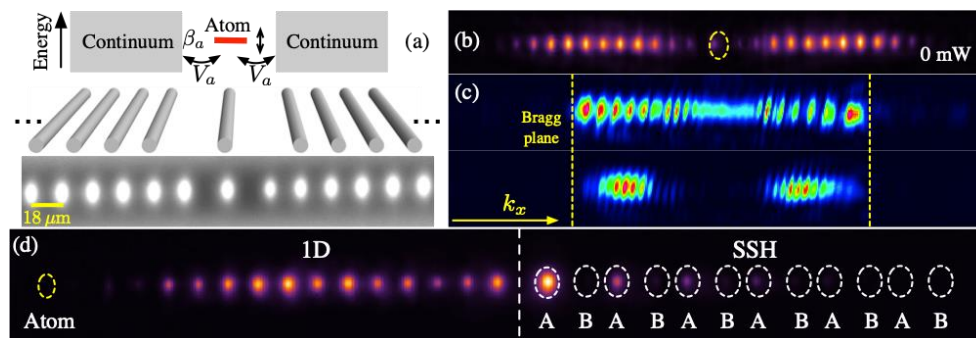


Figure 1. (a) Photonic analog of an atom coupled to a tight-binding continuum. Top panel schematizes the energy of the atom (red line) and the continuum. Middle, sketch of the photonic implementation. Bottom, output facet of the glass wafer after white illumination. (b) Output intensity profile when the atom is excited (yellow ellipse). (c) Fourier plane of both a discrete diffraction (top) and intensity pattern shown in (b) (bottom).

(d) Excitation of a SSH edge state using the wave-packet. Yellow circle denotes the atom, and white ellipses indicate the SSH lattice sites (A and B) with alternating distances among them.

REFERENCES

- [1] C. Cantillano *et al.*, *Sci. Bull.* 62, 339 (2017).
- [2] S. Longhi, *Phys. Rev. Lett.* 97, 110402 (2006).
- [3] F. Dreisow *et al.*, *Phys. Rev. Lett.* 101, 143602 (2008).
- [4] A. Szameit *et al.*, *Opt. Express* 13, 10552 (2005).

Multi-orbital lattices based on photonic molecules

R.A. Vicencio^{1,2}

¹*Departamento de Física, Facultad de Ciencias Físicas y Matemáticas, Universidad de Chile*

²*Millennium Institute for Research in Optics - MIRO*

e-mail: rvicencio@uchile.cl

The development of the femtosecond laser writing technique has revolutionized the fabrication of waveguide arrays and photonic systems due to its simplicity and versatility. Different configurations on different dimensions are possible by simply codifying the X, Y and Z positions of single waveguides inside a glass-like material [1,2]. However, the natural vertical ellipticity of fabricated waveguides is a major challenge that can be overcome by, for example, tuning the vertical distances among the waveguides to compensate the coupling constants anisotropy [3]. However, when having the need of, for example, exciting higher-order modes (orbitals) on single waveguides, this orientation destroys the mode degeneracy. Vertically oriented states are the first ones obtained experimentally [4], and the available degrees of freedom for studying more complex lattice interactions [5] are simply reduced.

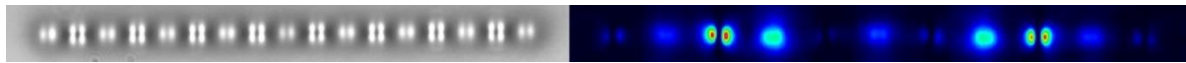


Figure 1. Left: SP Photonic lattice. Right: Output intensity after 20 mm of propagation.

In this work, we use the femtosecond laser writing technique to fabricate close waveguides, such that they can be treated as an effective “photonic molecule” [6]. We demonstrate that different higher order states can be excited depending on the excitation wavelength, and that the vertical restricted dipoles of single waveguides [4,5] can be oriented arbitrarily. This can be thought as a simple spatial rotation but has very important consequences when studying lattice dynamics on trivial and non-trivial configurations. To demonstrate these phenomena, we study different inter-orbital lattice geometries and show how the interaction between originally orthogonal states can induce effective magnetic fluxes that can control the light propagation on linear systems (see Figure 1). Specifically, we study a one-dimensional alternating SP lattice and its excitation with a zero-momentum Gaussian beam and observe a maximum dispersion with two well defined escaping lobes. This is in sharp contrast to the dynamics found in standard 1D lattices, where for zero momentum the energy is not transported at all. We also found that for a non-zero detuning in between S and P states, the 1D lattice can be mapped onto a diamond lattice exhibiting flat band and topological properties, which strongly affect the dynamics of this otherwise trivial lattice.

REFERENCES

- [1] A. Szameit, *Opt. Exp.* 13, 10552 (2005).
- [2] M. Wang *et al.*, paper AM2R.3, CLEO (2023).
- [3] R.A. Vicencio *et al.*, *Phys. Rev. Lett.* 114, 245503 (2015).
- [4] D. Guzmán-Silva *et al.*, *Phys. Rev. Lett.* 127, 066601 (2021).
- [5] G. Cáceres-Aravena *et al.*, *Phys. Rev. Lett.* 128, 256602 (2022).
- [6] S.V. Boriskina *et al.*, *Opt. Exp.* 19, 22024 (2011).

Pushing the boundaries of metasurface engineering: Hierarchical supercells and experimental validation

T. Contino^{1,2} and M. Tamagnone¹

¹Fondazione Istituto Italiano di Tecnologia, via Morego 30, 16163 Genova, Italy

²Dipartimento di Chimica e Chimica Industriale, Università di Genova, Genova, Italy

e-mail: tatiana.contino@iit.it

In this study, we propose a novel concept of metasurfaces based on generalized supercells, offering expanded capabilities and functionalities. Metasurfaces are planar artificial materials consisting of nanostructures arranged in arrays, enabling precise control over light properties such as phase, amplitude, and polarization. By utilizing supercells, which optimize multiple unit cells together, we can achieve diverse functions simultaneously [1,2].

Traditional metasurfaces employ subwavelength unit cells to impart specific phase profiles to light. This enables functionalities like focusing, holography, polarization control, and beam shaping. Supercells, arrangements of optimized multiple cells, allow for multiple functions in one device. When these supercells are periodically repeated, they act as gratings, diffracting light into multiple orders (*meta gratings*). Supercell size and arrangement determine diffraction order characteristics, while nanostructure geometry within the unit cell influences local light effects. This work expands supercells in two ways. Firstly, we introduce hierarchical supercells, combining cells with differences to achieve higher-order functionalities. Increasing the supercell order yields new diffraction orders, and engineering the unit cells enables different functions at each order. Secondly, we explore oblique supercells, extending design possibilities beyond horizontal and vertical orientations using a 2D integer Bravais lattice.

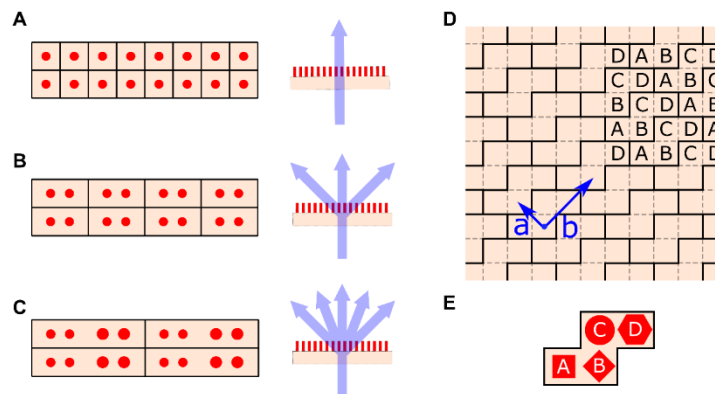


Figure 1. Generalized supercell metasurface concepts. A-C: Metagratings using supercells of increasing hierarchy. 0th-order supercells are just the unit cells of the metasurface; 1st-order create joining 0th cells, and so on. Increasing hierarchies generate an increased number of diffraction orders. D: An example of supercells based on a general integer Bravais lattice. E: Example of optical elements in a Bravais supercell.

REFERENCES

- [1] M. Khorasaninejad *et al.*, Science 352, 1190 (2016).
 [2] C. Spägle *et al.*, Nat. Commun. 12, 3787 (2021).

Unraveling the phononic mysteries: BIC revealed in hBN resonators through phonon polaritons

H. Gupta^{1,2}, J. Edgar³, F. De Angelis¹, A. Toma¹ and M. Tamagnone¹

¹*Istituto Italiano di Tecnologia (IIT), via Morego 30, 16163 Genova, Italy.*

²*Dipartimento di Chimica e Chimica Industriale, Università di Genova, Genova, Italy.*

³*Department of Chemical Engineering, Kansas State University, Manhattan, U.S.A*

e-mail: harsh.gupta@iit.it

Bound state in the continuum (BICs) refers to a special class of localized modes in open systems that exhibits resonance frequencies embedded within the continuous spectrum but do not radiate energy into the surrounding continuum. In fact, one of the main challenges is improving the quality factor Q by confining BICs, which is defined as,

$$\text{Quality Factor } (Q) = \frac{\text{Central Frequency of the Resonance } (f_0)}{\text{Full Width Half Maximum (FWHM) } (\Delta f)} \quad [1]$$

We studied phonon polaritons in hBN using the Lorentz model, considering the uniaxial in-plane isotropic crystal property of hBN with direction-dependent permittivity. Our model consisted of two elliptical hBN resonators arranged parallel along the y -axis. Initially, we simulated the system without any perturbation; we got the main resonance of hBN as bright mode at the resonant frequency of 1393.85 cm^{-1} along x -polarization and 1429.70 cm^{-1} along y -polarization. To demonstrate quasi-bound states in the continuum (Q-BIC) modes, we introduced a 25-degree rotation in opposite directions; we observed a new red-shifted Q-BIC or low-frequency dark mode at 1386.95 cm^{-1} and a blue-shifted Q-BIC or high-frequency dark mode at 1438.21 cm^{-1} . The quality factor is enhanced from 161 (bright mode) to 347(Q-BIC) by approximately 115 % (x -polarization). and enhancement in quality factor from 213 (bright high-frequency resonance) to 394 (blue-shifted Q-BIC) by nearly 85 % in y -polarization. The experimental FTIR results confirmed the presence of the low and high-frequency bright mode of hBN at 1396 cm^{-1} along x -polarization and 1427 cm^{-1} along y -polarization, respectively; the experimental spectra also showed a set of additional peaks corresponding to the quasi-BIC modes, as a low-frequency quasi-BIC mode at 1383 cm^{-1} along the major axis (x -polarization) and Q-BIC at 1437 cm^{-1} along the minor axis (y -polarization) in Figure (1), consistent with our theoretical prediction.

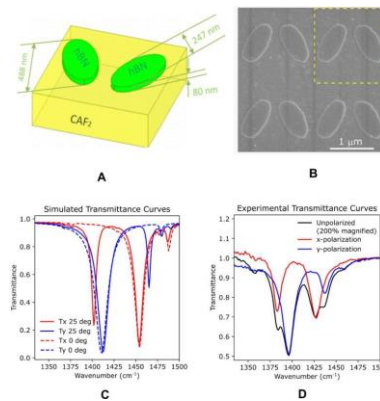


Figure 1. (a) hBN resonators with a major axis of 488 nm, minor axis of 247 nm, hBN thickness of 80 nm over the CAF2 substrate (b) SEM image of the hBN resonators having a period size of $1.7 \mu\text{m}$ with same measurements of simulated resonators (c) Simulated transmitted curves shows the main resonances at zero degrees rotation by dotted lines and 25 degrees rotation curves by solid lines, red and blue color shows the x and y polarization respectively (d) Experimental FTIR curves show by solid lines, black represents to the unpolarized curve (without polarizer), red and blue shows the transmission curves shows the x and y polarization respectively.

REFERENCES

[1] J. Shereena *et al.*, *Nanophotonics* 10, 4175 (2021).

Refractive index change caused by biomolecular adsorption and structural transformations of adsorbed molecules in ultrasensitive plasmonic biosensors

I. Jokić, O. Jakšić, M. Frantlović, Z. Jakšić and K. Radulović

University of Belgrade - Institute of Chemistry, Technology and Metallurgy - Department of Microelectronic Technologies - National Institute of the Republic of Serbia, Belgrade, Serbia

e-mail: ijokic@nanosys.ihm.bg.ac.rs

Adsorption-based plasmonic sensors have proven to be highly sensitive detectors of a broad range of chemical and biological analytes, with a great potential for application in environmental protection, medicine, industry, etc. [1]. The operating principle of plasmonic refractive index (RI) sensors is based on the RI change of the sensing area, which is a consequence of the change of the sensing layer effective relative permittivity, caused by the presence of adsorbed analyte particles on it. Since RI change is determined by the amount (number) of adsorbed particles of a certain type, and this amount depends on the concentration of analyte particles in the analyzed sample, RI change is used as a measurement parameter of this type of sensors. Mathematical modeling of the sensor response is therefore based on the modeling of the temporal change of the effective RI of the sensing area.

Particles of the biological analyte are reversibly adsorbed from the liquid sample onto the sensing area based on their affinity for surface adsorption sites. Ideally, the time response of the sensor will be determined only by the adsorption process. However, many biomolecules, especially proteins, undergo a structural transformation due to the change of external conditions, which may even be a contact with the surface of a solid body, such as the sensing surface. This phenomenon can significantly modify the sensor response kinetics [2]. In addition, the sensor response is also affected by the depletion of analyte molecules from the sample during adsorption, which is pronounced when working with minuscule sample amounts in which extremely low biomolecule concentrations are to be detected (one of the goals of the current research in the biosensors field) [3].

In this work, we derive the first mathematical model that describes the change in the effective RI of the sensing area by taking into account all three relevant processes: adsorption, transformation of adsorbed biomolecules and the sample depletion. We assume the following: 1) biomolecules are reversibly adsorbed in only one structural form, 2) a reversible transformation of the adsorbed biomolecules from the first to the second form occurs (which does not change the adsorption sites occupancy), 3) biomolecules can desorb with some probability even when they have the second form, 4) the concentration of biomolecules in the sample decreases with time due to adsorption process. We then use the devised model for the analysis of separate influences of the mentioned processes, as well as their joint influence on the RI change. We consider these influences in the concentration range of interest for protein biosensing.

The presented model of RI change is significant because it takes into account processes relevant for response generation in biosensors operating with small sample volumes, in which extremely low biomolecule concentrations must be detected. The results of the analysis demonstrate the importance of using a proper model of sensor response, because an inadequate model can lead to an erroneous interpretation of measurement results. In the authors' opinion, the presented model is a significant step in the development of reliable affinity-based plasmonic biosensors.

REFERENCES

- [1] Q. Duan *et al.*, *Sensors* 21, 5262 (2021).
- [2] I. Plikusiene *et al.*, *Biosens. Bioelectron.* 156, 112112 (2020).
- [3] I. Jokić *et al.*, *Meas. Sci. Technol.* 32, 95701 (2021).

Characterization and testing of fiber optic curvature sensor as an optical mode converter for deformation measurement

S. Babić, J.S. Bajić, M. Vasiljević Toskić, A. Joža and V. Rajs

University of Novi Sad, Faculty of Technical Sciences, Department of Power, Electronic and Telecommunication Engineering, Novi Sad, Serbia

e-mail: sladjana.babic@uns.ac.rs

Shortly after the discovery of optical fibers it was realized that optical fibers, except reliable data transmission, also possess excellent sensing capabilities. Main advantages of fiber optic sensors are: flexibility, immunity to electromagnetic interference, excellent resolution, wide measurement range, water and corrosion resistance, low-cost, small dimensions etc. A great number of fiber optic curvature sensors (FOCS) belong to the group of fiber optic sensors that are based on light intensity modulation. During the light propagation through the fiber, if the fiber bends, mode conversion occurs. Some of the light rays exit the optical fiber, leading to a decrease in light intensity at the fiber output. In order to increase the sensitivity of the optical fiber to bending, V-shaped notches are etched into the fiber forming a sensitive zone [1-3]. This sensitive zone can be also used for determining the bending direction, which is an advantage compared to other curvature sensors. In this paper, a fiber optic curvature sensor implemented using plastic optical fiber with a sensitive zone is tested. Essentially, the measurement is based on detecting changes in the output intensity distribution depending on the deformation (curvature) of the fiber. The testing is performed in function of different notch depth, their spacing and the angle at which they are etched into the fiber, in order to assess the impact of these parameters on the sensor's performance. The results presented in paper [2] indicate that the optimal number of notches is 55. Therefore, in this measurement, a sensitive zone including about 50 notches is investigated. Additionally, in paper [1], it is demonstrated how the position of the FOCS sensitive zone, whether it is on the concave or convex side of the bent fiber, affects the output signal. This aspect is also tested in this experiment, where deformations are applied in both directions.

In Figure 1 the experimental setup used in this work is shown. LED is used as a light source, and its intensity can be controlled. Therefore, the influence of the source intensity on the measurements is tested. Additionally, a mode converter is placed between the LED and FOCS. Its role is to excite multiple modes and ensure that the same radiation distribution is injected into all tested sensors. Unlike in paper [4], where a quadrant photodetector was used, here the output intensity distribution is recorded using a CCD sensor, where the mode conversion can be clearly observed. Due to this capability, the FOCS sensor is also referred to as an optical mode converter or mode filter.

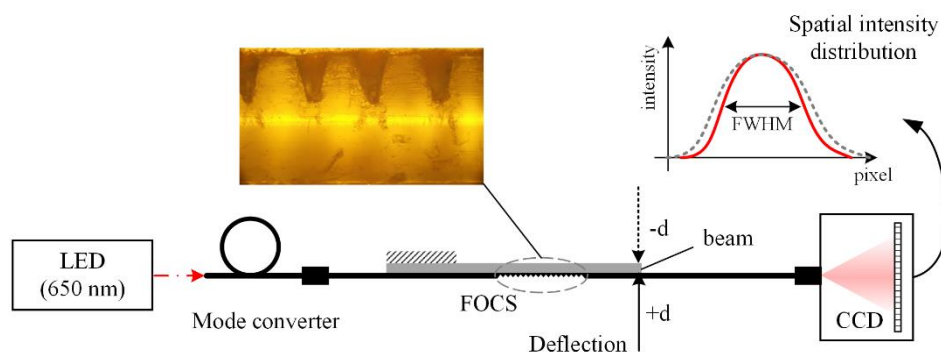


Figure 1. Experimental setup for the characterization and testing of the proposed FOCS sensor.

REFERENCES

- [1] H. Di, *Opt. Laser Technol.* 62, 44 (2014).
- [2] Y. Fu, H. Di, *Opt. Laser Technol.* 43, 586 (2011).
- [3] Y. Fu *et al.*, *Opt. Laser Technol.* 42, 594 (2010).
- [4] J.S. Bajić *et al.*, *Sens. Actuators A: Phys.* 267, 278 (2017).

Application of polymer optical fiber sensor for urine parameter measurements: a preliminary study

P. Sokołowski¹, K. Cierpiak¹, P. Wityk², A. Drabik-Kruczkowska³ and M. Szczerska¹

¹*Department of Metrology and Optoelectronics, Faculty of Electronics, Telecommunications and Informatics, Gdańsk University of Technology, 11/12 Narutowicza Street, Gdańsk, Poland*

²*Department of Molecular Biotechnology and Microbiology, Faculty of Chemistry, Gdańsk University of Technology, Narutowicza 11/12 Street, Gdańsk, Poland*

³*Department of Obstetrics, Faculty of Medicine, Ludwik Rydygier Collegium Medicum in Bydgoszcz, Nicolaus Copernicus University in Toruń, 85-094, Bydgoszcz, Poland*

e-mail: patsokol@pg.edu.pl

The use of polymer optical fiber (POF) sensor as sensors seems to be an expanding application field. There are numerous beneficial properties of polymer fiber, such as small size, flexibility, biocompatibility, immunity to electromagnetic interference, capability for direct optical measurements and ease of coupling light into fiber. With POF different kind of sensors can be designed and working under different principles such as: intensity sensor, interferometric, Bragg grating, optical time domain reflectometry [1-3].

In preliminary study we prepared U-Shape fiber, which is bent fiber sensor and mainly based on intensity modulation. For intensity modulation, changes are detected by optical loss, which can be changed through coupling condition, optical absorption characteristics, evanescent field. In order to improve the accuracy of the POF sensor, the part of the cladding was removed. The sensor can additionally be modified by applying additional layers, e.g. for bacteria detection. The U-shape sensor probe was dipped into a solution. A fiber optic sensor was applied to detect changes in spectra and the refractive index of its surrounding environment. Observed changes with support of machine learning can be used to diagnose patients' urine [4-7].

POF sensors leads to the creation of new applications. The advancement of technologies for the ways of functionalization and geometrical modification provides numerous opportunities for the modification and optimization U-shape sensors.

REFERENCES

- [1] W.R. Habel, K. Krebber, *Photonic Sens.* 1, 268 (2011).
- [2] A. Gowri *et al.*, *Opt. Fiber Technol.* 47, 15 (2019).
- [3] G. Wandemur *et al.*, *Biosens. Bioelectron.* 54, 661 (2014).
- [4] P. Wityk *et al.*, *J. Biophotonics* e202300095 (2023).
- [5] C.G. Danny *et al.*, *J. Light. Technol.* 38, 1580 (2020).
- [6] M. Szczerska, *Chemosensors* 10, 228 (2022).
- [7] M. Kruczkowski *et al.*, *Sci Rep* 12, 3762 (2022).

Index

A

Abramović D	87
Abu el Rub A	78,79,80
Aleksić N B	55,56
Algarra M	78,79,121
Alwashahi S	55
Andjus P	93
Andreeva C	139
Anfertev V	29
Angelova L	71
Antić A	93
Antić Ž	26
Antonov L	139
Apostolakis A	29
Arsenović D	44
Atanasijevic P	89
Atanassova V	111
Atić A	100
Aygun G	132

B

Babić S	146
Bader A	98
Bajić J S	105,136,146
Banović M	135
Bassi A	9
Batinić B	105
Belić M R	55,56
Beličev P P	53
Berger M	131
Birner S	65
Blažić L	91
Bobrovsky A	67
Bokic B	138
Bonacina L	20
Boskovic N	39
Boteva V	112
Boukherroub R	25
Bouzin M	72
Boychuk A	67
Božanić D K	35,66,69
Bozhevolnyi S I	4
Bozic D	124
Božinović N	60,117
Brestovacki L	136
Buchvarov I	71

Bugarski K	101,102
Bukumira M	90
Bunjac A	46

C

Cáceres-Aravena G	140
Cerullo G	72
Chen X	124
Chirico G	72
Cid-Lara C	103
Cierpiak K	147
Cigl M	67
Colciaghi P	11
Collini M	72
Conci C	72
Contino T	143
Credi C	19,21,76
Crnjanski J	135
Cubrovic M	43
Ćurčić M M	44,46,62,113
Cvejić Ž	91

D

Dallari C	76
Damljanović V	59
Danilović D	35
Daskalova A	71
De Angelis F	144
Demić A	99
Demirhan Y	132
Demoli N	87
Denčevski A	75,90
Deneva V	139
Denker A	115
Dér A	24
Dezfouli A M	87
Diamanti E	27
Diaspro A	3
Dikovska A	71
Dimova V	139
Djoković V	35,66,69
Dojcilovic R	69
Donato S	19
Đorđević K Lj	38
dos Santos Martins L	27
Drabik-Kruczkowska A	147
Dragaš M A	38
Drvenica I T	95

Dučić T	121	Hartmann F	98
E		Hasar E	122
Eden J G	32	Hermann Avigliano C	42
Edgar J	144	Hinkel J	113
Eftimov T	77	Höfling S	98
Elahi P	122	Hunt B D	32
F		I	
Farsari M	72	Ilić A Ž	107,108
Fernandes M H	71	Ilić M M	107,108
Filipov E	71	Ilić V Lj	95
Filipović Tričković J	78,79	Imas J J	121
Frantlović M	145	Indjin D	99
Fuenzalida J	94	Inverso D	72
G		Isić G	130
Gaković B	118	Ivanov I	77
Galović S P	38,123	Ivliev N	119
Garcia G A	35	J	
Genova S	112	Jabeen F	98
Genova Ts	82,83,139	Jacchetti E	72
Gensch M	54,115	Jakšić O	145
Gentscheva G	77	Jakšić Z	127,145
Georgieva D	77,131	Jamme F	10
Gilaberte M	94	Jelenković B	44,64,81
Gili V	94	Jelić J Z	90,92
Gligorić G	51,53	Ji M	22
Gojanovic J	104	Jokić I	145
Golub I	119	Jovanovic D	85
Golubovic M	136	Joža A	136,146
Gräfe M	94	Jugović D	63
Grass E	108	K	
Grujic D	89,91	Kabouraki E	72
Grujić Z D	46,110,113	Kahraman M	73,74
Gueckstock O	115	Kalinić A	128,129
Guo R	22	Kampfrath T	115
Gupta H	144	Karagoz I D	73
Guzmán-Silva D	141	Karbunar L	128,129
Gvozdić D	135	Kariman B S	72
H		Karpeev S	120
Ha Y	115	Khonina S	119,120
Hadzic B	62	Kolaric B	138
Hafezi M	15	Korićanac L	36,78,79
Hamplová V	67	Kostadinov I	97
		Kostic Lj	123
		Kourfakas G	115

Kovačević A	64	Milovanović D	118
Kozakijevic S	84	Mincheva R	71
Krmpot A J	75,84,90,92,95,115	Mircheva V	82
Krsic J	102	Mišković Z L	128,129
Krstajic M	33	Mladenović I	127
Krstić M	135	Mojović M	36
Kuzmanovic M	124	Mrakovic A	85
		Murić B	64
L		Mutavdzic D	85
Lainović T	91	N	
Lefevbre P	27	Nahon L	5,35
Leguay L	65	Nakarada Đ	36
León-Torres J R	94	Nardini A	72
Leykam D	52	Nedić M	51,52
Li Y	11	Nenadović M	60
Lorenz V O	32	Neshev D	131
Loveridge T	32	Nesic M	123
Löw R	17	Nešić M D	36,78,79,80,121
Lutz D	93	Neves S	27
M		Nikolić M G	110,134
Ma J	22	Nikolić S N	55,92
Mączko H	65	Nikolova K	77
Maletić N	108	Nocentini S	19
Maluckov A	51,52,53,102	Noga P	63
Mančić A	52	Novaković M	34,60,63
Manojlović L	105	Novotná V	67
Mara D	61	Novta E	91
Marić T	35	O	
Marini M	72	Obradov M	127
Marinovic Cincovic M	85	Omerasevic M	85
Markham D	27	Oolman K	32
Markovic D	43	Osellame R	72
Markovic S	34	Ozyuzer L	132
Markovski A	82,139	P	
Markushev D D	38	Pagnacco M	138
Markushev D K	38	Pajic T	84
Martella D	19	Pajovic J	10,35,66
Martínez Vázquez R	72	Palibrk A	93
Mashanovich G Z	101	Pan R	115
Matijević M	36,79,80	Pankov N	83
Mi L	22	Pantelić D	64,86,88,89,91
Mihailov V	111	Panzeri D	72
Mihailovic P	89,135	Park S	32
Mihalev M	112	Parmeggiani C	19
Milenković A	46,113		
Miletic V	123		
Milošević M	93		

Paunovic N	62	Real B	140,141
Pavlicevic T	104	Recati A	7,48
Pavlovic D	86,88,89	Rechtsman M	18
Pavlovic V	50	Réfrégiers M	10
Pavone F S	76	Resan B	30
Pereira M F	29	Roccuzzo S M	48
Perić M	46	Román-Cortés D	140
Pesic J	68	Romcevic M	62
Petkova N	77	Romcevic N	62
Petković M	36,78,79,80,121	Ruzic J	124
Petričević S	135		
Petrović B	98	S	
Petrovic J	23,51,101,102,115	Salatic B	86,88,89
Petrovic M S	56	Santos L	48
Petrović N	57	Saralieva E	77
Petrović S	117,118	Saridağ A M	73,74
Pevicharova G	112	Savić S V	107,108
Pirovska A	111	Savić-Šević S	64,91
Pjević D	63	Savovic J	124
Polzik E S	2	Savva K	117
Popović I	78,79,80	Schliwa A	65
Popović M	34,60,63	Scholtes T	46,113
Popovic M	123	Seifert T	115
Porfirev A	119,120	Senkić A	90
Porfirev D	120	Setzpfandt F	16
Potočnik J	60,117	Sevic D	134
		Shibaev V	67
R		Shinbrough K	32
Rabasovic M	115	Shu X	28
Rabasović M D	75,84,90,92,95,110	Simic M	124
Rabasovic M S	134	Simovic Pavlovic M	138
Rac V	34	Sindik M	48
Radjenovic B	39	Siogka C	118
Radmilović M D	95	Sironi L	72
Radmilovic-Radjenovic M	39	Skapin S D	34
Radoičić M	36,80	Skenderović H	87,88
Radojevic V	62	Slaveeva S	97
Radovanović J	99,100	Slavova V	112
Radović I	128,129	Smirnova O	13
Radulovic A	138	Soavi G	8
Radulović K	145	Sokołowski P	147
Rahmani M	131	Solajic A	68
Raimondi M T	72	Soto J	79,121
Rajic V	34	Sredojević D	66
Rajs V	136,146	Stanic V	85
Rakić M	87,88	Stanojević N	99
Ralevic U	132	Stasic J	124,125
Ralić V	78,79,80	Stepić M	36,78,79,80,121
Rašljić Rafajilović M	127	Stevanovic Lj	47,50

Stević Z	93	Veerman P	102
Stojadinovic S	34	Veljovic Dj	85
Stojanovic D B	132	Veselinovic Lj	34
Stojanovic M	101,102	Vicencio R A	101,103,140,141,142
Stojanovic N	54,102,115	Vildoso P	101
Stojkovic Simatovic I	34	Vinić M	37
Stoyanova M	139	Vladimirov B	83
Stratakis E	117	Vladimirova–Mihaleva L	77,112,131
Stringari S	48	Vozzi C	12
Strinic A I	56	Vučičević J	45
Su W	22	Vujičić N	90
Šupić I	27	Vukojević V	92
Supina A	90	Vuković N	99,100
Szczerska M	147		
		W	
T		Weih R	98
Tamagnone M	143,144	Wien F	10
Tankova V	111	Wiersma D S	19
Tanovska M	131	Wityk P	147
Temelkov K	97	Woeste J	54
Todorovic N V	84		
Toma A	144	Y	
Töpfer S	94	Yacoub V	27
Tošić D	66,67	Yankov G	97
Toth E	91		
Trajković J Z	107,108	Z	
Treutlein P	11	Zafar H	29
Troyanova P	82	Zaharieva L	139
Trpkov Dj	66,69	Žakula J	36,78,79,80
Trtica M	124,125	Zelenika S	110
Tsibidis G	118	Zhelyazkova Al	82,83
Tzoneva R	131	Zibold T	11
		Zivanovic S	104
U		Zivic M	84
Urrutia A	121	Zografopoulos D C	130
Ustinov A	119		
		V	
Vaks V	29	Vaks V	29
Valenta Šobot A	78,79	Valenta Šobot A	78,79
Vaňa D	63	Vaňa D	63
Vasić B	130	Vasić B	130
Vasić I	45	Vasić I	45
Vasiljevic D	138	Vasiljevic D	138
Vasiljević Radović D	127	Vasiljević Radović D	127
Vasiljević Toskić M	105,146	Vasiljević Toskić M	105,146
Vassilev V	131	Vassilev V	131

